Electronic Supporting Information

Photo-triggered hydrogen atom transfer from an iridium hydride complex to unactivated olefins

Mirjam R. Schreier, Björn Pfund, Xingwei Guo,[*‡] and Oliver S. Wenger[*]

Department of Chemistry, University of Basel, St. Johanns-Ring 19, 4056 Basel, Switzerland

[‡] Current address: Center of Basic Molecular Science (CMBS), Department of Chemistry, Tsinghua University, Beijing 100084, China

Table of Contents

1 Equipment and methods

General

Unless stated otherwise, all air- or moisture-sensitive syntheses were performed under inert conditions (N_2 atmosphere). Dry solvents were used as received and if necessary were degassed using the freeze, pump, thaw method. Dry diethyl ether, tetrahydrofuran (THF) and dichloromethane (DCM) were obtained from a commercial solvent purification system by Innovative Technology. Commercially available chemicals were purchased from ABCR, Acros Organics, Fluorochem, or Sigma-Aldrich and used as received.

Chromatography

Column chromatography was performed with silica gel from Silicycle (silica flash, 40-63 µm, (230-400 mesh ASTM) for flash column chromatography). Thin layer chromatography (TLC) was performed with pre-coated aluminium sheets (precoated with silica 60, from Merck, layer thickness of 0.25 mm), coated with fluorescence indicator F254. Visualization of the compounds occurred either under UV light (using either the 254 nm or 365 nm output of a UV lamp) or using a $KMnO_4$-stain.

NMR spectroscopy

NMR spectra were measured on a Bruker Avance III operating at 400 MHz or 500 MHz proton frequencies. All chemical shifts are reported in δ values in ppm and were referenced to the signals of the residual non-perdeuterated solvent used.[1] The deuterated solvents for NMR-spectroscopy were obtained from Cambridge Isotope Laboratories. All coupling constants *J* are given in Hertz (Hz) and the following abbreviations are used to describe their coupling patterns: s (singlet), br s (broad singlet), d (doublet), t (triplet), q (quartet), pent. (quintet), sext. (sextet), m (multiplet), dd (doublet of doublets), dq (doublet of quartets), tq (triplet of quartets), ddd (doublet of doublets of doublets).

GC-MS spectrometry

GC-MS spectrometry was performed using a GC-MS-QP2010 SE gas chromatograph system with a ZB-5HT inferno column (30 m x 0.25 mm x 0.25 mm) that was operated at a 1 mL/min He flow rate (split = 20:1). The different analytes were separated using the methods summarized in Table S1. The retention times (t_R) of the substrates and products are reported in minutes in the experimental sections S2 and S3.

The mass system consisted of a Shimadzu mass detector (EI, 70 eV). The quotients of mass to charge (*m/z*) are given and the relative intensities related to the basis peak (I=100) are reported in brackets.

Table S1. Different methods for analysis by GC-MS spectrometry.

	Oven Temperature Program
Method A	100 °C, 35 °C/min, 200 °C, 100 °C/min, 350 °C
Method B	100 °C, 30 °C/min, 200 °C, 5 °C/min, 230 °C, 100 °C/min, 350 °C

Steady-state absorption spectroscopy

Optical absorption spectroscopy was measured on a Cary 5000 UV-Vis-NIR instrument from Varian.

Time-resolved luminescence spectroscopy

Time-resolved luminescence spectroscopy was performed on a LP920-KS instrument from Edinburgh Instruments. Excitation occurred at 455 nm using a Quantel Brilliant b laser combined with an optical parametric oscillator (OPO) from Opotek as excitation source. The laser pulse duration was ~10 ns and the pulse frequency was 10 Hz. Kinetics at single detection wavelengths were recorded using a photomultiplier tube.

Transient absorption spectroscopy

Transient absorption spectroscopy was performed on a LP920-KS instrument from Edinburgh Instruments. Excitation of the complexes occurred at 445 nm using a frequency-tripled Nd:YAG laser (Quantel Brilliant, ca. 10 ns pulse width) equipped with an OPO from Opotek and the typical pulse energy was ca 9 mJ. A beam expander (GBE02-A from Thorlabs) was used to improve the excitation homogeneity in the detection volume. The transient absorption spectra were detected with an iCCD camera from Andor.

Set-up for photocatalysis

Photoirradiation was performed using a home-built photoreactor (Fig. S1). The setup consists of LED strips (470 nm) that are arranged around the outside of a glass beaker. The photoreactor is divided into 8 compartments, each corresponding to an irradiation power of ca. 7.5 W. The beaker is filled with water and incorporates copper tubing through which water is flowed. The tubes are connected to an external thermostat, enabling a steady temperature throughout the irradiation process. For all experiments, the water temperature was adjusted to 50 °C and the reactions were performed in NMR tubes that were irradiated in individual compartments.

For the UV-Vis irradiation experiment, continuous-wave photo-irradiation of the sample occurred at room temperature using a 455 nm (~1000 mW power output) collimated LED purchased from ThorLabs.

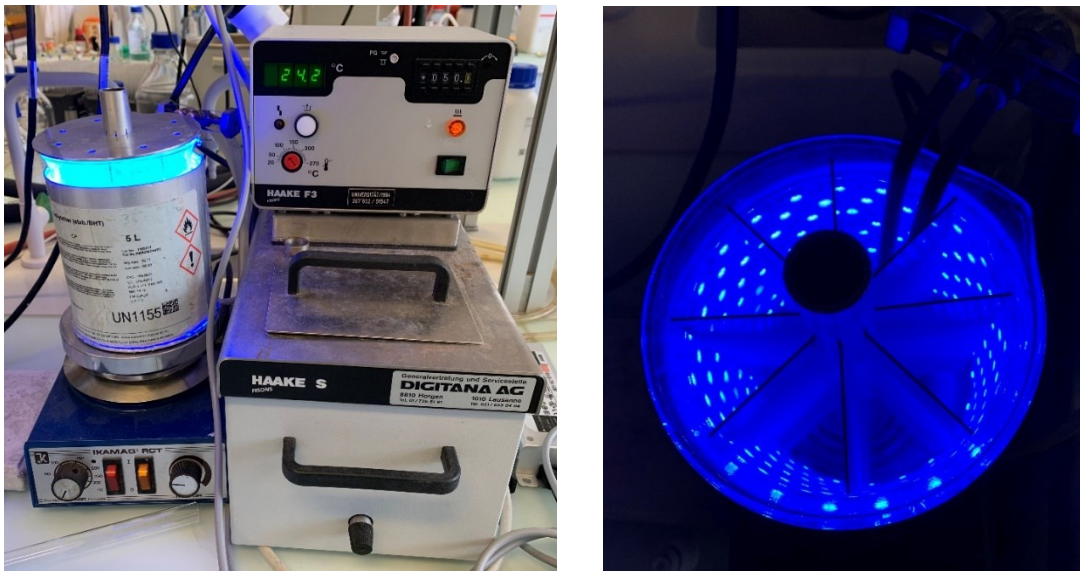

Figure S1. Home-built photoreactor (λ = 470 nm), connected to an external thermostat (left). Different compartments of the photoreactor (viewed from the top), each corresponding to an irradiation power of ca. 7.5 W (right).

2 Experimental procedures

2.1 Catalyst syntheses

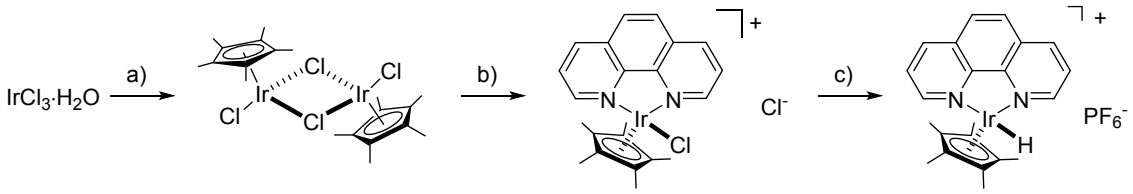

Scheme S1. Synthesis of different iridium complexes: a) C_5Me_5H, MeOH, reflux, 2 days, 80%; b) phen, MeOH, rt, overnight, 70%; c) aq. formic acid (3 M, pH 5), rt, 5 h, then KPF_6, 84%.

$[Cp^*IrCl_2]_2$

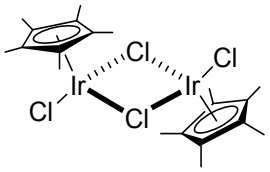

The synthesis of **$[Cp^*IrCl_2]_2$** was adapted from a previously published protocol.[2] Iridium(III) chloride hydrate (501 mg, 1.58 mmol, 2.0 eq.) was dissolved in dry MeOH (10 mL) and pentamethyl-cyclopentadiene (0.40 mL, 2.55 mmol, 3.2 eq.) was added dropwise. The reaction mixture was heated at reflux for 2 days. The resulting suspension was cooled to 0 °C. The formed orange-red precipitate was collected by filtration and washed with cold methanol to afford **$[Cp^*IrCl_2]_2$** (506 mg, 635 µmol, 80%) as an orange solid. Analytical data matches the literature.[2]

$C_{20}H_{30}Ir_2Cl_4$ (797 g/mol):

^{1}H-NMR (400 MHz, 298 K, $CDCl_3$, δ/ppm): 1.59 (s, 30H).

^{13}C-{^{1}H}-NMR (126 MHz, 298 K, $CDCl_3$, δ/ppm): 86.4, 9.5.

[Cp*Ir(phen)Cl]Cl

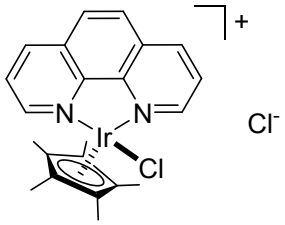

The synthesis of **[Cp*Ir(phen)Cl]Cl** was adapted from a previously published protocol.[3] A round-bottomed flask was charged with **$[Cp^*IrCl_2]_2$** (200 mg, 251 µmol, 1.0 eq.), 1,10-phenanthroline (92.0 mg, 511 µmol, 2.0 eq.) and dry methanol (20 mL). After the reaction mixture was stirred at room

temperature overnight, the solvent was evaporated under reduced pressure. The residue was redissolved in DCM and added dropwise to diethyl ether. The formed yellow precipitate was collected by filtration and washed with diethyl ether to afford **[Cp*Ir(phen)Cl]Cl** (203 mg, 351 µmol, 70%) as a yellow solid. Analytical data matches the literature.[4]

$C_{22}H_{23}N_2IrCl_2$ (579 g/mol):

^{1}H-NMR (400 MHz, 298 K, $CDCl_3$, δ/ppm): δ 9.41 (d, *J* = 5.2 Hz, 2H), 8.76 (d, *J* = 8.2 Hz, 2H), 8.32 (dd, *J* = 8.2 Hz, *J* = 5.2 Hz, 2H), 8.17 (s, 2H), 1.85 (s, 15H).

^{13}C-{^{1}H}-NMR (126 MHz, 298 K, $CDCl_3$, δ/ppm): 151.8, 146.6, 139.4, 131.2, 128.4, 128.1, 89.6, 9.2.

[Cp*Ir(phen)(H)](PF$_6$)

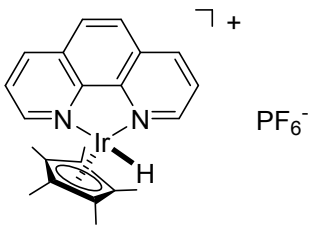

The synthesis of **[Cp*Ir(phen)(H)](PF$_6$)** was adapted from a previously published protocol.[5] The entire synthesis was performed in the dark and under argon atmosphere. **[Cp*Ir(phen)Cl]Cl** (100 mg, 172 µmol, 1.0 eq.) was dissolved in aq. formic acid solution (3 M, 5.7 mL, adjusted to pH 5 by addition of grounded KOH pellets) and the reaction mixture was stirred at room temperature in the dark for 5 hours. The resulting orange solution was filtered over Celite and **[Cp*Ir(phen)(H)](PF$_6$)** was precipitated from the filtrate through the addition of KPF_6 (283 mg, 1.54 mmol, 9.0 eq.). The resulting yellow suspension was filtered over Celite and the formed yellow precipitate was washed with previously degassed water (3 mL) and diethyl ether (3 mL). The residue was eluted with previously degassed MeCN (5 mL) and the filtrate was concentrated under reduced pressure. **[Cp*Ir(phen)(H)](PF$_6$)** (95.0 mg, 146 µmol, 84%) was obtained as a yellow solid. Analytical data is in agreement with the literature data obtained for **[Cp*Ir(phen)(H)](BF$_4$)**.[4]

$C_{22}H_{24}N_2IrPF_6$ (654 g/mol):

^{1}H-NMR (400 MHz, 298 K, CD_3CN, δ/ppm): 9.22 (dd, *J* = 5.4 Hz, 1.2 Hz, 2H), 8.64 (dd, *J* = 8.2 Hz, 1.2 Hz, 2H), 8.15 (s, 2H), 7.96 (dd, *J* = 8.2 Hz, 5.4 Hz, 2H), 1.90 (s, 15H), -11.46 (s, 1H).

[Cp*Ir(phen)]^0

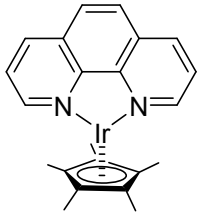

A reference spectrum of **[Cp*Ir(phen)]^0** was obtained after deprotonation of **[Cp*Ir(phen)(H)](PF$_6$)** (3.2 mg, 4.9 µmol, 1.0 eq.) dissolved in CD_3CN (0.5 mL) in presence of KO^{t}Bu (700 µg, 6.25 µmol, 1.3eq.).

^{1}H-NMR (400 MHz, 298 K, CD_3CN, δ/ppm): 9.04 (d, *J* = 6.5 Hz, 2H), 7.48 (s, 2H), 7.37 (d, *J* = 6.9 Hz, 2H), 6.73 (t, *J* = 6.7 Hz, 2H), 1.99 (s, 15H).

2.2 Substrate syntheses

2.2.1 Synthesis of allylic ethers

Table S2. Synthesis of different allylic ether substrates (**1-SM**, **7-SM**, **10-SM** and **11-SM**):

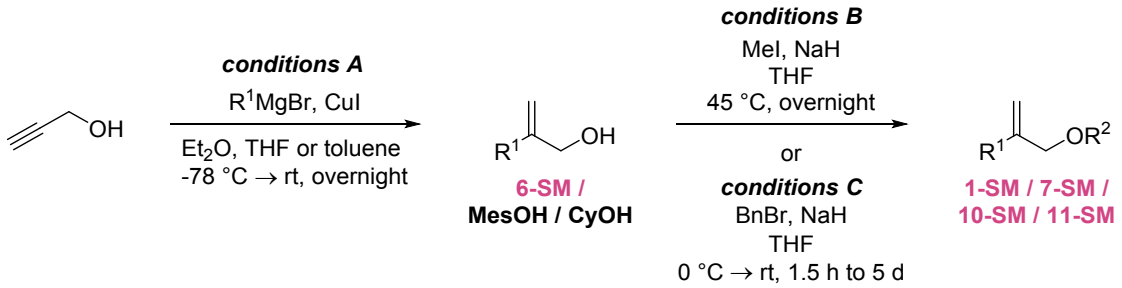

Allylic alcohol	R^1	Conditions	Yield / %	Allylic ether	R^2	Conditions	Yield / %
6-SM	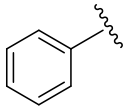	***conditions A*** with Et_2O	91	1-SM	Me	***conditions B***	93
MesOH	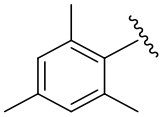	***conditions A*** with THF	69	7-SM	Bn	***conditions C***	69
CyOH	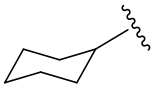	***conditions A*** with toluene/THF	27	10-SM	Bn	***conditions C***	81
	Me	-[a]	-[a]	11-SM	Bn	***conditions C***	89

[a] 2-Methylprop-2-en-1-ol was obtained from commercial sources.

2-Phenylprop-2-en-1-ol (6-SM)

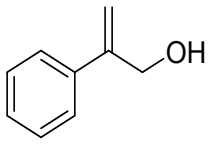

Propargyl alcohol (1.07 g, 19.1 mmol, 1.0 eq.) and CuI (1.66 g, 8.72 mmol, 0.5 eq.) were suspended in dry diethyl ether (25 mL) and the resulting suspension was cooled to −78 °C with an acetone/dry ice bath. Phenylmagnesium bromide (3.0 M in diethyl ether, 18.0 mL, 54.0 mmol, 2.8 eq.) was added dropwise and the reaction was stirred at −78 °C for 15 minutes. The reaction mixture was then allowed to reach room temperature and was stirred at this temperature overnight. After cooling to 0 °C, the

reaction was quenched with sat. aq. NH_4Cl solution (40 mL), the layers were separated, and the aqueous layer was extracted with diethyl ether (3 x 40 mL). The combined organic layers were dried over anhydrous sodium sulfate, filtered and concentrated under reduced pressure. The crude product was purified by flash column chromatography (SiO_2, diethyl ether/pentane 1:5) to afford 2-phenylprop-2-en-1-ol (**6-SM**, 2.34 g, 17.4 mmol, 91%) as a light-yellow liquid. Analytical data matches the literature.[6]

$C_9H_{10}O$ (134 g/mol):

^{1}H-NMR (400 MHz, 298 K, $CDCl_3$, δ/ppm): 7.48-7.43 (m, 2H), 7.39-7.28 (m, 3H), 5.48 (pseudo-q, *J* = 0.9 Hz, 1H), 5.36 (pseudo-q, *J* = 1.3 Hz, 1H), 4.55 (s, 2H), 1.75 (br s, 1H).

^{13}C-{^{1}H}-NMR (101 MHz, 298 K, $CDCl_3$, δ/ppm): 147.4, 138.6, 128.6, 128.1, 126.2, 112.7, 65.2.

2-Mesitylprop-2-en-1-ol (MesOH)

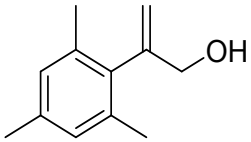

Propargyl alcohol (2.00 g, 35.7 mmol, 1.0 eq.) and CuI (3.40 g, 17.8 mmol, 0.5 eq.) were suspended in dry THF (50 mL) and the resulting suspension was cooled to −78 °C with an acetone/dry ice bath. Mesitylmagnesium bromide [freshly prepared from mesitylbromide (16.5 mL, 108 mmol, 3.0 eq.) and magnesium (3.90 g, 161 mmol, 4.5 eq.) in dry THF (107 mL)] was added dropwise and the reaction was stirred at −78 °C for 15 minutes. The reaction mixture was then allowed to reach room temperature and was stirred at this temperature overnight. After cooling to 0 °C, the reaction was quenched with sat. aq. NH_4Cl solution (40 mL), the layers were separated, and the aqueous layer was extracted with diethyl ether (3 x 40 mL). The combined organic layers were dried over anhydrous sodium sulfate, filtered and concentrated under reduced pressure. The crude product was purified by gradient flash column chromatography (SiO_2, diethyl ether/pentane 1:5 then diethyl ether/pentane 1:3) to afford 2-mesitylprop-2-en-1-ol (**MesOH**, 4.37 g, 24.8 mmol, 69%) as a yellowish liquid. Analytical data matches the literature.[7]

$C_{12}H_{16}O$ (176 g/mol):

^{1}H-NMR (400 MHz, 298 K, $CDCl_3$, δ/ppm): 6.86 (s, 2H), 5.51 (pseudo-q, *J* = 2.1 Hz, 1H), 4.84 (pseudo-q, *J* = 1.8 Hz, 1H), 4.02 (dt, *J* = 6.1 Hz, 1.9 Hz, 2H), 3.06 (t, *J* = 6.1 Hz, 1H), 2.23 (s, 3H), 2.17 (s, 6H).

^{13}C-{^{1}H}-NMR (101 MHz, 298 K, CD_3CN, δ/ppm): 150.3, 137.7, 137.3, 136.4, 128.8, 112.0, 64.9, 21.0, 19.8.

2-Cyclohexylprop-2-en-1-ol (CyOH)

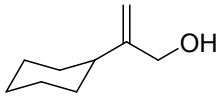

Propargyl alcohol (990 mg, 17.7 mmol, 1.0 eq.) and CuI (1.70 g, 8.93 mmol, 0.5 eq.) were suspended in dry toluene (24 mL) and the resulting suspension was cooled to −78 °C with an acetone/dry ice bath. Cyclohexylmagnesium bromide (1.3 M in toluene/THF (1:1 *v:v*), 40 mL, 52.0 mmol, 2.9 eq.) was added dropwise and the reaction was stirred at −78 °C for 15 minutes. The reaction mixture was then allowed to reach room temperature and was stirred at this temperature overnight. After cooling to 0 °C, the reaction was quenched with sat. aq. NH_4Cl solution (40 mL), the layers were separated, and the aqueous layer was extracted with diethyl ether (3 x 40 mL). The combined organic layers were dried over anhydrous sodium sulfate, filtered and concentrated under reduced pressure. The crude product was purified by gradient flash column chromatography (SiO_2, diethyl ether/pentane 1:10 then diethyl ether/pentane 1:1) to afford 2-cyclohexylprop-2-en-1-ol (**CyOH**, 672 mg, 4.79 mmol, 27%) as a yellowish liquid. Analytical data matches the literature.[6,8]

$C_9H_{16}O$ (140 g/mol):

^{1}H-NMR (400 MHz, 298 K, $CDCl_3$, δ/ppm): 4.94 (pseudo-q, *J* = 1.7 Hz, 1H), 4.81-4.79 (m, 1H), 3.98 (dt, *J* = 5.9 Hz, 1.5 Hz, 2H), 2.76-2.71 (m, 1H), 1.94-1.87 (m, 1H), 1.79-1.72 (m, 4H), 1.70-1.62 (m, 1H), 1.36-1.15 (m, 5H).

^{13}C-{^{1}H}-NMR (126 MHz, 298 K, CD_3CN, δ/ppm): 155.9, 106.5, 64.3, 41.6, 32.9, 27.1, 26.7.

(3-Methoxyprop-1-en-2-yl)benzene (1-SM)

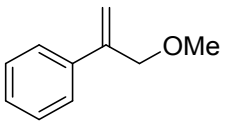

Sodium hydride (95%, 856 mg, 21.4 mmol, 1.2 eq.) was suspended in dry THF (35 mL) and iodomethane (1.6 mL, 25.7 mmol, 1.5 eq.) was added dropwise. After the suspension was heated to 45 °C, 2-phenylprop-2-en-1-ol (**6-SM**, 2.34 g, 17.4 mmol, 1.0 eq.) was added and the reaction mixture was stirred at 45 °C overnight. The crude mixture was cooled to 0 °C and was then quenched with water (25 mL). The layers were separated, and the aqueous layer was extracted with diethyl ether (3 x 50 mL). The combined organic layers were dried over anhydrous sodium sulfate, filtered and

concentrated under reduced pressure. The crude product was purified by flash column chromatography (SiO_2, pentane/ethyl acetate 30:1) to afford (3-methoxyprop-1-en-2-yl)benzene (**1-SM**, 2.41 g, 16.3 mmol, 93%) as a colorless liquid. Analytical data matches the literature.[9]

$C_{10}H_{12}O$ (148 g/mol):

^{1}H-NMR (400 MHz, 298 K, $CDCl_3$, δ/ppm): 7.52-7.46 (m, 2H), 7.39-7.27 (m, 3H), 5.52 (s, 1H), 5.31 (pseudo-q, *J* = 1.3 Hz, 1H), 4.31 (s, 2H), 3.30 (s, 3H).

^{13}C-{^{1}H}-NMR (126 MHz, 298 K, CD_3CN, δ/ppm): 145.7, 139.8, 129.3, 128.7, 127.0, 114.8, 75.0, 58.0.

GC (achiral phase, 62.7 kPa He, method A): t_R = 3.62 min.

GC-MS (EI, 70 eV) *m/z* (%): 147 (15), 133 (6), 118 (100), 103 (49), 91 (15), 77 (34), 63 (6).

2-(3-(Benzyloxy)prop-1-en-2-yl)-1,3,5-trimethylbenzene (7-SM)

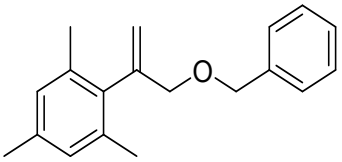

Sodium hydride (60%, dispersed in mineral oil, 500 mg, 12.5 mmol, 1.1 eq.) was suspended in dry THF (15 mL) and the resulting suspension was cooled to 0 °C. 2-Mesitylprop-2-en-1-ol (**MesOH**, 2.01 g, 11.4 mmol, 1.0 eq.) dissolved in dry THF (5 mL) was added dropwise and the reaction mixture was stirred at this temperature for 30 minutes. At 0 °C, benzyl bromide (1.5 mL, 12.5 mmol, 1.1 eq.) was added and the reaction mixture was stirred at room temperature for 1.5 hours. The reaction was quenched with water (50 mL), the layers were separated, and the aqueous layer was extracted with diethyl ether (3 x 100 mL). The combined organic layers were dried over anhydrous sodium sulfate, filtered and concentrated under reduced pressure. The crude product was purified by gradient flash column chromatography (SiO_2, neat pentane then pentane/diethyl ether 30:1) to afford 2-(3-(benzyloxy)prop-1-en-2-yl)-1,3,5-trimethylbenzene (**7-SM**, 2.10 g, 7.88 mmol, 69%) as a colorless liquid.

$C_{19}H_{22}O$ (266 g/mol):

^{1}H-NMR (400 MHz, 298 K, $CDCl_3$, δ/ppm): 7.39-7.32 (m, 4H), 7.31-7.26 (m, 1H), 6.86 (s, 2H), 5.57 (pseudo-q, *J* = 1.8 Hz, 1H), 4.92-4.90 (m, 1H), 4.57 (s, 2H), 4.06 (*t*, J = 1.5 Hz, 2H), 2.23 (s, 3H), 2.17 (s, 6H).

^{13}C-{^{1}H}-NMR (126 MHz, 298 K, CD_3CN, δ/ppm): 146.8, 139.7, 137.5, 137.4, 136.5, 129.3, 128.9, 128.4, 128.4, 114.3, 73.2, 73.1, 21.0, 19.9.

GC (achiral phase, 62.7 kPa He, method A): t_R = 5.96 min.

GC-MS (EI, 70 eV) *m/z* (%): 266 (4, M^+), 235 (9), 175 (16), 160 (100), 157 (54), 145 (69), 129 (35), 120 (27), 115 (22), 105 (21), 91 (75), 77 (11), 65 (16).

(((2-Cyclohexylallyl)oxy)methyl)benzene (10-SM)

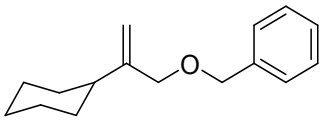

Sodium hydride (60%, dispersed in mineral oil, 420 mg, 10.5 mmol, 1.1 eq.) was suspended in dry THF (15 mL) and the resulting suspension was cooled to 0 °C. 2-Cyclohexylprop-2-en-1-ol (**CyOH**, 1.33 g, 9.48 mmol, 1.0 eq.) dissolved in dry THF (2.5 mL) was added dropwise. The reaction mixture was stirred at this temperature for 30 minutes. At 0 °C, benzyl bromide (1.25 mL, 10.4 mmol, 1.1 eq.) was added and the reaction mixture was stirred at room temperature for 5 days. At 0 °C, the reaction was quenched with water (50 mL), the layers were separated, and the aqueous layer was extracted with diethyl ether (3 x 100 mL). The combined organic layers were dried over anhydrous sodium sulfate, filtered and concentrated under reduced pressure. The crude product was purified by gradient flash column chromatography (SiO_2, neat pentane then pentane/diethyl ether 10:1) to afford (((cyclohexylallyl)oxy)methyl)benzene (**10-SM**, 1.77 g, 7.68 mmol, 81%) as a colorless liquid.

$C_{16}H_{22}O$ (230 g/mol):

^{1}H-NMR (400 MHz, 298 K, CD_3CN, δ/ppm): 7.39-7.32 (m, 4H), 7.31-7.26 (m, 1H), 5.00 (pseudo-q, *J* = 1.6 Hz, 1H), 4.91-4.89 (m, 1H), 4.46 (s, 2H), 3.99 (s, 2H), 2.03-1.95 (m, 1H), 1.82-1.73 (m, 4H), 1.71-1.64 (m, 1H), 1.35-1.12 (m, 5H).

^{13}C-{^{1}H}-NMR (126 MHz, 298 K, CD_3CN, δ/ppm): 152.9, 139.9, 129.3, 128.6, 128.4, 109.9, 73.1, 72.6, 42.1, 33.1, 27.5, 27.1.

GC (achiral phase, 62.7 kPa He, method B): t_R = 8.43 min.

GC-MS (EI, 70 eV) *m/z* (%): 124 (29), 104 (8), 91 (100), 67 (22), 79 (19), 55 (14).

((2-Methylallyloxy)methyl)benzene (11-SM)

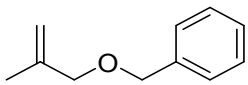

Sodium hydride (60%, dispersed in mineral oil, 1.22 g, 30.5 mmol, 1.1 eq.) was suspended in dry THF (50 mL) and the resulting suspension was cooled to 0 °C. 2-Methylprop-2-en-1-ol (1.96 g, 27.2 mmol, 1.0 eq.) was added and the reaction mixture was stirred at this temperature for 1 hour. At 0 °C, benzyl bromide (3.6 mL, 30.3 mmol, 1.1 eq.) was added dropwise and the reaction was stirred at room temperature for 4 hours. The reaction was quenched with water (50 mL), the layers were separated, and the aqueous layer was extracted with diethyl ether (3 x 100 mL). The combined organic layers were dried over anhydrous sodium sulfate, filtered and concentrated under reduced pressure. The crude product was purified by gradient flash column chromatography (SiO_2, neat pentane then pentane/diethyl ether 30:1) to afford ((2-methylallyloxy)methyl)benzene (**11-SM**, 3.92 g, 24.2 mmol, 89%) as a colorless liquid. Analytical data matches the literature.[10]

$C_{11}H_{14}O$ (162 g/mol):

^{1}H-NMR (400 MHz, 298 K, $CDCl_3$, δ/ppm): 7.38-7.27 (m, 5H), 5.01 (s, 1H), 4.93 (s, 1H), 4.50 (s, 2H), 3.94 (s, 2H), 1.78 (s, 3H).

^{13}C-{^{1}H}-NMR (101 MHz, 298 K, $CDCl_3$, δ/ppm): 142.4, 138.6, 128.5, 127.8, 127.7, 112.5, 74.3, 72.0, 19.7.

GC (achiral phase, 62.7 kPa He, method A): t_R = 3.85 min.

GC-MS (EI, 70 eV) *m/z* (%): 118 (9), 107 (44), 91 (100), 79 (12), 65 (17), 55 (6).

2.2.2 Synthesis of terminal olefins

Table S3. Synthesis of terminal olefins (2-SM to 5-SM) in a Wittig reaction.

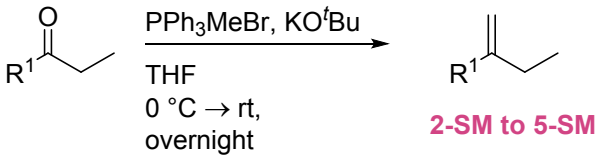

2-SM to 5-SM

Terminal Olefin	R^1	Yield / %
2-SM	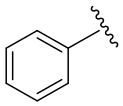	86
3-SM	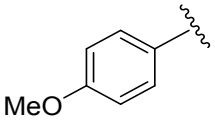	92
4-SM	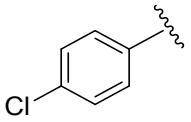	92
5-SM	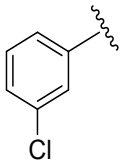	68

General procedure A: Wittig reaction for the synthesis of terminal olefins

Methyltriphenylphosphonium bromide (3.0 eq.) was suspended in dry THF (5 mL per mmol ketone) under a nitrogen atmosphere. At 0 °C, potassium *tert*-butoxide (3.0 eq.) was added and the resulting yellow suspension was stirred at this temperature for 30 minutes. The desired ketone (1.0 eq.) was added at 0 °C and the reaction mixture was stirred at room temperature overnight. The reaction was quenched with water (5 mL per mmol ketone), the layers were separated, and the aqueous layer was extracted with diethyl ether (3 x 10 mL per mmol ketone). The combined organic layers were dried over anhydrous sodium sulfate, filtered and concentrated under reduced pressure. The crude product was purified by flash column chromatography.

But-1-en-2-ylbenzene (2-SM)

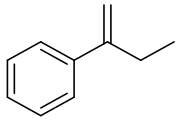

According to general procedure A, methyltriphenylphosphonium bromide (16.1 g, 45.0 mmol, 3.0 eq.) and potassium *tert*-butoxide (5.10 g, 45.5 mmol, 3.0 eq.) in dry THF (75 mL) were stirred at 0 °C for 30 minutes. After the addition of 1-phenyl-propan-1-one (2.00 g, 15.0 mmol, 1.0 eq.), the reaction was stirred at room temperature overnight. The crude product was purified by flash column chromatography (SiO_2, pentane/ethyl acetate 10:1) to afford but-1-en-2-ylbenzene (**2-SM**, 1.70 g, 12.9 mmol, 86%) as a colorless liquid. Analytical data matches the literature.[11]

$C_{10}H_{12}$ (132 g/mol):

^{1}H-NMR (400 MHz, 298 K, $CDCl_3$, δ/ppm): 7.44-7.39 (m, 2H), 7.35-7.30 (m, 2H), 7.28-7.23 (m, 1H), 5.27 (s, 1H), 5.06 (pseudo-q, *J* = 1.5 Hz, 1H), 2.52 (q, *J* = 7.4 Hz, 2H), 1.11 (t, *J* = 7.4 Hz, 3H).

^{13}C-{^{1}H}-NMR (101 MHz, 298 K, $CDCl_3$, δ/ppm): 150.2, 141.7, 128.4, 127.4, 126.2, 111.1, 28.2, 13.1.

GC (achiral phase, 62.7 kPa He, method A): t_R = 3.03 min.

GC-MS (EI, 70 eV) *m/z* (%): 132 (82, M^+), 117 (100), 103 (43), 91 (29), 77 (30), 65 (10), 51 (21).

1-(But-1-en-2-yl)-4-methoxybenzene (3-SM)

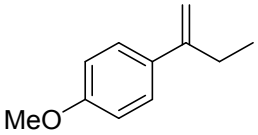

According to general procedure A, methyltriphenylphosphonium bromide (16.1 g, 45.0 mmol, 3.0 eq.) and potassium *tert*-butoxide (5.10 g, 45.5 mmol, 3.0 eq.) in dry THF (75 mL) were stirred at 0 °C for 2 h. After the addition of 1-(4-methoxyphenyl)propan-1-one (2.46 g, 15.0 mmol, 1.0 eq.), the reaction was stirred at room temperature overnight. The crude product was purified by flash column chromatography (SiO_2, pentane/ethyl acetate 10:1) to afford 1-(but-1-en-2-yl)-4-methoxybenzene (**3-SM**, 2.24 g, 13.8 mmol, 92%) as a colorless liquid. Analytical data matches the literature.[12]

$C_{11}H_{14}O$ (162 g/mol):

^{1}H-NMR (400 MHz, 298 K, CD_3CN, δ/ppm): 7.42-7.37 (m, 2H), 6.92-6.86 (m, 2H), 5.22 (s, 1H), 4.99 (pseudo-q, *J* = 1.4 Hz, 1H), 3.79 (s, 3H), 2.50 (q, *J* = 7.4 Hz, 2H), 1.07 (t, *J* = 7.4 Hz, 3H).

^{13}C-{^{1}H}-NMR (126 MHz, 298 K, CD_3CN, δ/ppm): 160.2, 150.4, 134.4, 128.0, 1114.6, 109.8, 55.9, 28.6, 13.5.

GC (achiral phase, 62.7 kPa He, method A): t_R = 4.21 min.

GC-MS (EI, 70 eV) *m/z* (%): 162 (100, M^+), 147 (64), 133 (88), 103 (16), 91 (37), 77 (22), 63 (12).

1-(But-1-en-2-yl)-4-chlorobenzene (4-SM)

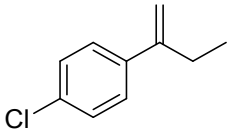

According to general procedure A, methyltriphenylphosphonium bromide (16.1 g, 45.0 mmol, 3.0 eq.) and potassium *tert*-butoxide (5.10 g, 45.5 mmol, 3.0 eq.) in dry THF (75 mL) were stirred at 0 °C for 30 minutes. After the addition of 1-(4-chlorophenyl)propan-1-one (2.54 g, 15.1 mmol, 1.0 eq.), the reaction was stirred at room temperature overnight. The crude product was purified by flash column chromatography (SiO_2, pentane/ethyl acetate 10:1) to afford 1-(but-1-en-2-yl)-4-chlorobenzene (**4-SM**, 2.32 g, 13.9 mmol, 92%) as a colorless liquid. Analytical data matches the literature.[12]

$C_{10}H_{11}Cl$ (167 g/mol):

^{1}H-NMR (400 MHz, 298 K, CD_3CN, δ/ppm): 7.48-7.39 (m, 2H), 7.39-7.30 (m, 2H), 5.31 (s, 1H), 5.12-5.10 (m, 1H), 2.50 (q, *J* = 7.4 Hz, 2H), 1.06 (t, *J* = 7.4 Hz, 3H).

^{13}C-{^{1}H}-NMR (126 MHz, 298 K, CD_3CN, δ/ppm): 150.0, 140.9, 133.6, 129.3, 128.5, 112.2, 28.5, 13.3.

GC (achiral phase, 62.7 kPa He, method A): t_R = 3.93 min.

GC-MS (EI, 70 eV) *m/z* (%): 166 (88, M^+), 151 (46), 131 (100), 115 (65), 102 (40), 91 (28), 75 (26), 63 (13).

1-(But-1-en-2-yl)-3-chlorobenzene (5-SM)

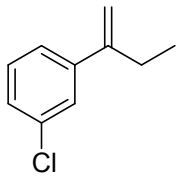

According to general procedure A, methyltriphenylphosphonium bromide (16.1 g, 45.0 mmol, 3.0 eq.) and potassium *tert*-butoxide (5.10 g, 45.5 mmol, 3.0 eq.) in dry THF (75 mL) were stirred at 0 °C for 2 h.

After the addition of 1-(3-chlorophenyl)propan-1-one (2.53 g, 15.0 mmol, 1.0 eq.), the reaction was stirred at room temperature overnight. The crude product was purified by flash column chromatography (SiO_2, pentane/ethyl acetate 10:1) to afford 1-(but-1-en-2-yl)-3-chlorobenzene (**5-SM**, 10.2 mmol, 1.70 g, 68%) as a colorless liquid. Analytical data matches the literature.[12]

$C_{10}H_{11}Cl$ (167 g/mol):

^{1}H-NMR (400 MHz, 298 K, $CDCl_3$, δ/ppm): 7.46 (s, 1H), 7.40-7.19 (m, 3H), 5.33 (s, 1H), 5.13 (s, 1H), 2.50 (q, *J* = 7.4 Hz, 2H), 1.07 (t, *J* = 7.4 Hz, 3H).

^{13}C-{^{1}H}-NMR (126 MHz, 298 K, $CDCl_3$, δ/ppm): 150.0, 144.4, 134.8, 130.9, 128.2, 126.9, 125.5, 112.9, 28.5, 13.2.

GC (achiral phase, 62.7 kPa He, method A): t_R = 3.89 min.

GC-MS (EI, 70 eV) *m/z* (%): 166 (72, M^+), 151 (23), 131 (100), 115 (57), 91 (36), 75 (22), 63 (12).

2.2.3 Synthesis of 9-SM

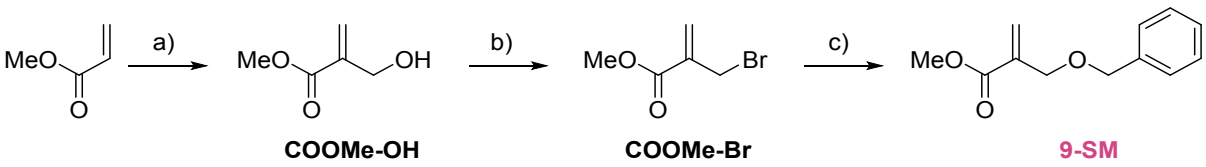

Scheme S2. Synthesis of 9-SM: a) $(CH_2O)_n$, DABCO, dioxane/H_2O (1:1 *v:v*), rt, 4.5 h, quant.; b) PBr_3, Et_2O, rt, 3 h, 97%; c) benzyl alcohol, DABCO, THF, 70 °C, overnight, 78%.

Methyl 2-(hydroxymethyl)acrylate (COOMe-OH)

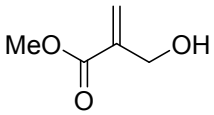

The synthesis of methyl 2-(hydroxymethyl)acrylate (**COOMe-OH**) was adapted from a previously published protocol.[13] Paraformaldehyde (10.2 g, 113 mmol, 1.0 eq.) and 1,4-diazabicyclo[2.2.2]octane (DABCO, 12.6 g, 112 mmol, 1.0 eq.) were suspended in a dioxane/H_2O mixture (20 mL, 1:1 *v:v*). Methyl acrylate (30 mL, 336 mmol, 3.0 eq.) was added and the reaction mixture was stirred at room temperature for 4.5 hours, resulting in full dissolution of the reagents. Water (50 mL) and diethyl ether (50 mL) were added, the layers were separated, and the aqueous layer was extracted with diethyl ether (2 x 100 mL). The combined organic layers were dried over anhydrous sodium sulfate, filtered and concentrated under reduced pressure. The crude product was purified by

gradient flash column chromatography (SiO_2, cyclohexane/ethyl acetate 5:1 then neat ethyl acetate) to afford the product (**COOMe-OH**, 13.1 g, 113 mmol, quant.) as a colorless liquid. Analytical data matches the literature.[14]

$C_5H_8O_3$ (116 g/mol):

^{1}H-NMR (400 MHz, 298 K, $CDCl_3$, δ/ppm): 6.04 (pseudo-q, *J* = 1.4 Hz, 1H), 5.67 (pseudo-q, *J* = 1.6 Hz, 1H), 4.09 (s, 2H), 3.86 (br s, 1H), 3.55 (s, 3H).

^{13}C-{^{1}H}-NMR (101 MHz, 298 K, $CDCl_3$, δ/ppm): 166.4, 139.3, 124.8, 60.9, 51.5.

Methyl 2-(bromomethyl)acrylate (COOMe-Br)

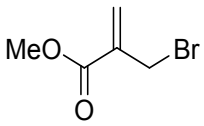

The synthesis of methyl 2-(bromomethyl)acrylate (**COOMe-Br**) was adapted from a previously published protocol.[13] Methyl 2-(hydroxymethyl)acrylate (**COOMe-OH**, 13.0 g, 113 mmol, 1.0 eq.) was dissolved in dry diethyl ether (150 mL) and the solution was cooled to 0 °C. PBr_3 (5.5 mL, 58.5 mmol, 0.5 eq.) was added dropwise and the reaction mixture was stirred at room temperature for 3 hours. At 0 °C, the reaction was quenched with water (50 mL), the layers were separated, and the aqueous layer was extracted with diethyl ether (3 x 100 mL). The combined organic layers were dried over anhydrous sodium sulfate, filtered and concentrated under reduced pressure to afford the product (**COOMe-Br**, 19.7 g, 110 mmol, 97%) as a yellow liquid. Analytical data matches the literature.[14]

$C_5H_7O_2Br$ (179 g/mol):

^{1}H-NMR (400 MHz, 298 K, $CDCl_3$, δ/ppm): 6.34 (d, *J* = 0.7 Hz, 1H), 5.96 (pseudo-q, *J* = 0.9 Hz, 1H), 4.18 (d, *J* = 1.0 Hz, 2H), 3.82 (s, 3H).

^{13}C-{^{1}H}-NMR (101 MHz, 298 K, $CDCl_3$, δ/ppm): 165.4, 137.4, 129.4, 52.4, 29.4.

Methyl 2-((benzyloxy)methyl)acrylate (9-SM)

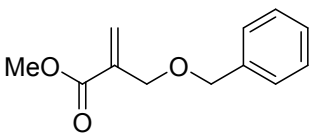

The synthesis of methyl 2-((benzyloxy)methyl)acrylate (**9-SM**) was adapted from a previously published protocol.[15] Methyl 2-(bromomethyl)acrylate (**COOMe-Br**, 5.03 g, 28.1 mmol, 1.0 eq.) and benzyl alcohol (5.2 mL, 50.0 mmol, 1.8 eq.) were dissolved in dry THF (5.0 mL) and the solution was cooled to 0 °C. A solution of 1,4-diazabicyclo[2.2.2]octane (4.62 g, 41.2 mmol, 1.5 eq.) dissolved in THF (30 mL) was added dropwise and the resulting white suspension was heated to 70 °C overnight. The suspension was filtered and the residue was washed with diethyl ether. The filtrate was washed with aq. HCl solution (0.5 M, 50 mL), sat. aq. $NHCO_3$ solution (50 mL) and brine (50 mL). The layers were separated, and the organic layer was dried over anhydrous sodium sulfate, filtered and concentrated under reduced pressure. The crude product was purified by flash column chromatography (SiO_2, neat DCM) to afford the product (**9-SM**, 4.49 g, 21.8 mmol, 78%) as a colorless liquid. Analytical data matches the literature.[15]

$C_{12}H_{14}O_3$ (206 g/mol):

^{1}H-NMR (500 MHz, 298 K, CD_3CN, δ/ppm): 7.39-7.33 (m, 4H), 7.33-7.28 (m, 1H), 6.23 (pseudo-q, *J* = 1.3 Hz, 1H), 5.89 (pseudo-q, *J* = 1.7 Hz, 1H), 4.55 (s, 2H), 4.21 (pseudo-t, *J* = 1.5 Hz, 2H), 3.72 (s, 3H).

^{13}C-{^{1}H}-NMR (126 MHz, 298 K, CD_3CN, δ/ppm): 167.1, 139.5, 138.7, 129.3, 128.6, 128.5, 126.3, 73.2, 69.2, 52.3.

GC (achiral phase, 62.7 kPa He, method A): t_R = 4.99 min.

GC-MS (EI, 70 eV) *m/z* (%): 107 (79), 100 (51), 91 (100), 83 (14), 79 (28), 77 (19), 69 (28), 65 (23).

2.3 Synthesis of hydrogenation products

Table S4. Synthesis of the different hydrogenation products (**1-H** to **5-H** and **9-H** to **12-H**) as a reference for ^{1}H-NMR and GC-MS analysis. Hydrogenation products **6-H** and **8-H** were obtained from commercial sources.

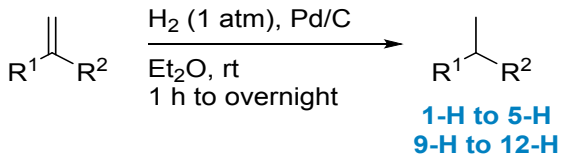

Hydrogenation Product	R^1	R^2	Yield / %
1-H	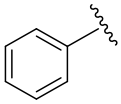	CH_2OMe	94
2-H	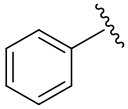	Et	94
3-H	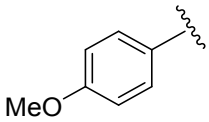	Et	96
4-H	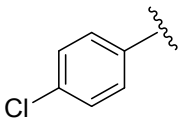	Et	94
5-H	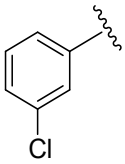	Et	92
9-H	COOMe	CH_2OBn	56
10-H		CH_2OBn	46
11-H	Me	CH_2OBn	89
12-H	H	OBn	74

General procedure B: Hydrogenation of terminal olefins

The terminal olefin was dissolved in dry diethyl ether (3.5 mL per mmol olefin) and Pd/C (10% Pd basis, 10% *w:w* with respect to the terminal olefin) was added. The reaction mixture was stirred under hydrogen atmosphere (1 atm) for several hours. The suspension was filtered over Celite and the filtrate was concentrated under reduced pressure to afford the hydrogenation product. If necessary, the crude product was further purified by flash column chromatography.

2-Phenyl-1-propyl methyl ether (1-H)

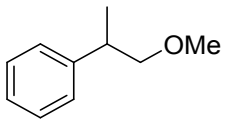

2-Phenyl-1-propyl methyl ether (**1-H**) was synthesized according to general procedure B. (3-Methoxyprop-1-en-2-yl)benzene (**1-SM**, 510 mg, 3.44 mmol, 1.0 eq.) and Pd/C (10% Pd basis, 50.9 mg) in diethyl ether (10 mL) were stirred under hydrogen atmosphere (1 atm) for 4 hours. 2-Phenyl-1-propyl methyl ether (**1-H**, 488 mg, 3.25 mmol, 94%) was obtained as a colorless liquid. Analytical data matches the literature.[16]

$C_{10}H_{14}O$ (150 g/mol):

^{1}H-NMR (400 MHz, 298 K, $CDCl_3$, δ/ppm): 7.34-7.28 (m, 2H), 7.25-7.19 (m, 3H) 3.55-3.40 (m, 2H), 3.34 (s, 3H), 3.03 (sext., *J* = 7.0 Hz, 1H), 1.29 (d, *J* = 7.0 Hz, 3H).

^{13}C-{^{1}H}-NMR (101 MHz, 298 K, CD_3CN, δ/ppm): 146.0, 129.2, 128.3, 127.1, 79.0, 58.7, 40.6, 18.7.

GC (achiral phase, 62.7 kPa He, method A): t_R = 3.53 min.

GC-MS (EI, 70 eV) *m/z* (%): 150 (14, M^+), 118 (6), 105 (100), 91 (7), 79 (14).

***sec*-Butylbenzene (2-H)**

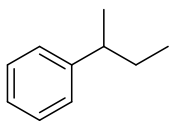

sec-Butylbenzene (**2-H**) was synthesized according to general procedure B. But-1-en-2-ylbenzene (**2-SM**, 998 mg, 7.55 mmol, 1.0 eq.) and Pd/C (10% Pd basis, 100 mg) in diethyl ether (20 mL) were stirred under hydrogen atmosphere (1 atm) for 3 hours. *sec*-Butylbenzene (**2-H**, 955 mg, 7.13 mmol, 94%) was obtained as a colorless liquid. Analytical data matches the literature.[17]

$C_{10}H_{14}$ (134 g/mol):

^{1}H-NMR (400 MHz, 298 K, CD_3CN, δ/ppm): 7.32-7.26 (m, 2H), 7.23-7.15 (m, 3H), 2.61 (sext., *J* = 7.0 Hz, 1H), 1.60 (pent., *J* = 7.3 Hz, 2H), 1.22 (d, *J* = 7.0 Hz, 3H), 0.80 (t, *J* = 7.3 Hz, 3H).

^{13}C-{^{1}H}-NMR (101 MHz, 298 K, CD_3CN, δ/ppm): 148.7, 129.3, 128.0, 126.8, 42.4, 31.8, 22.3, 12.6.

GC (achiral phase, 62.7 kPa He, method A): t_R = 2.82 min.

GC-MS (EI, 70 eV) *m/z* (%): 134 (25, M^+), 105 (100), 91 (18), 77 (14).

1-(*sec*-Butyl)-4-methoxybenzene (3-H)

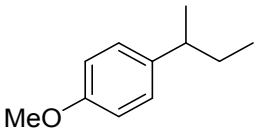

1-(*sec*-Butyl)-4-methoxybenzene (**3-H**) was synthesized according to general procedure B. 1-(But-1-en-2-yl)-4-methoxybenzene (**3-SM**, 998 mg, 6.15 mmol, 1.0 eq.) and Pd/C (10% Pd basis, 100 mg) in diethyl ether (20 mL) were stirred under hydrogen atmosphere (1 atm) for 5 hours. 1-(*sec*-Butyl)-4-methoxybenzene (**3-H**, 967 mg, 5.89 mmol, 96%) was obtained as a colorless liquid. Analytical data matches the literature.[12]

$C_{11}H_{16}O$ (164 g/mol):

^{1}H-NMR (400 MHz, 298 K, CD_3CN, δ/ppm): 7.17-7.08 (m, 2H), 6.89-6.81 (m, 2H), 3.75 (s, 3H), 2.62-2.48 (m, 1H), 1.62-1.49 (m, 2H), 1.19 (d, *J* = 7.0 Hz, 3H), 0.79 (t, *J* = 7.4 Hz, 3H).

^{13}C-{^{1}H}-NMR (126 MHz, 298 K, CD_3CN, δ/ppm): 158.8, 140.6, 128.8, 114.6, 55.8, 41.6, 32.0, 22.4, 12.6.

GC (achiral phase, 62.7 kPa He, method A): t_R = 3.98 min.

GC-MS (EI, 70 eV) *m/z* (%): 164 (18, M^+), 135 (100), 121 (11), 91 (14), 77 (10), 65 (6).

1-(*sec*-Butyl)-4-chlorobenzene (4-H)

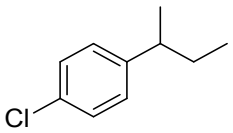

1-(*sec*-Butyl)-4-chlorobenzene (**4-H**) was synthesized according to general procedure B. 1-(But-1-en-2-yl)-4-chlorobenzene (**4-SM**, 998 mg, 5.99 mmol, 1.0 eq.) and Pd/C (10% Pd basis, 100 mg) in diethyl ether (20 mL) were stirred under hydrogen atmosphere (1 atm) for 5 hours. 1-(*sec*-Butyl)-4-chlorobenzene (**4-H**, 953 mg, 5.64 mmol, 94%) was obtained as a colorless liquid. Analytical data matches the literature.[12]

$C_{10}H_{13}Cl$ (169 g/mol):

^{1}H-NMR (400 MHz, 298 K, CD_3CN, δ/ppm): 7.32-7.27 (m, 2H), 7.21-7.17 (m, 2H), 2.61 (sext., *J* = 7.0 Hz, 1H), 1.65-1.49 (m, 2H), 1.20 (d, *J* = 7.0 Hz, 3H), 0.79 (t, *J* = 7.4 Hz, 3H).

^{13}C-{^{1}H}-NMR (126 MHz, 298 K, CD_3CN, δ/ppm): 147.6, 131.8, 129.7, 129.2, 41.8, 31.7, 22.1, 12.4.

GC (achiral phase, 62.7 kPa He, method A): t_R = 3.76 min.

GC-MS (EI, 70 eV) *m/z* (%): 168 (21, M^+), 141 (32), 139 (100), 125 (14), 103 (51), 77 (19).

1-(*sec*-Butyl)-3-chlorobenzene (5-H)

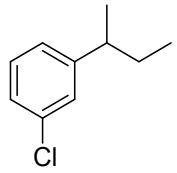

1-(*sec*-Butyl)-3-chlorobenzene (**5-H**) was synthesized according to general procedure B. 1-(But-1-en-2-yl)-3-chlorobenzene (**5-SM**, 998 mg, 5.99 mmol, 1.0 eq.) and Pd/C (10% Pd basis, 100 mg) in diethyl ether (20 mL) were stirred under hydrogen atmosphere (1 atm) for 5 hours. 1-(*sec*-Butyl)-3-chlorobenzene (**5-H**, 937 mg, 5.54 mmol, 92%) was obtained as a colorless liquid. Analytical data matches the literature.[12]

$C_{10}H_{13}Cl$ (169 g/mol):

^{1}H-NMR (400 MHz, 298 K, CD_3CN, δ/ppm): 7.31-7.13 (m, 4H), 2.62 (sext., *J* = 7.0 Hz, 1H), 1.64-1.54 (m, 2H), 1.21 (d, *J* = 7.0 Hz, 3H), 0.79 (t, *J* = 7.4 Hz, 3H).

^{13}C-{^{1}H}-NMR (126 MHz, 298 K, CD_3CN, δ/ppm): 150.8, 134.1, 130.5, 127.6, 126.4, 126.2, 41.8, 31.2, 21.6, 12.0.

GC (achiral phase, 62.7 kPa He, method A): t_R = 3.71 min.

GC-MS (EI, 70 eV) *m/z* (%): 168 (26, M^+), 141 (32), 139 (100), 125 (15), 103 (58), 91 (5), 77 (23).

Methyl 3-(benzyloxy)-2-methylpropanoate (9-H)

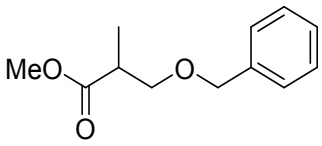

Methyl 3-(benzyloxy)-2-methylpropanoate (**9-H**) was synthesized according to general procedure B. Methyl 2-((benzyloxy)methyl)acrylate (**9-SM**, 994 mg, 4.82 mmol, 1.0 eq.) and Pd/C (10% Pd basis, 101 mg) in diethyl ether (15 mL) were stirred under hydrogen atmosphere (1 atm) for 3 h. The crude product was purified by gradient flash column chromatography (SiO_2, cyclohexane/ethyl acetate 20:1 then cyclohexane/ethyl acetate 5:1) to afford methyl 3-(benzyloxy)-2-methylpropanoate (**9-H**, 559 mg, 2.69 mmol, 56%) as a colorless liquid. Analytical data matches the literature.[18]

$C_{12}H_{16}O_3$ (208 g/mol):

^{1}H-NMR (500 MHz, 298 K, CD_3CN, δ/ppm): 7.43-7.17 (m, 5H), 4.47 (d, *J* = 1.9 Hz, 2H), 3.63 (s, 3H), 3.60 (dd, *J* = 9.2 Hz, 7.2 Hz, 1H), 3.52 (dd, *J* = 9.2 Hz, 5.5 Hz, 1H), 2.80-2.69 (m, 1H), 1.11 (d, *J* = 7.1 Hz, 3H).

^{13}C-{^{1}H}-NMR (126 MHz, 298 K, CD_3CN, δ/ppm): 157.6, 139.2, 128.9, 128.2, 128.1, 73.1, 72.6, 51.7, 40.5, 13.8.

GC (achiral phase, 62.7 kPa He, method A): t_R = 4.83 min.

GC-MS (EI, 70 eV) *m/z* (%): 121 (16), 107 (46), 102 (20), 91 (100), 87 (27), 79 (14), 65 (16).

((2-Cyclohexylpropoxy)methyl)benzene (10-H)

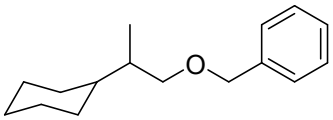

((2-Cyclohexylpropoxy)methyl)benzene (**10-H**) was synthesized according to general procedure B. (((2-Cyclohexylallyl)oxy)methyl)benzene (**10-SM**, 816 mg, 3.55 mmol, 1.0 eq.) and Pd/C (10% Pd basis, 88 mg) in diethyl ether (16 mL) were stirred under hydrogen atmosphere (1 atm) for 1.5 hours. The crude product was purified by gradient flash column chromatography (SiO_2, pentane/diethyl ether 10:1 then pentane/diethyl ether 3:1) to afford ((2-cyclohexylpropoxy)methyl)benzene (**10-H**, 379 mg, 1.63 mmol, 46%) as a colorless liquid. Analytical data matches the literature.[19]

$C_{16}H_{24}O$ (232 g/mol):

^{1}H-NMR (400 MHz, 298 K, CD_3CN, δ/ppm): 7.38-7.14 (m, 5H), 4.45 (s, 2H), 3.42 (dd, *J* = 9.2 Hz, 5.9 Hz, 1H), 3.28 (dd, *J* = 9.2 Hz, 6.7 Hz, 1H), 1.75-1.68 (m, 2H), 1.67-1.55 (m, 4H), 1.40-0.95 (m, 6H), 0.87 (d, *J* = 6.9 Hz, 3H).

^{13}C-{^{1}H}-NMR (101 MHz, 298 K, CD_3CN, δ/ppm): 140.2, 129.2, 128.5, 128.3, 74.6, 73.4, 40.7, 39.4, 31.6, 29.6, 27.6, 27.5, 27.4, 14.3.

GC (achiral phase, 62.7 kPa He, method B): t_R = 8.35 min.

GC-MS (EI, 70 eV) *m/z* (%): 124 (32), 111 (8), 91 (100), 81 (42), 69 (51), 55 (34).

Benzyl *iso*-butyl ether (11-H)

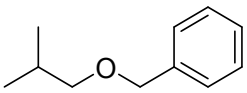

Benzyl *iso*-butyl ether (**11-H**) was synthesized according to general procedure B. ((2-Methylallyloxy)-methyl)benzene (**11-SM**, 1.01 g, 6.23 mmol, 1.0 eq.) and Pd/C (10% Pd basis, 92.5 mg) in diethyl ether (20 mL) were stirred under hydrogen atmosphere (1 atm) for 4 hours. Benzyl *iso*-butyl ether (**11-H**, 905 mg, 5.52 mmol, 89%) was obtained as a colorless liquid. Analytical data matches the literature.[20]

$C_{11}H_{16}O$ (164 g/mol):

^{1}H-NMR (400 MHz, 298 K, CD_3CN, δ/ppm): 7.36-7.33 (m, 4H), 7.31-7.27 (m, 1H), 4.51 (s, 2H), 3.25 (d, *J* = 6.7 Hz, 2H), 1.98-1.85 (m, 1H), 0.93 (d, *J* = 6.7 Hz, 6H).

^{13}C-{^{1}H}-NMR (126 MHz, 298 K, $CDCl_3$, δ/ppm): 140.2, 129.2, 128.5, 128.3, 77.9, 73.4, 29.3, 19.7.

GC (achiral phase, 62.7 kPa He, method A): t_R = 3.70 min.

GC-MS (EI, 70 eV) *m/z* (%): 91 (100), 65 (14).

Benzyl propyl ether (12-H)

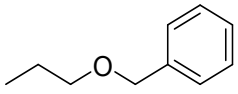

Benzyl propyl ether (**12-H**) was synthesized according to general procedure B. Benzyl allyl ether (**12-SM**, 514 mg, 3.47 mmol, 1.0 eq.) and Pd/C (10% Pd basis, 51.5 mg) in diethyl ether (10 mL) were stirred under hydrogen atmosphere (1 atm) for 4 hours. Benzyl propyl ether (**12-H**, 386 mg, 2.57 mmol, 74%) was obtained as a colorless liquid. Analytical data matches the literature.[21]

$C_{10}H_{14}O$ (150 g/mol):

^{1}H-NMR (298 K, $CDCl_3$, δ/ppm): 7.37-7.32 (m, 4H), 7.32-7.26 (m, 1H), 4.52 (s, 2H), 3.44 (t, *J* = 6.7 Hz, 2H), 1.72-1.58 (m, 2H), 0.95 (t, *J* = 7.4 Hz, 3H).

^{13}C-{^{1}H}-NMR (101 MHz, 298 K, $CDCl_3$, δ/ppm): 138.9, 128.5, 127.8, 127.6, 73.0, 72.3, 23.1, 10.8.

GC (achiral phase, 62.7 kPa He, method A): t_R = 3.47 min.

GC-MS (EI, 70 eV) *m/z* (%): 107 (11), 91 (100), 79 (16), 65 (17).

2.4 Synthesis of the radical clock substrate and reference products

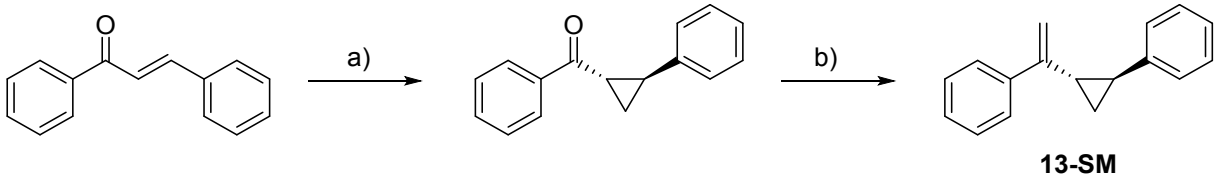

Scheme S3. Synthesis of the cyclopropane substrate (**13-SM**): a) Me_3SOI, NaH, DMSO, 0 °C → rt, 2 days, 76%; b) $MePPh_3Br$, KO^{t}Bu, THF, 0 °C → rt, overnight, 90%.

1-Benzoyl-2-phenylcyclopropane

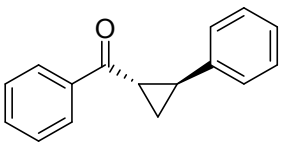

Sodium hydride (60%, dispersed in mineral oil, 1.15 g, 28.8 mmol, 1.2 eq.) and trimethylsulfoxonium iodide (5.88 g, 26.7 mmol, 1.1 eq.) were suspended in dry DMSO (40 mL). After the reaction mixture was cooled to 0 °C, (*E*)-chalcone (5.06 g, 24.3 mmol, 1.0 eq.) in dry DMSO (14 mL) was added and the reaction was stirred at room temperature for 2 days. The reaction was quenched with water (50 mL), the layers were separated, and the aqueous layer was extracted with diethyl ether (3 x 50 mL). The combined organic layers were dried over anhydrous sodium sulfate, filtered and concentrated under reduced pressure. The crude product was purified by flash column chromatography (SiO_2, pentane/diethyl ether 20:1) to afford 1-benzoyl-2-phenylcyclopropane (4.09 g, 18.4 mmol, 76%) as a colorless liquid. Analytical data matches the literature.[22]

$C_{16}H_{14}O$ (222 g/mol):

^{1}H-NMR (400 MHz, 298 K, $CDCl_3$, δ/ppm): 8.02-7.97 (m, 2H), 7.59-7.53 (m, 1H), 7.49-7.43 (m, 2H), 7.34-7.28 (m, 2H), 7.25-7.21 (m, 1H), 7.20-7.16 (m, 2H), 2.91 (ddd, *J* = 8.0 Hz, 5.3 Hz, 4.0 Hz, 1H), 2.70 (ddd,

J = 9.2 Hz, 6.6 Hz, 4.0 Hz, 1H), 1.93 (ddd, *J* = 9.2 Hz, 5.3 Hz, 4.1 Hz, 1H), 1.56 (ddd, *J* = 8.0 Hz, 6.6 Hz, 4.1 Hz, 1H).

^{13}C-{^{1}H}-NMR (101 MHz, 298 K, $CDCl_3$, δ/ppm): 198.7, 140.6, 137.9, 133.1, 128.7, 128.3, 126.7, 126.4, 30.2, 29.5, 19.4.

(*trans*)-(1-(2-Phenylcyclopropyl)vinyl)benzene (13-SM)

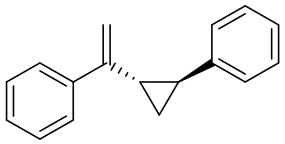

According to general procedure A, methyltriphenylphosphonium bromide (2.42 g, 6.77 mmol, 3.0 eq.) and potassium *tert*-butoxide (762 mg, 6.79 mmol, 3.0 eq.) in dry THF (11 mL) were stirred at 0 °C for 30 minutes. After addition of 1-benzoyl-2-phenylcyclopropane (497 mg, 2.23 mmol, 1.0 eq.) the reaction was stirred at room temperature overnight to afford a racemic mixture of *trans*-**13-SM**. The crude product was purified by flash column chromatography (SiO_2, neat cyclohexane) to afford (1-(2-phenylcyclopropyl)vinyl)benzene (**13-SM**, 444 mg, 2.02 mmol, 90%) as a colorless liquid. Analytical data matches the literature.[22]

$C_{17}H_{16}$ (220 g/mol):

^{1}H-NMR (400 MHz, 298 K, $CDCl_3$, δ/ppm): 7.54-7.49 (m, 2H), 7.34-7.25 (m, 5H), 7.22-7.14 (m, 3H), 5.37 (s, 1H), 5.05 (t, *J* = 1.1 Hz, 1H), 2.04-1.92 (m, 2H), 1.41 (ddd, *J* = 8.7 Hz, 6.2 Hz, 5.0 Hz, 1H), 1.28 (ddd, *J* = 8.5 Hz, 5.8 Hz, 5.0 Hz, 1H).

^{13}C-{^{1}H}-NMR (101 MHz, 298 K, $CDCl_3$, δ/ppm): 148.4, 142.7, 141.2, 128.6, 128.4, 127.7, 126.2, 125.9, 109.5, 28.0, 26.6, 16.0.

GC (achiral phase, 62.7 kPa He, method A): t_R = 5.70 min.

GC-MS (EI, 70 eV) *m/z* (%): 220 (50, M^+), 205 (34), 191 (8), 142 (74), 129 (100), 115 (49), 91 (41), 77 (28), 65 (11).

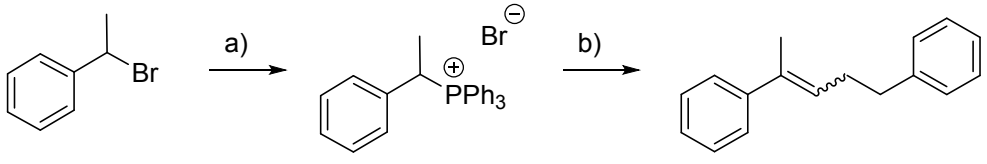

13-RO

Scheme S4. Synthesis of the ring-opened product (**13-RO**): a) PPh_3, toluene, reflux, 3 d, 91%; b) hydrocinnamaldehyde, *n*-BuLi, THF, −78 °C → 0 °C → rt, overnight, 36%.

(1-Phenethyl)triphenylphosphonium bromide

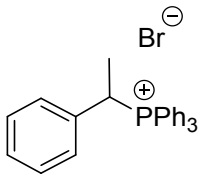

A solution of triphenylphosphane (1.50 g, 5.72 mmol, 1.1 eq.) in dry toluene (6 mL) was treated with (1-bromoethyl)benzene (0.74 mL, 5.42 mmol, 1.0 eq.) and the reaction mixture was stirred at reflux for 3 days. The resulting suspension was allowed to cool to room temperature. The white precipitate was collected by filtration, washed with toluene (10 mL) and dried *in vacuo* to afford (1-phenethyl)triphenylphosphonium bromide (2.20 g, 4.92 mmol, 91%) as a white solid. Analytical data matches the literature.[23]

$C_{26}H_{24}PBr$ (447 g/mol):

^{1}H-NMR (400 MHz, 298 K, $CDCl_3$, δ/ppm): 7.87-7.79 (m, 6H), 7.78-7.72 (m, 3H), 7.67-7.59 (m, 6H), 7.25-7.21 (m, 1H), 7.20-7.12 (m, 4H), 6.84 (dq, *J* = 14.3 Hz, *J* = 7.2 Hz, 1H), 1.82 (dd, *J* = 19.1 Hz, *J* = 7.2 Hz, 3H).

^{31}P-{^{1}H}-NMR (162 MHz, 298 K, $CDCl_3$, δ/ppm): 27.3.

^{13}C-{^{1}H}-NMR (101 MHz, 298 K, $CDCl_3$, δ/ppm): 134.9 (d, *J* = 3.0 Hz), 134.7 (d, *J* = 9.2 Hz), 133.5 (d, *J* = 5.5 Hz), 130.5 (d, *J* = 5.9 Hz), 130.2 (d, *J* = 12.2 Hz), 128.9 (d, *J* = 3.5 Hz), 128.8 (d, *J* = 2.6 Hz), 117.8 (d, *J* = 82.6 Hz), 35.0 (d, *J* = 42.9 Hz), 17.1 (d, *J* = 1.6 Hz).

Pent-3-ene-1,4-diyldibenzene (13-RO)

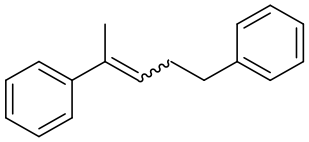

A suspension of (1-phenethyl)triphenylphosphonium bromide (917 mg, 2.05 mmol, 1.1 eq.) in dry THF (2 mL) was cooled to −78 °C. *n*-BuLi (2.5 M in hexanes, 0.93 mL, 2.33 mmol, 1.2 eq.) was added dropwise and the reaction mixture was stirred at 0 °C for 30 minutes. At 0 °C, a solution of hydrocinnamaldehyde (0.25 mL, 1.88 mmol, 1.0 eq.) in dry THF (1 mL) was added dropwise and the

reaction mixture was stirred at room temperature overnight. The reaction was quenched with aq. sat. NH_4Cl solution (5 mL), the layers were separated, and the aqueous layer was extracted with diethyl ether (3 x 10 mL). The combined organic layers were dried over anhydrous sodium sulfate, filtered and concentrated under reduced pressure. The crude product was purified and the isomers were separated by gradient flash column chromatography (SiO_2, neat cyclohexane then cyclohexane/ethyl acetate 10:1) to afford (*E*)-pent-3-ene-1,4-diyldibenzene (**(*E*)-13-RO**, 121 mg, 545 µmol, 29%) and (*Z*)-pent-3-ene-1,4-diyldibenzene (**(*Z*)-13-RO** 27.4 mg, 123 µmol, 6.5%) as colorless liquids. Analytical data matches the literature.[24]

$C_{17}H_{18}$ (222 g/mol):

(*E*)-Pent-3-ene-1,4-diyldibenzene

^{1}H-NMR (400 MHz, 298 K, $CDCl_3$, δ/ppm): δ 7.39-7.11 (m, 10H), 5.81 (tq, *J* = 7.1 Hz, 1.4 Hz, 1H), 2.81-2.72 (m, 2H), 2.52 (q, *J* = 7.5 Hz, 2H), 1.97 (q, *J* = 1.0 Hz, 3H).

^{13}C-{^{1}H}-NMR (101 MHz, 298 K, $CDCl_3$, δ/ppm): 144.0, 142.2, 135.6, 128.7, 128.5, 128.3, 127.5, 126.7, 126.0, 125.8, 36.0, 30.9, 15.9.

GC (achiral phase, 62.7 kPa He, method A): t_R = 5.73 min.

GC-MS (EI, 70 eV) *m/z* (%): 222 (6, M^+), 131 (100), 115 (10), 91 (37), 65 (6).

(*Z*)-Pent-3-ene-1,4-diyldibenzene

^{1}H-NMR (400 MHz, 298 K, $CDCl_3$, δ/ppm): 7.36-7.07 (m, 10H), 5.50 (tq, *J* = 7.3 Hz, 1.5 Hz, 1H), 2.64 (dd, *J* = 8.9 Hz, 6.7 Hz, 2H), 2.33-2.24 (m, 2H), 2.02 (q, *J* = 1.3 Hz, 3H).

^{13}C-{^{1}H}-NMR (101 MHz, 298 K, $CDCl_3$, δ/ppm): 142.2, 142.1, 137.1, 128.6, 128.4, 128.2, 128.0, 126.8, 126.6, 125.9, 36.5, 31.1, 25.7.

GC (achiral phase, 62.7 kPa He, method A): t_R = 5.46 min.

GC-MS (EI, 70 eV) *m/z* (%): 222 (7, M^+), 131 (100), 115 (11), 91 (39), 77 (5), 65 (6).

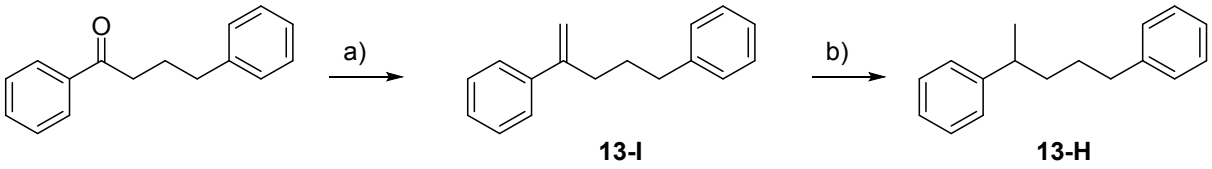

Scheme S5. Synthesis of the isomerization product (**13-I**) and the ring-opened hydrogenation product (**13-H**): a) PPh_3MeBr, KO^tBu, THF, 0 °C → rt, overnight, 91%; b) H_2 (1 atm), Pd/C, Et_2O, rt, 2 h, 97%.

Pent-4-ene-1,4-diyldibenzene (13-I)

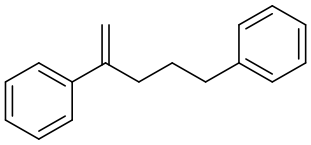

According to general procedure A, methyltriphenylphosphonium bromide (2.41 g, 6.75 mmol, 3.0 eq.) and potassium *tert*-butoxide (752 mg, 6.70 mmol, 3.0 eq.) in dry THF (10 mL) were stirred at 0 °C for 30 minutes. After the addition of 1,4-diphenylbutan-1-one (501 mg, 2.23 mmol, 1.0 eq.), the reaction was stirred at room temperature overnight. The crude product was purified by flash column chromatography (SiO_2, neat petroleum ether) to afford pent-4-ene-1,4-diyldibenzene (**13-I**, 450 mg, 2.03 mmol, 91%) as a colorless liquid. Analytical data matches the literature.[25]

$C_{17}H_{18}$ (222 g/mol):

^{1}H-NMR (400 MHz, 298 K, $CDCl_3$, δ/ppm): 7.41-7.36 (m, 2H), 7.34-7.23 (m, 5H), 7.20-7.12 (m, 3H), 5.32-5.21 (m, 1H), 5.07 (pseudo-q, *J* = 1.4 Hz, 1H), 2.69-2.60 (m, 2H), 2.59-2.49 (m, 2H), 1.84-1.73 (m, 2H).

^{13}C-{^{1}H}-NMR (126 MHz, 298 K, CD_3CN, δ/ppm): 149.5, 143.5, 142.0, 129.3, 129.3, 129.2, 128.4, 127.0, 126.6, 113.0, 35.8, 35.3, 30.9.

GC (achiral phase, 62.7 kPa He, 100 °C, 35 °C/min, 200 °C, 100 °C/min, 350 °C): t_R = 5.64 min.

GC-MS (EI, 70 eV) *m/z* (%): 118 (100), 104 (29), 91 (20), 77 (12), 65 (7).

Pentane-1,4-diyldibenzene (13-H)

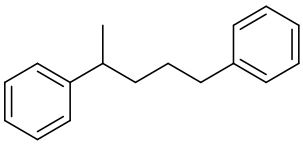

According to general procedure B, pent-4-ene-1,4-diyldibenzene (**13-I**, 221 mg, 994 µmol, 1.0 eq.) and Pd/C (10% Pd basis, 19 mg) in diethyl ether (4 mL) were stirred under hydrogen atmosphere for 2 hours. Pent-4-ene-1,4-diyldibenzene (**13-H**, 215 mg, 960 µmol, 97%) was obtained as a colorless liquid.

$C_{17}H_{20}$ (224 g/mol):

^{1}H-NMR (500 MHz, 298 K, CD_3CN, δ/ppm): 7.34-7.25 (m, 4H), 7.24-7.13 (m, 6H), 2.79-7.71 (m, 1H), 2.66-2.53 (m, 2H), 1.66-1.50 (m, 3H), 1.49-1.41 (m, 1H), 1.23 (d, *J* = 6.9 Hz, 3H).

^{13}C-{^{1}H}-NMR (126 MHz, 298 K, CD_3CN, δ/ppm): 148.7, 143.7, 129.3, 129.3, 129.2, 127.9, 126.8, 126.5, 40.4, 38.6, 36.3, 30.5, 22.6.

GC (achiral phase, 62.7 kPa He, method A): t_R = 5.54 min.

GC-MS (EI, 70 eV) *m/z* (%): 224 (20, M^+), 105 (100), 91 (25), 77 (9), 65 (6).

2.5 Synthesis of the deuterated substrate (1-SM-*d*$_4$)

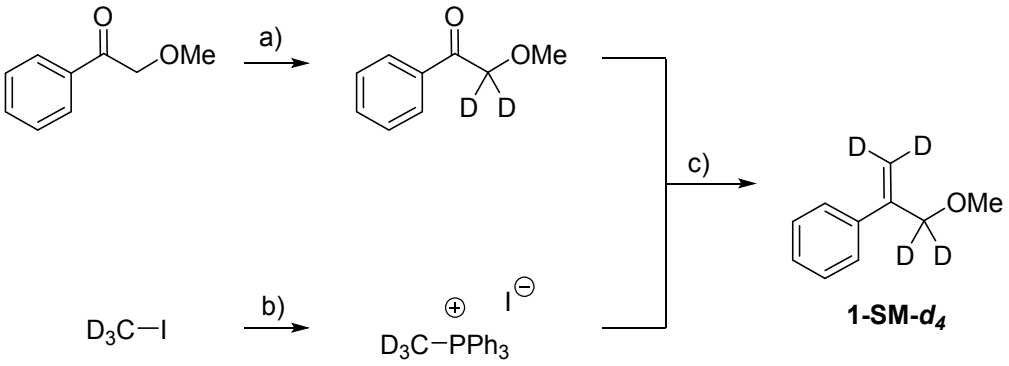

Scheme S6. Synthesis of the deuterated substrate **1-SM-*d*$_4$**: a) NaOH, D_2O, reflux, 1 h, 92%; b) PPh_3, THF, reflux, 45 min., quant.; c) KO^{t}Bu, THF, 0 °C → rt, overnight, 33%.

2-Methoxy-1-phenylethan-1-one-*2,2-d*$_2$

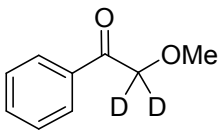

2-Methoxy-1-phenylethan-1-one (499 mg, 3.32 mmol, 1.0 eq.) and grinded NaOH (5.7 mg, 143 µmol, 0.04 eq.) were dissolved in D_2O and stirred under reflux for 1 hour. After cooling to rt, DCM (10 mL) was added, the layers were separated, and the aqueous layer was extracted with DCM (2 x 10 mL). The combined organic layers were dried over anhydrous sodium sulfate, filtered and concentrated under reduced pressure to afford 2-methoxy-1-phenylethan-1-one-*2,2-d*$_2$ (464 mg, 3.05 mmol, 92%, contains 4.1% of the monodeuterated product) as a yellow liquid. Analytical data matches the literature.[26]

$C_9H_8D_2O_2$ (152 g/mol):

^{1}H-NMR (400 MHz, 298 K, CD_3CN, δ/ppm): 7.94-7.89 (m, 2H), 7.67-7.60 (m, 1H), 7.54-7.48 (m, 2H), 3.41 (s, 3H).

^{13}C-{^{1}H}-NMR (101 MHz, 298 K, CD_3CN, δ/ppm): 197.6, 136.1, 134.3, 129.7, 128.6, 59.3.

The deuterated carbon atom is not visible in the ^{13}C-{^{1}H}-NMR spectrum.

(Methyl-*d*$_3$)triphenylphosphonium iodide

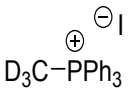

Triphenylphosphane (1.55 g, 5.91 mmol, 1.0 eq.) was dissolved in dry THF (7 mL). Iodomethane-*d*$_3$ (0.43 mL, 6.91 mmol, 1.2 eq.) was added and the reaction mixture was stirred at reflux for 45 minutes. The resulting white suspension was allowed to cool to room temperature. The white precipitate was collected by filtration, washed with toluene (10 mL) and dried *in vacuo* to afford (methyl-*d*$_3$)triphenylphosphonium iodide (2.41 g, 5.91 mmol, quant.) as a white solid. Analytical data matches the literature.[27]

$C_{19}H_{15}D_3PI$ (407 g/mol):

^{1}H-NMR (400 MHz, 298 K, $CDCl_3$, δ/ppm): 7.85-7.65 (m, 15H).

^{31}P-{^{1}H}-NMR (162 MHz, 298 K, $CDCl_3$, δ/ppm): 21.5.

^{13}C-{^{1}H}-NMR (101 MHz, 298 K, $CDCl_3$, δ/ppm): 135.4 (d, *J* = 2.9 Hz), 133.5 (d, *J* = 10.8 Hz), 130.6 (d, *J* = 12.9 Hz), 119.0 (d, *J* = 88.5 Hz).

The deuterated carbon atom is not visible in the ^{13}C-{^{1}H}-NMR spectrum.

(3-Methoxyprop-1-en-2-yl-*1,1,3,3-d*$_4$)benzene (1-SM-*d*$_4$)

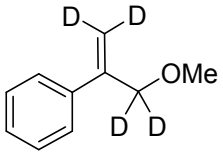

(Methyl-d_3)triphenylphosphonium iodide (2.76 g, 6.78 mmol, 2.5 eq.) was suspended in dry THF (20 mL). At 0 °C, potassium *tert*-butoxide (608 mg, 5.42 mmol, 2.0 eq) was added and the resulting yellow suspension was stirred at 0 °C for 30 minutes. 2-Methoxy-1-phenylethan-1-one-*2,2*-d_2 (412 mg, 2.71 mmol, 1.0 eq.) was added and the reaction mixture was stirred at room temperature overnight. The reaction was quenched with water (20 mL), the layers were separated, and the aqueous layer was extracted with diethyl ether (3 x 20 mL). The combined organic layers were dried over anhydrous sodium sulfate, filtered and concentrated under reduced pressure. The resulting crude product was purified by gradient flash column chromatography (SiO_2, cyclohexane/ethyl acetate 20:1 then cyclohexane/ethyl acetate 10:1) to afford (3-methoxyprop-1-en-2-yl-*1,1,3,3*-d_4)benzene (**1-SM-*d*$_4$**, 135 mg, 888 µmol, 33%, contains 6% of non-deuterated olefin) as a light yellow liquid.

$C_{10}H_8D_4O$ (152 g/mol):

^{1}H-NMR (500MHz, 298 K, CD_3CN, δ/ppm): 7.57-7.47 (m, 2H), 7.40-7.33 (m, 2H), 7.32-7.28 (m, 1H), 3.30 (s, 3H).

^{13}C-{^{1}H}-NMR (126 MHz, 298 K, CD_3CN, δ/ppm): 129.3, 128.7, 127.0, 57.9.

The deuterated and the quaternary carbon atoms are not visible in the ^{13}C-{^{1}H}-NMR spectrum.

GC-MS (EI, 70 eV) *m/z* (%): 152 (6), 151 (9), 122 (100), 109 (18), 105 (45), 78 (20), 51 (13).

2.6 Synthesis of the triarylamine donor

Tris(4-anisyl)amine (TAA-OMe)

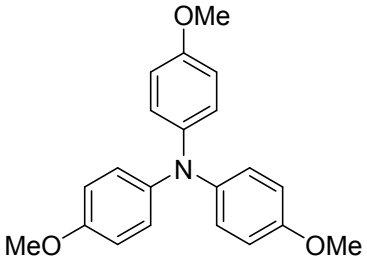

Tris(4-anisyl)amine was synthesized following a previously published protocol.[28] *p*-Anisidine (2.00 g, 16.2 mmol, 1.0 eq.), *p*-bromoanisole (9.09 g, 48.6 mmol, 3.0 eq.) and NaO^{t}Bu (3.89 g, 40.5 mmol, 2.5 eq.) were dissolved in dry toluene and the reaction mixture was degassed by bubbling N_2 through

the solution for 15 min. [$Pd_2(dba)_3$] (297 mg, 324 µmol, 2.0 mol%) and SPhos (333 mg, 810 µg, 5.0 mol%) were added and the reaction mixture was degassed for another 10 min. The suspension was heated at reflux for 3 days. After cooling to room temperature, the reaction mixture was filtered over Celite and washed with DCM. The filtrate was concentrated under reduced pressure and the crude product was purified by gradient flash column chromatography (SiO_2, pure pentane then pentane/ethyl acetate 9:1). The resulting yellow liquid was treated with *n*-hexane and the formed precipitate was collected by filtration. Recrystallization from *n*-hexane (150 mL) afforded tris(4-anisyl)amine (4.57 g, 13.6 mmol, 84%) as off-white needles. Analytical data matches the literature.[29]

^{1}H-NMR (500 MHz, 298 K, $CDCl_3$, δ/ppm): 6.97 (d, *J* = 7.1 Hz, 6H), 6.82-6.76 (m, 6H), 3.78 (s, 9H).

^{13}C-{^{1}H}-NMR (126 MHz, 298 K, $CDCl_3$, δ/ppm): 155.1, 142.2, 124.9, 114.6, 55.6.

3 Visible-light driven hydrogenation of unactivated olefins

3.1 General procedure and methods

General procedure C: Light-induced hydrogenation of olefins

The work-flow for the visible-light driven hydrogenation of olefins is depicted in Fig. S2. Degassed stock solutions of the substrate (150 µL, 500mM in CD_3CN, 75.0 µmol, 1.0 eq.), [Cp*Ir(phen)Cl]Cl (375 µL, 10 mM in CD_3CN, 3.75 µmol, 5.0 mol%), 1,10-phenanthroline (150 µL, 150 mM, 22.5 µmol, 30 mol%) and *tert*-butylbenzene (150 µL, 500 mM in CD_3CN, 75.0 µmol, 1.0 eq.) as an internal standard were combined and further diluted with degassed CD_3CN (675 µL). TEA (52 µL, 375 µmol, 5.0 eq.) was added and 0.5 mL of the reaction mixture were transferred to an NMR-tube. The reaction was then irradiated at 470 nm for 44 h, while the temperature was kept at 50 °C using an external thermostat (see section S1 for details about the home-built photoreactor). The conversion was determined both by ^{1}H-NMR spectroscopy (see section S3.1.1 for details) and GC-MS spectrometry (see section S3.1.2 for details). For GC-MS analysis, 200 µL of the reaction mixture were diluted with hexane (2.0 mL) and aq. HCl solution (0.5 M, 1.0 mL) was added. The layers were separated, and the organic layer was dried over anhydrous sodium sulfate, passed through a syringe filter and injected into the GC-MS spectrometer.

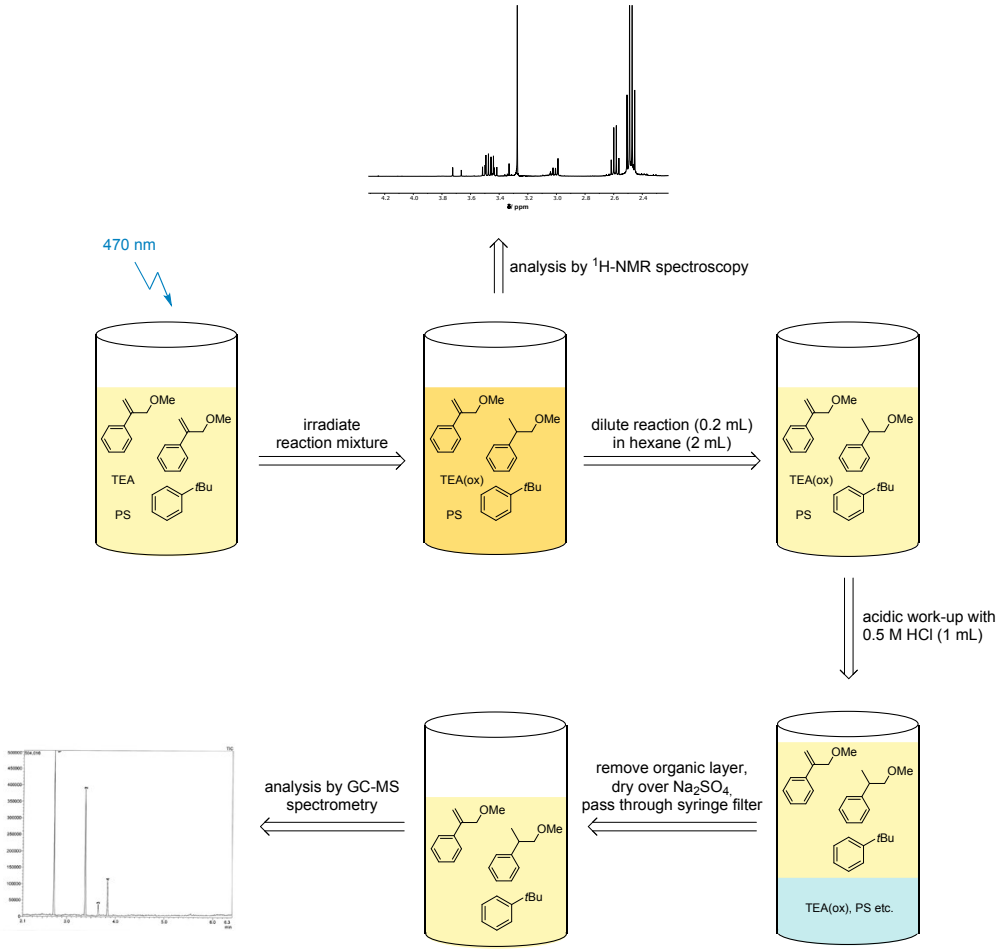

Figure S2. Typical work-flow for the light-induced hydrogenation of unactivated olefins catalyzed by iridium-hydrides. TEA(ox) stands for oxidation products of triethylamine. See text for further details.

3.1.1 Reaction monitoring based on ^{1}H-NMR spectroscopy

The reaction progress of the visible-light driven hydrogenation of olefins was monitored by ^{1}H-NMR spectroscopy. The conversion was determined by relative integration of the characteristic signals of each compound with respect to *tert*-butylbenzene (9H at 1.31 ppm in CD_3CN) as an internal standard. We estimate that the experimental uncertainty associated with this procedure is on the order of 10%.

3.1.2 Reaction monitoring based on GC-MS spectrometry

The NMR yield of the hydrogenation product was further confirmed by GS-MS spectrometry (see section S1 for instrumental details and methods). For this purpose, calibration curves were established for the different hydrogenation products (H) with respect to *tert*-butylbenzene as an internal standard (ISTD, t_R = 2.74 min.). To do so, the A_H/A_{ISTD} ratios were plotted against the c_H/c_{ISTD} ratios, where A is the area obtained in the GC trace and c is the concentration of the analytes. The slope and the intercept of the calibration curves were determined based on linear regression using equation S1.

$$\frac{A_H}{A_{ISTD}} = a + b\frac{c_H}{c_{ISTD}} \qquad \text{(eq. S1)}$$

The GC-MS yield of the hydrogenation product was determined based on relative integration of the GC-trace with respect to the area of the ISTD. The concentration of the hydrogenation product (c_H) was then determined by solving the linear equation S1 for C_H:

$$c_H = \frac{(A_H / A_{ISTD} - a)/b}{c_{ISTD}} \qquad \text{(eq. S2)}$$

3.2 Substrate scope

3.2.1 Light-driven hydrogenation of (3-methoxyprop-1-en-2-yl)benzene (1-SM)

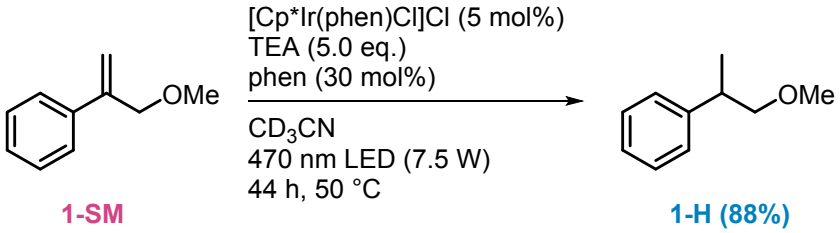

(3-Methoxyprop-1-en-2-yl)benzene (**1-SM**) was reduced to 2-phenyl-1-propyl methyl ether (**1-H**) according to general procedure C. Based on ^{1}H-NMR spectroscopy, the conversion of **1-SM** was determined to be 94%, affording **1-H** in 88% yield. Isomerization to (1-methoxyprop-1-en-2-yl)benzene (**1-R**) was observed in minor amounts (6%). The formation of 2-phenyl-1-propyl methyl ether (**1-H**) was further confirmed by GC-MS spectrometry (90% formation of hydrogenation product **1-H** with respect to *tert*-butylbenzene as an internal standard).

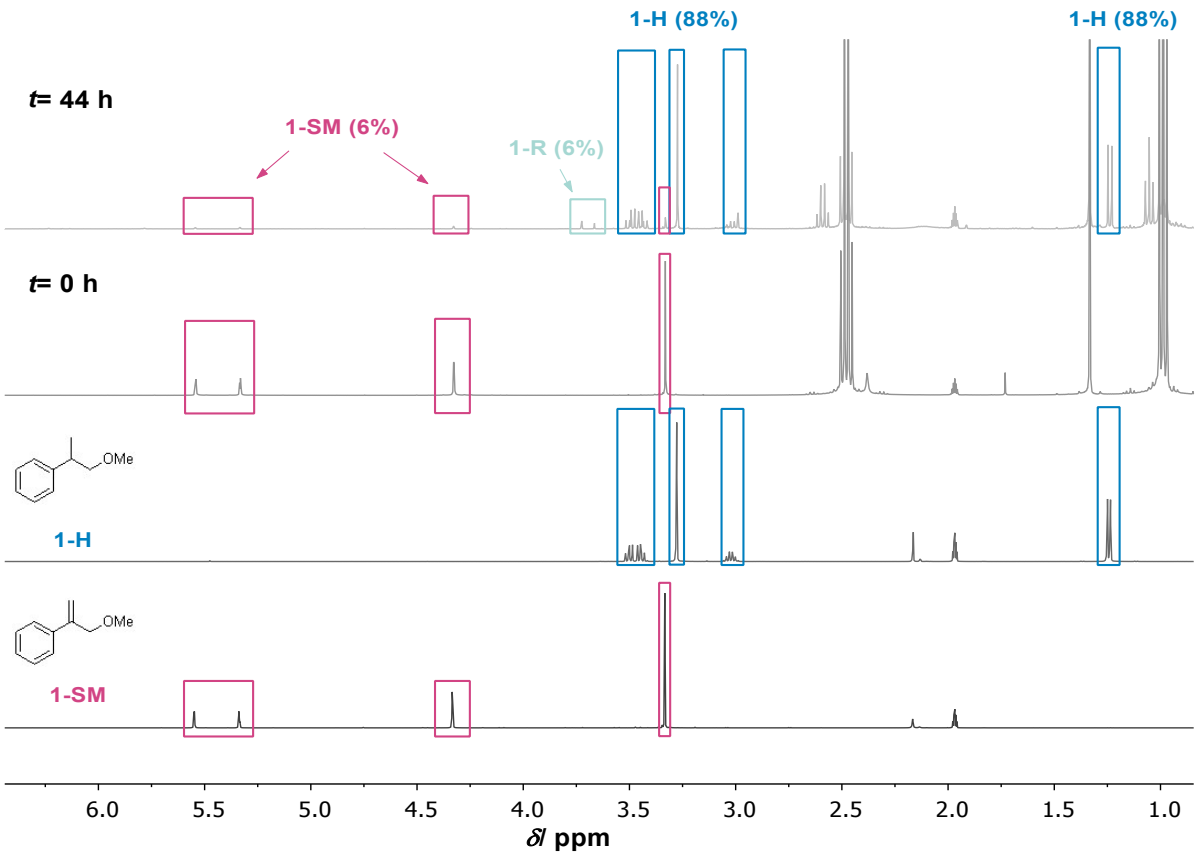

Figure S3. ^{1}H-NMR spectra for the light-driven hydrogenation of (3-methoxyprop-1-en-2-yl)benzene (**1-SM**) in CD_3CN: The ^{1}H-NMR spectra of the reaction mixture before (t = 0 h) and after (t = 44 h) irradiation are shown in comparison to the ^{1}H-NMR spectra of neat (3-methoxyprop-1-en-2-yl)benzene (**1-SM**) and 2-phenyl-1-propyl methyl ether (**1-H**). The triplet at 1.02 ppm and the quartet at 2.56 ppm in the top spectrum are due to diethylamine resulting from TEA oxidation.

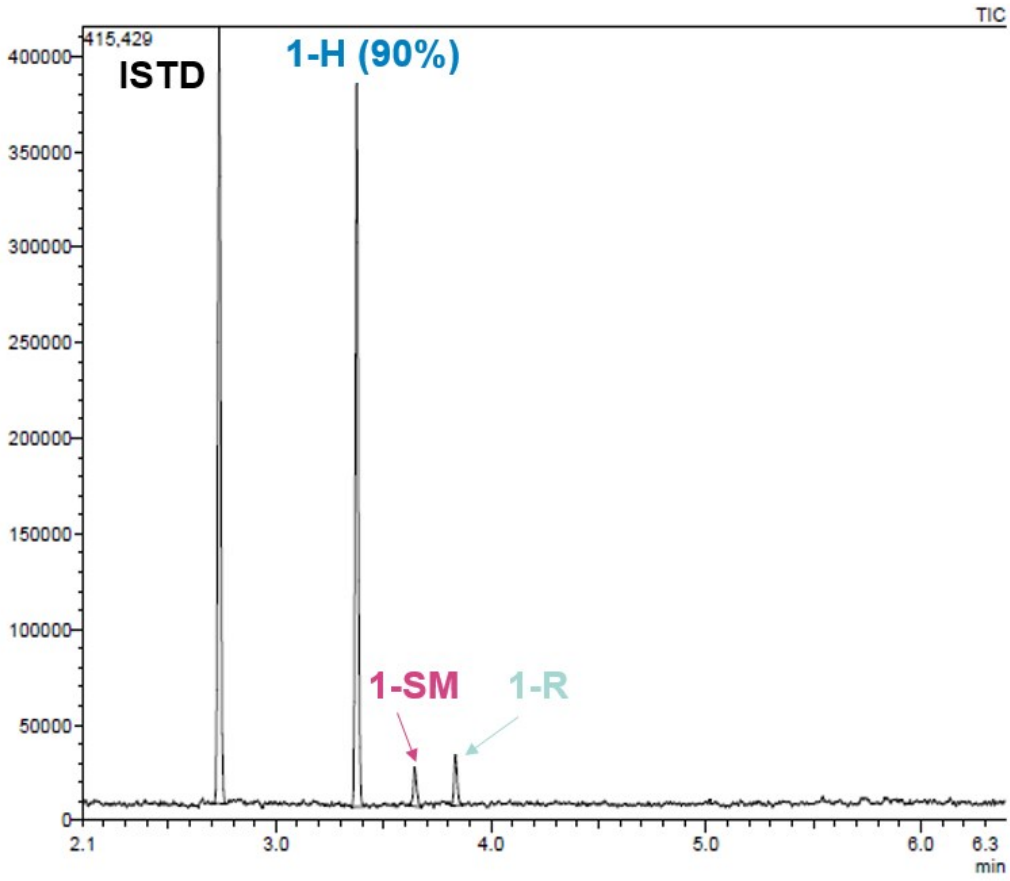

Figure S4. GC-MS trace of the light-induced hydrogenation of (3-methoxyprop-1-en-2-yl)benzene (**1-SM**) to afford 2-phenyl-1-propyl methyl ether (**1-H**) and (1-methoxyprop-1-en-2-yl)benzene (**1-R**). The different analytes were separated using GC method A (see section S1 for details).

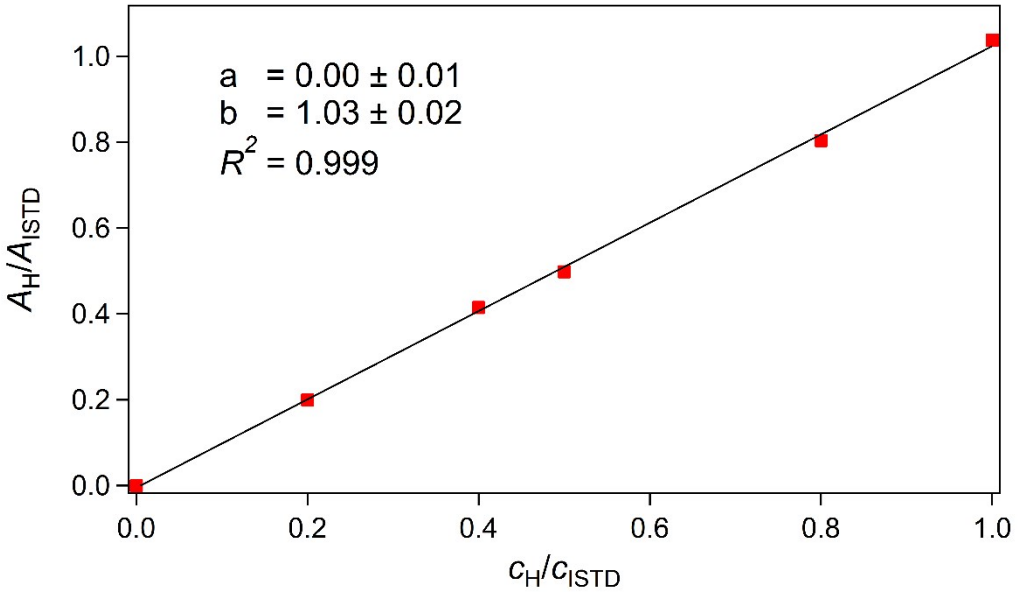

Figure S5. GC-MS calibration curve of 2-phenyl-1-propyl methyl ether (**1-H**) with respect to *tert*-butylbenzene (**ISTD**, 5 mM).

3.2.2 Light-driven hydrogenation of but-1-en-2-ylbenzene (2-SM)

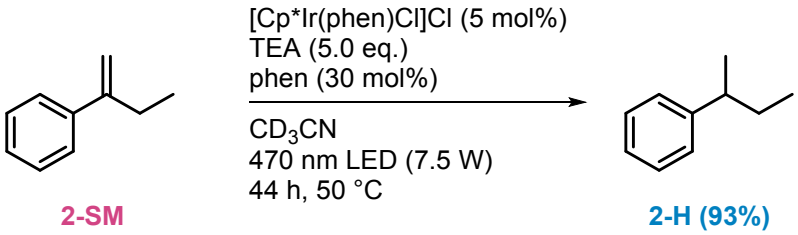

But-1-en-2-ylbenzene (**2-SM**) was reduced to *sec*-butylbenzene (**2-H**) according to general procedure C. Based on ^{1}H-NMR spectroscopy, 97% conversion of **2-SM** was achieved, affording **2-H** in 93% yield. Isomerization to but-2-en-2-ylbenzene (**2-R**) was observed in minor amounts (4%). The formation of *sec*-butylbenzene (**2-H**) was further confirmed by GC-MS spectrometry (92% formation of hydrogenation product **2-H** with respect to *tert*-butylbenzene as an internal standard).

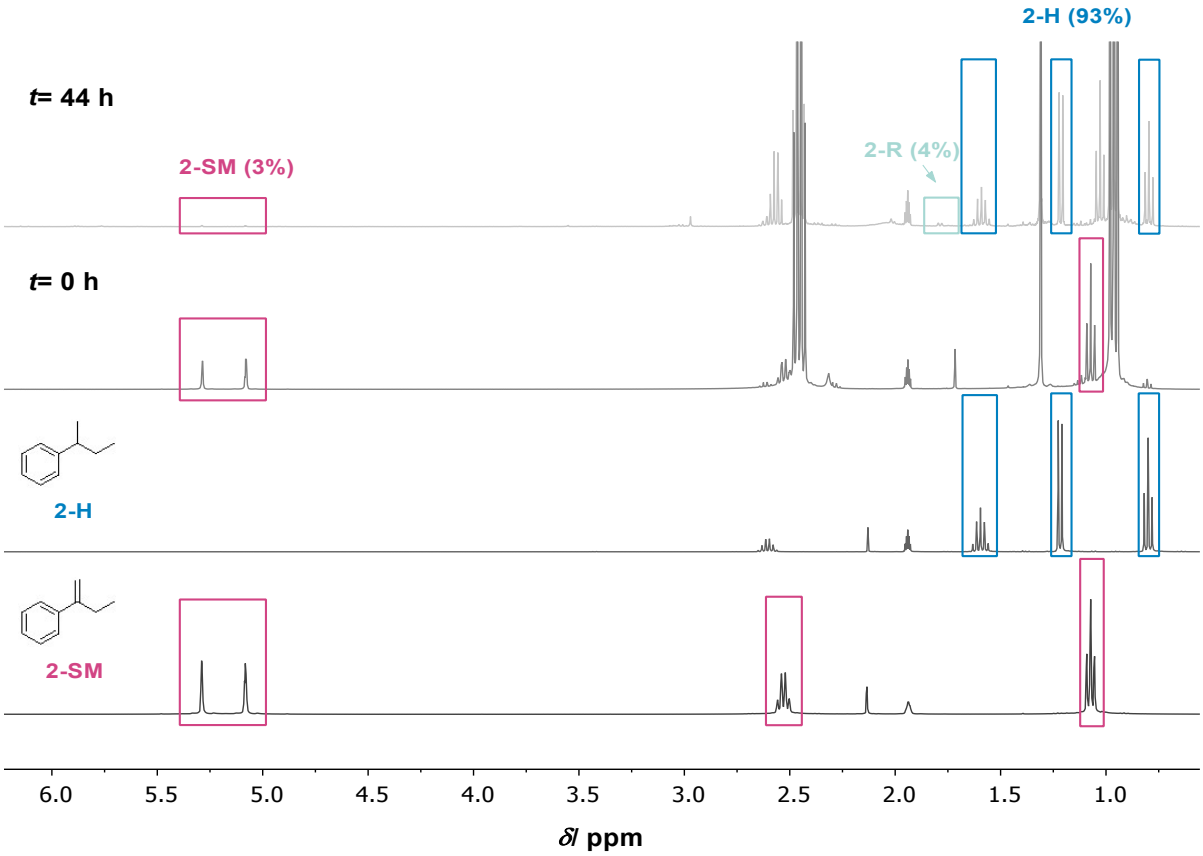

Figure S6. ^{1}H-NMR spectra of the light-driven hydrogenation of but-1-en-2-ylbenzene (**2-SM**) in CD_3CN: The ^{1}H-NMR spectra of the reaction mixture before (t = 0 h) and after (t = 44 h) irradiation are shown in comparison to the ^{1}H-NMR spectra of neat but-1-en-2-ylbenzene (**2-SM**) and *sec*-butylbenzene (**2-H**). The triplet at 1.02 ppm and the quartet at 2.56 ppm in the top spectrum are due to diethylamine resulting from TEA oxidation.

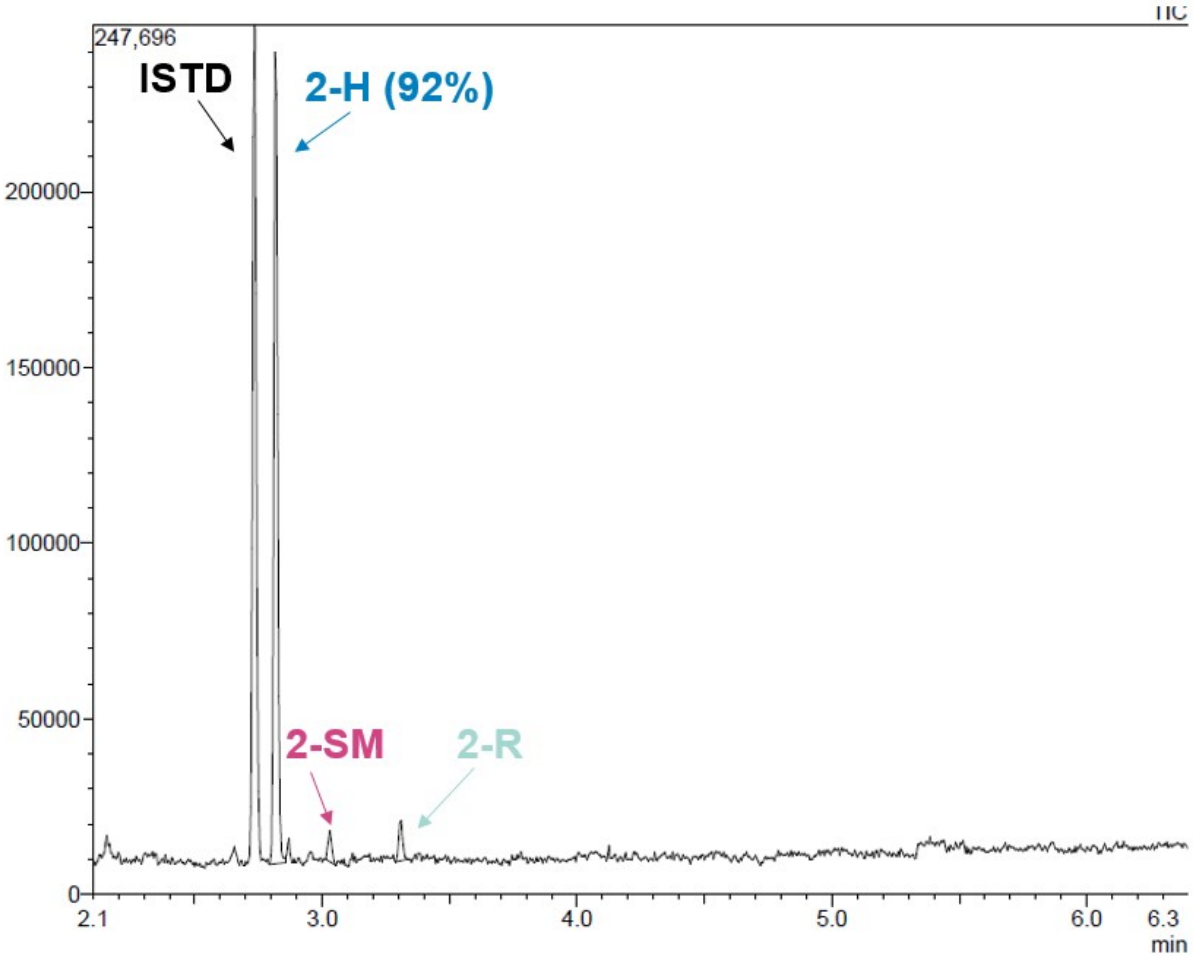

Figure S7. GC-MS trace of the light-induced hydrogenation of but-1-en-2-ylbenzene (**2-SM**) to afford *sec*-butylbenzene (**2-H**) and but-2-en-2-ylbenzene (**2-R**). The different analytes were separated using GC method A (see section S1 for details).

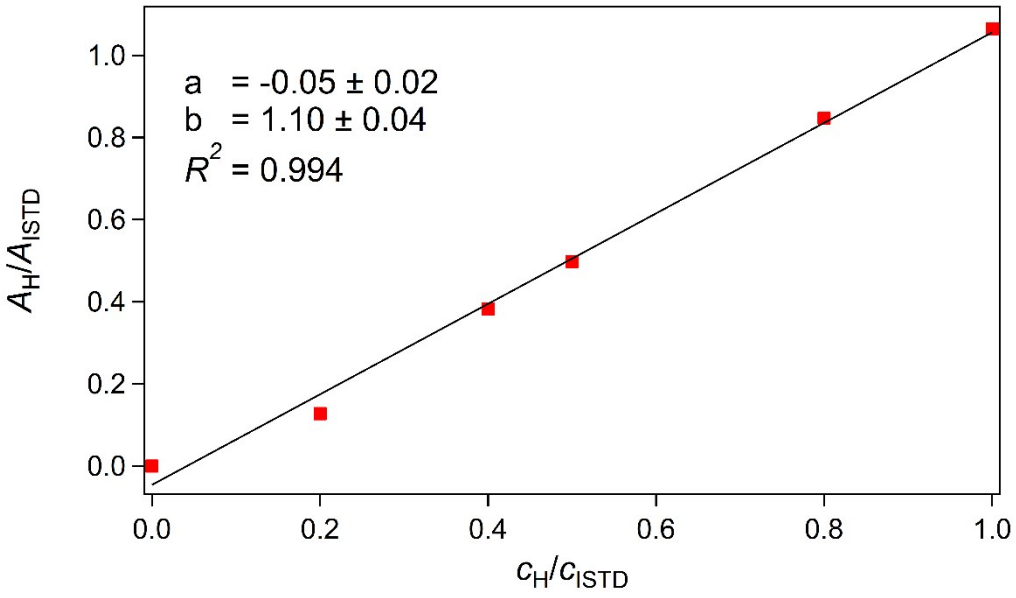

Figure S8. GC-MS calibration curve of *sec*-butylbenzene **(2-H)** with respect to *tert*-butylbenzene (**ISTD**, 5 mM).

3.2.3 Light-driven hydrogenation of 1-(but-1-en-2-yl)-4-methoxybenzene (3-SM)

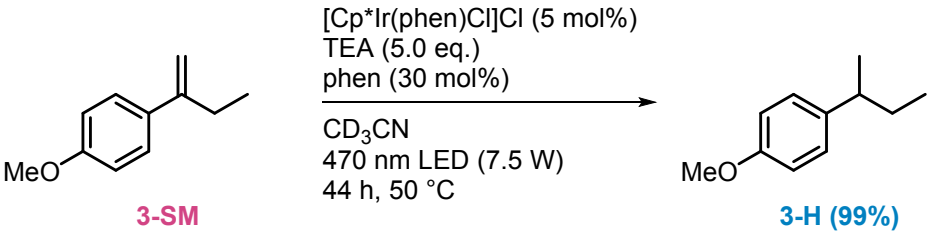

1-(But-1-en-2-yl)-4-methoxybenzene (**3-SM**) was reduced to 1-(*sec*-butyl)-4-methoxybenzene (**3-H**) according to general procedure C. Based on ^{1}H-NMR spectroscopy, the conversion of **3-SM** was determined to be essentially quantitative, giving hydrogenation product **3-H** in 99% analytical yield. Isomerization to 1-(but-2-en-2-yl)-4-methoxybenzene (**3-R**) was observed in minor amounts (~1%). The formation of 1-(*sec*-butyl)-4-methoxybenzene (**3-H**) was further confirmed by GC-MS spectrometry (95% formation of hydrogenation product **3-H** with respect to *tert*-butylbenzene as an internal standard).

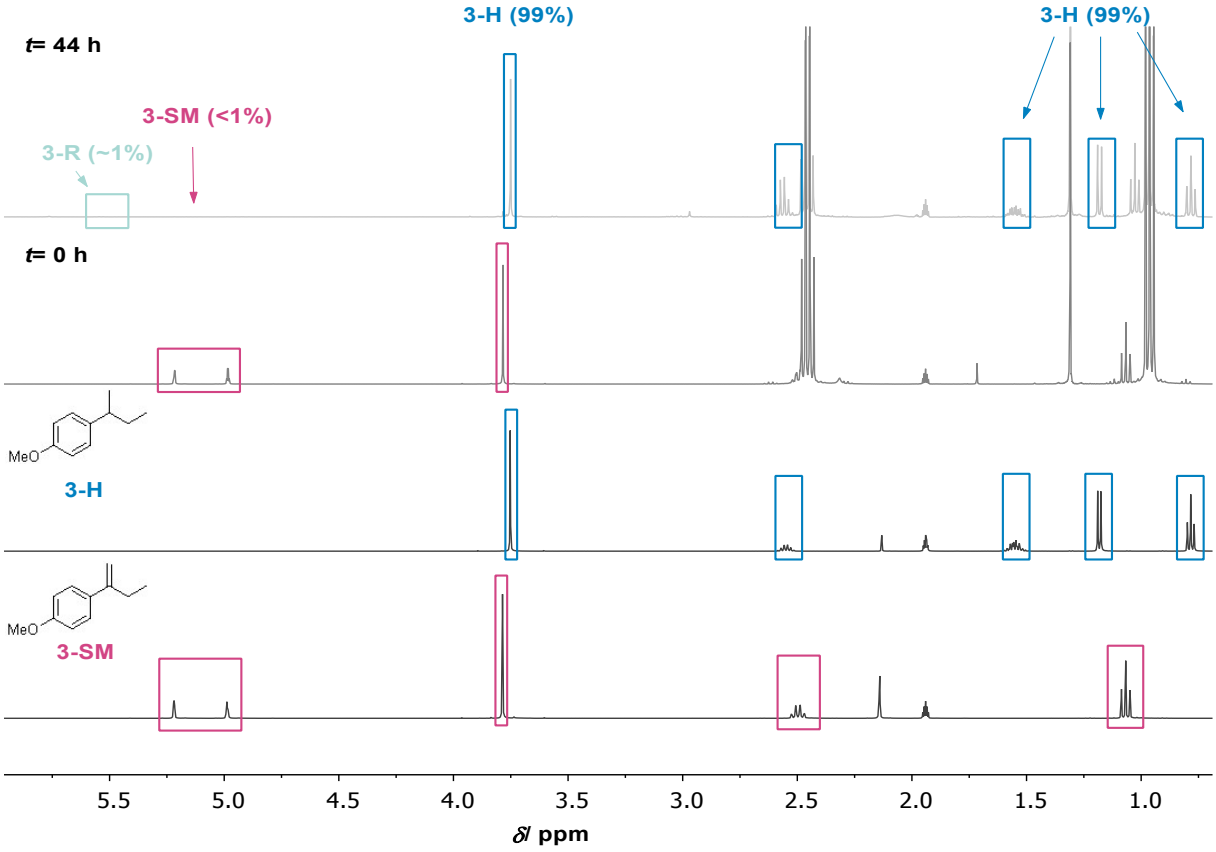

Figure S9. ^{1}H-NMR spectra of the light-driven hydrogenation of 1-(but-1-en-2-yl)-4-methoxybenzene (**3-SM**) in CD_3CN: The ^{1}H-NMR spectra of the reaction mixture before (t = 0 h) and after (t = 44 h) irradiation are shown in comparison to the ^{1}H-NMR spectra of neat 1-(but-1-en-2-yl)-4-methoxybenzene (**3-SM**) and 1-(*sec*-butyl)-4-methoxybenzene (**3-H**). The triplet at 1.02 ppm and the quartet at 2.56 ppm in the top spectrum are due to diethylamine resulting from TEA oxidation.

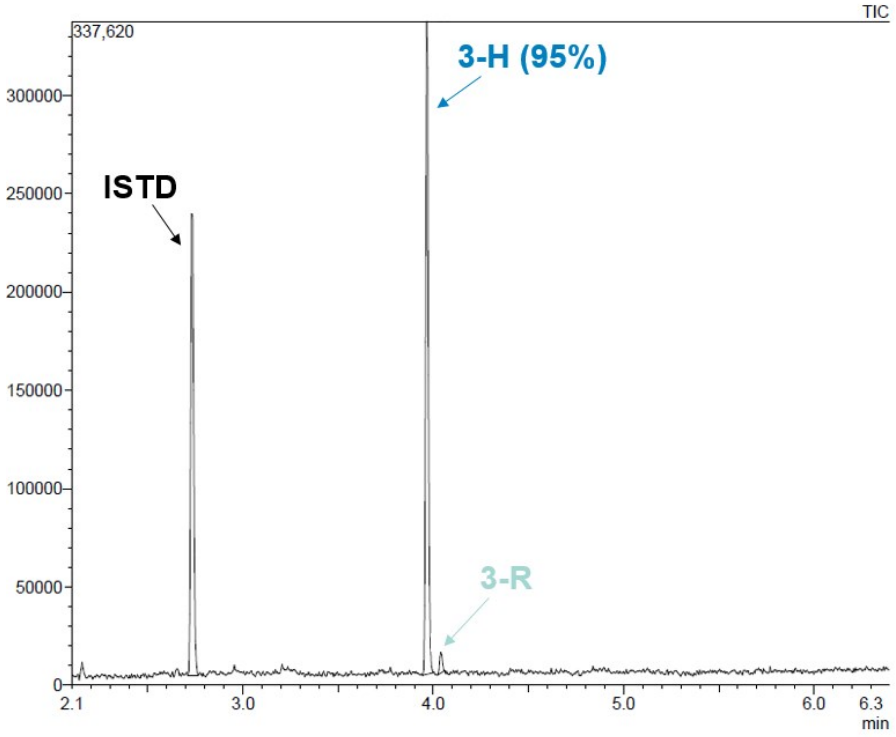

Figure S10. GC-MS trace of the light-induced hydrogenation of 1-(but-1-en-2-yl)-4-methoxybenzene (**3-SM**) to afford 1-(*sec*-butyl)-4-methoxybenzene (**3-H**) and 1-(but-2-en-2-yl)-4-methoxybenzene (**3-R**). The different analytes were separated using GC method A (see section S1 for details).

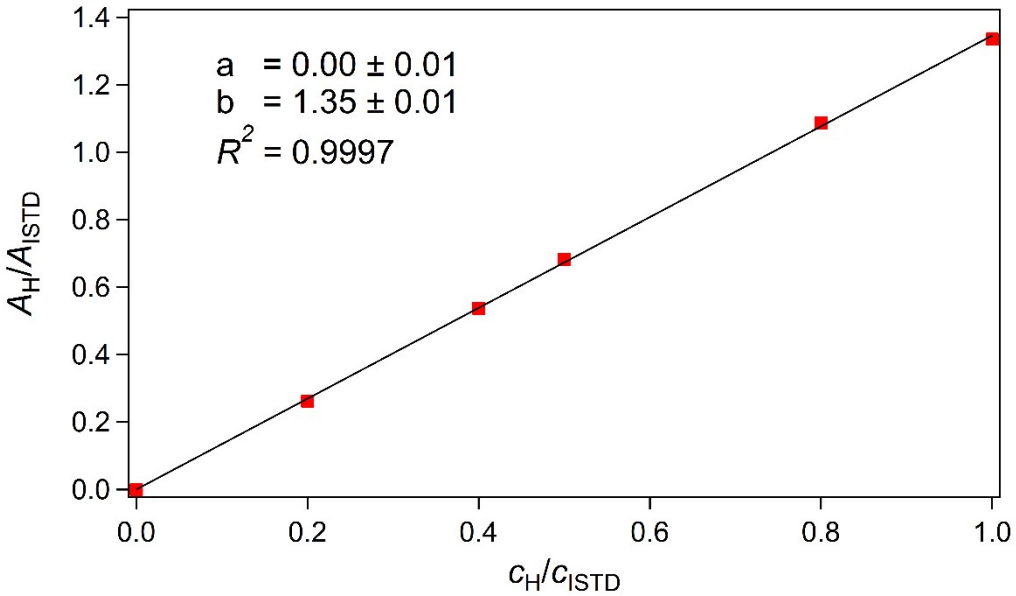

Figure S11. GC-MS calibration curves of 1-(*sec*-butyl)-4-methoxybenzene (**3-H**) with respect to *tert*-butylbenzene (**ISTD**, 5 mM).

3.2.4 Light-driven hydrogenation of 1-(but-1-en-2-yl)-4-chlorobenzene (4-SM)

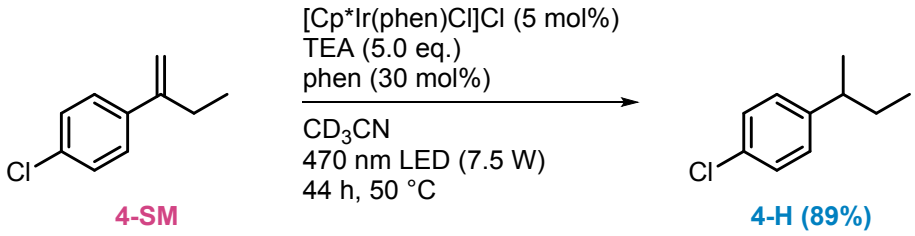

1-(But-1-en-2-yl)-4-chlorobenzene (**4-SM**) was reduced to 1-(*sec*-butyl)-4-chlorobenzene (**4-H**) according to general procedure C. Based on ^{1}H-NMR spectroscopy, 96% conversion of **4-SM** was achieved, resulting in **4-H** in 89% yield. Isomerization to 1-(but-2-en-2-yl)-4-chlorobenzene (**4-R**) was observed in minor amounts (7%). The formation of 1-(*sec*-butyl)-4-chlorobenzene (**4-H**) was further confirmed by GC-MS spectrometry (91% formation of hydrogenation product **4-H** with respect to *tert*-butylbenzene as an internal standard).

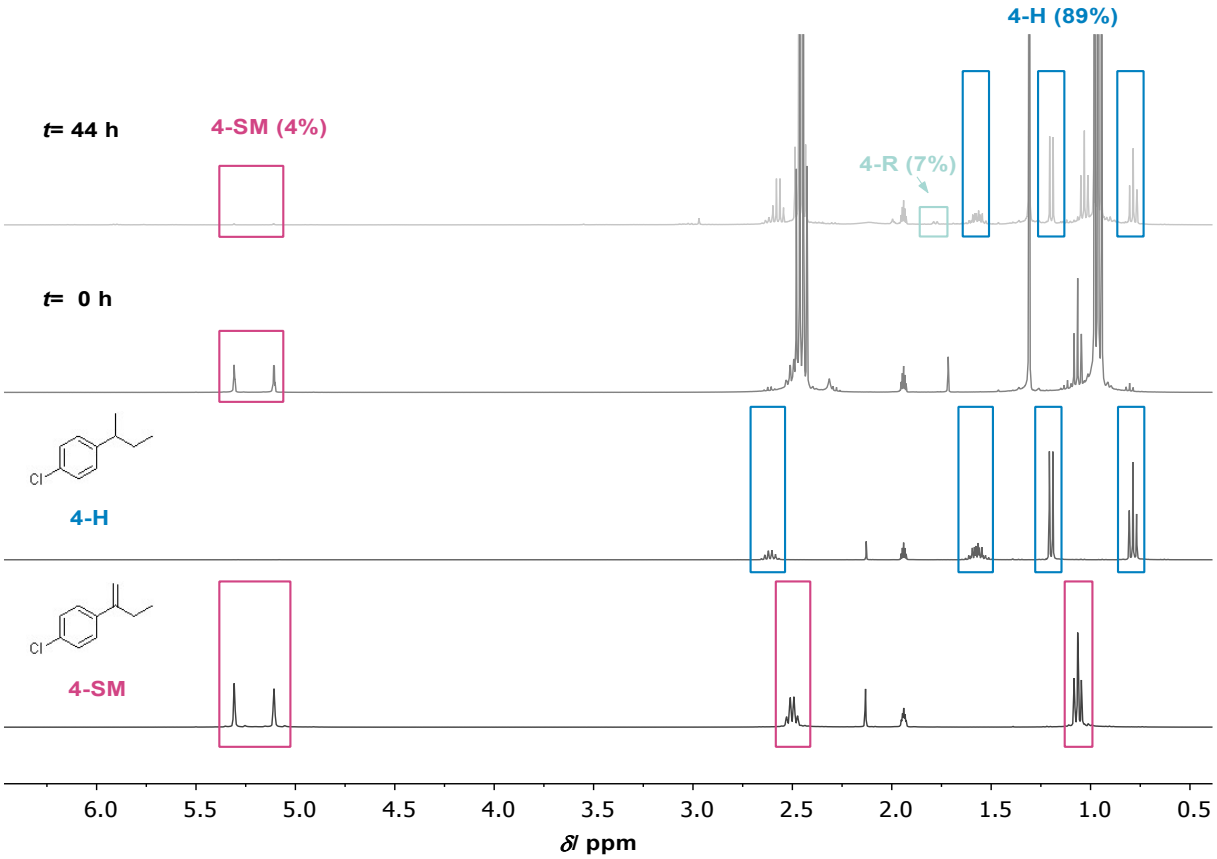

Figure S12. ^{1}H-NMR spectra of the light-driven hydrogenation of 1-(but-1-en-2-yl)-4-chlorobenzene (**4-SM**) in CD_3CN: The ^{1}H-NMR spectra of the reaction mixture before (*t* = 0 h) and after (*t* = 44 h) irradiation are shown in comparison to the ^{1}H-NMR spectra of neat 1-(but-1-en-2-yl)-4-chlorobenzene (**4-SM**) and 1-(*sec*-butyl)-4-chlorobenzene (**4-H**). The triplet at 1.02 ppm and the quartet at 2.56 ppm in the top spectrum are due to diethylamine resulting from TEA oxidation.

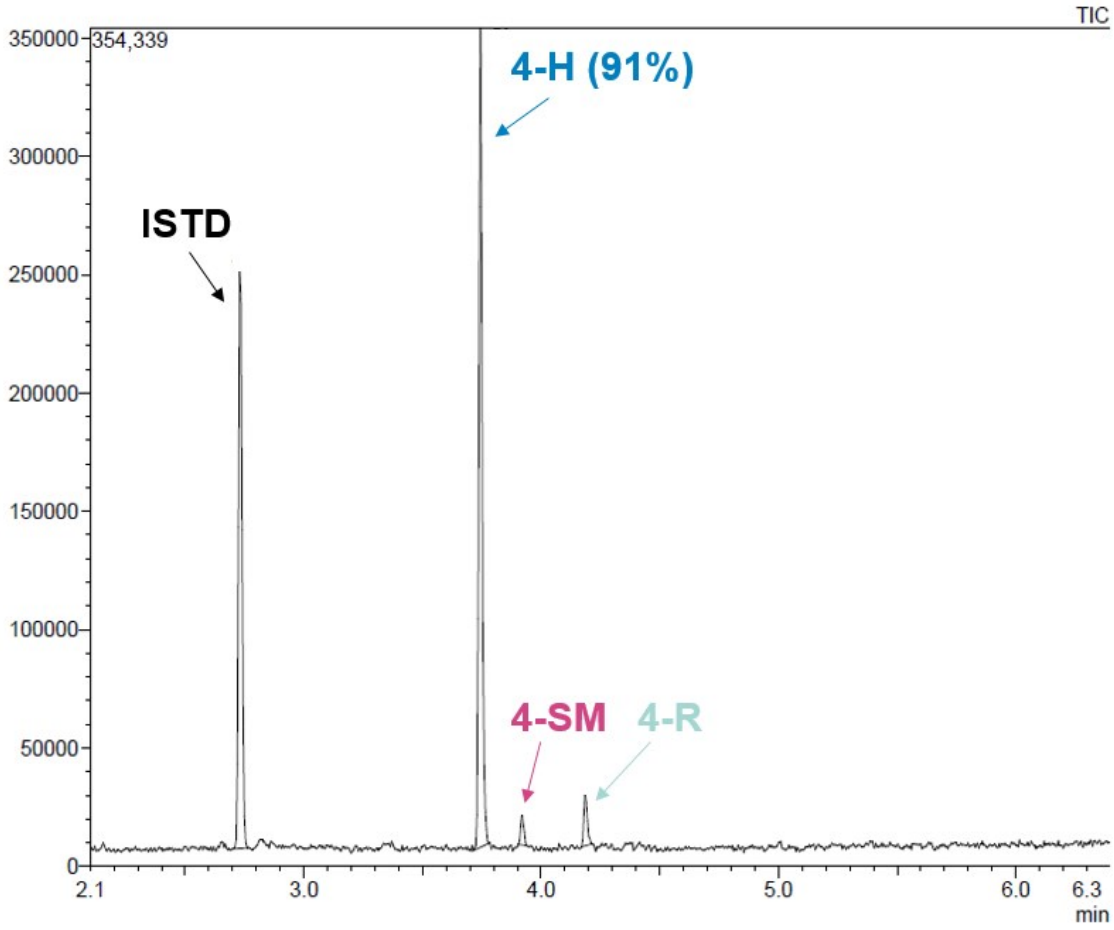

Figure S13. GC-MS trace of the light-induced hydrogenation of 1-(but-1-en-2-yl)-4-chlorobenzene (**4-SM**) to afford 1-(*sec*-butyl)-4-chlorobenzene (**4-H**) and 1-(but-2-en-2-yl)-4-chlorobenzene (**4-R**). The different analytes were separated using GC method A (see section S1 for details).

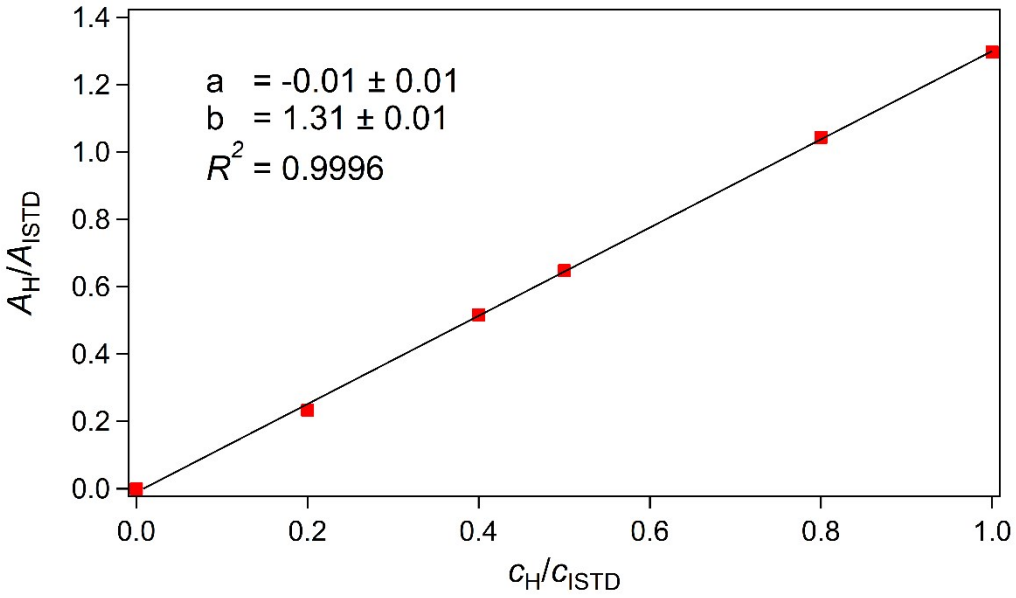

Figure S14. GC-MS calibration curve of 1-(*sec*-butyl)-4-chlorobenzene (**4-H**) with respect to *tert*-butylbenzene (**ISTD**, 5 mM).

3.2.5 Light-driven hydrogenation of 1-(but-1-en-2-yl)-3-chlorobenzene (5-SM)

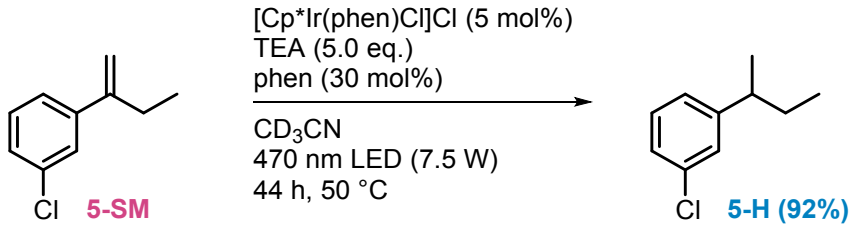

1-(But-1-en-2-yl)-3-chlorobenzene (**5-SM**) was reduced to 1-(*sec*-butyl)-3-chlorobenzene (**5-H**) according to general procedure C. Based on ^{1}H-NMR spectroscopy, the conversion of **5-SM** was 96%, affording **5-H** in 92% analytical yield. Isomerization to 1-(but-2-en-2-yl)-3-chlorobenzene (**5-R**) was observed in minor amounts (4%). The formation of 1-(*sec*-butyl)-3-chlorobenzene (**5-H**) was further confirmed by GC-MS spectrometry (89% formation of hydrogenation product **5-H** with respect to *tert*-butylbenzene as an internal standard).

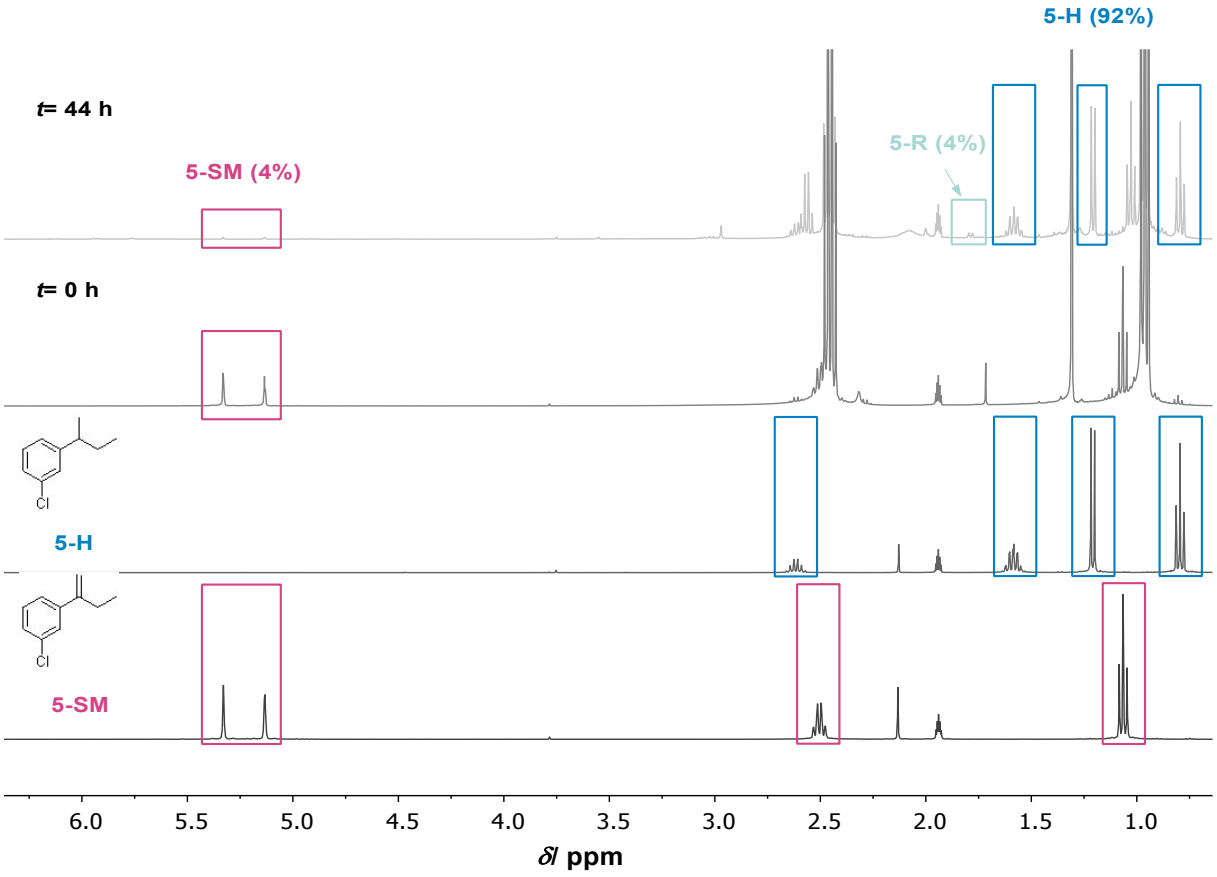

Figure S15. ^{1}H-NMR spectra of the light-driven hydrogenation of 1-(but-1-en-2-yl)-3-chlorobenzene (**5-SM**) in CD_3CN: The ^{1}H-NMR spectra of the reaction mixture before (t = 0 h) and after (t = 44 h) irradiation are shown in comparison to the ^{1}H-NMR spectra of neat 1-(but-1-en-2-yl)-3-chlorobenzene (**5-SM**) and 1-(*sec*-butyl)-3-chlorobenzene (**5-H**). The triplet at 1.02 ppm and the quartet at 2.56 ppm in the top spectrum are due to diethylamine resulting from TEA oxidation.

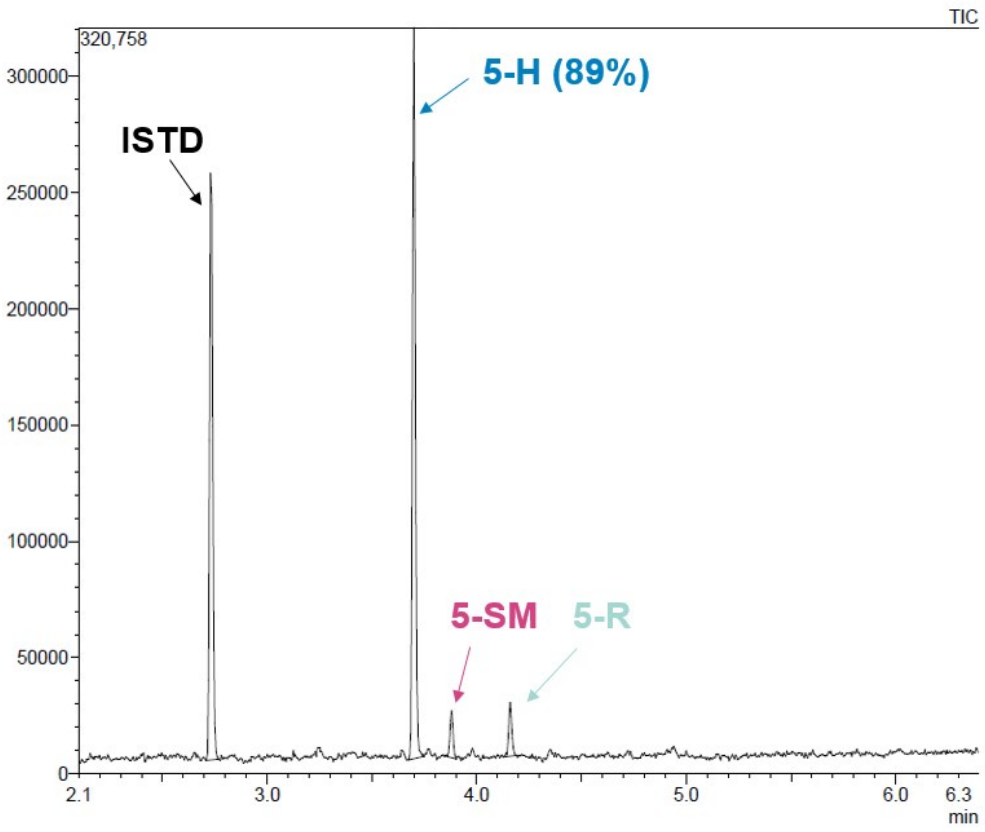

Figure S16. GC-MS trace of the light-induced hydrogenation of 1-(but-1-en-2-yl)-3-chlorobenzene (**5-SM**) to afford 1-(*sec*-butyl)-3-chlorobenzene (**5-H**) and 1-(but-2-en-2-yl)-3-chlorobenzene (**5-R**). The different analytes were separated using GC method A (see section S1 for details).

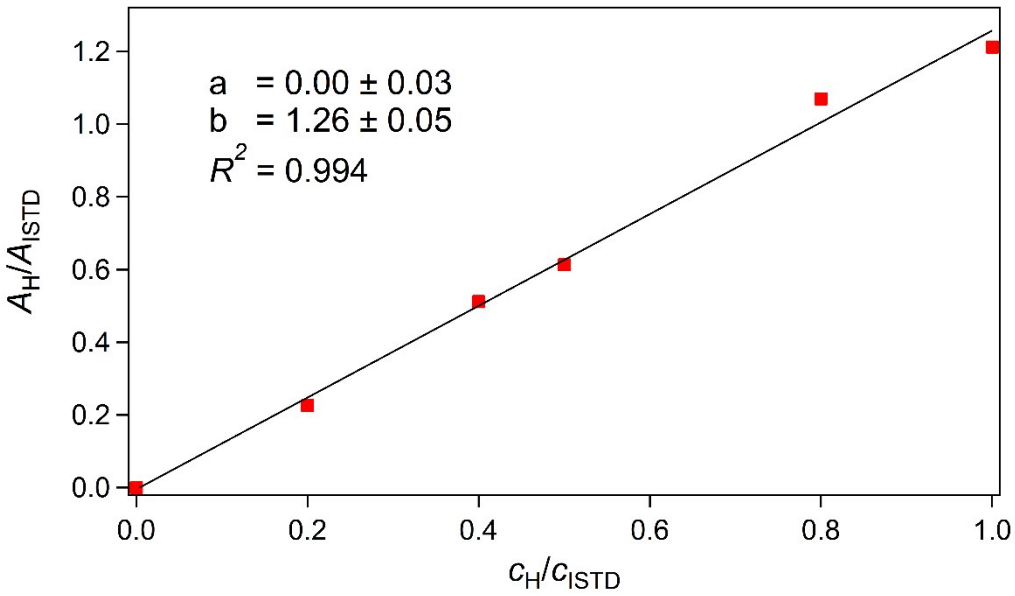

Figure S17. GC-MS calibration curve of 1-(*sec*-butyl)-3-chlorobenzene (**5-H**) with respect to *tert*-butylbenzene (**ISTD**, 5 mM).

3.2.6 Light-driven hydrogenation of 2-phenylprop-2-en-1-ol (6-SM)

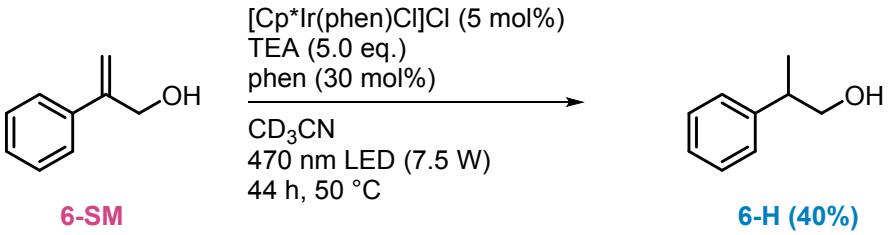

2-Phenylprop-2-en-1-ol (**6-SM**) was reduced to 2-phenylpropan-1-ol (**6-H**) according to general procedure C. Based on ^{1}H-NMR spectroscopy, the conversion of **6-SM** was 41% affording **6-H** in 40% analytical yield. No significant isomerization of **6-SM** was observed.

Since analysis by GC-MS was not possible for substrate **6-SM**, in this particular case the conversions were determined based on ^{1}H-NMR spectroscopy exclusively.

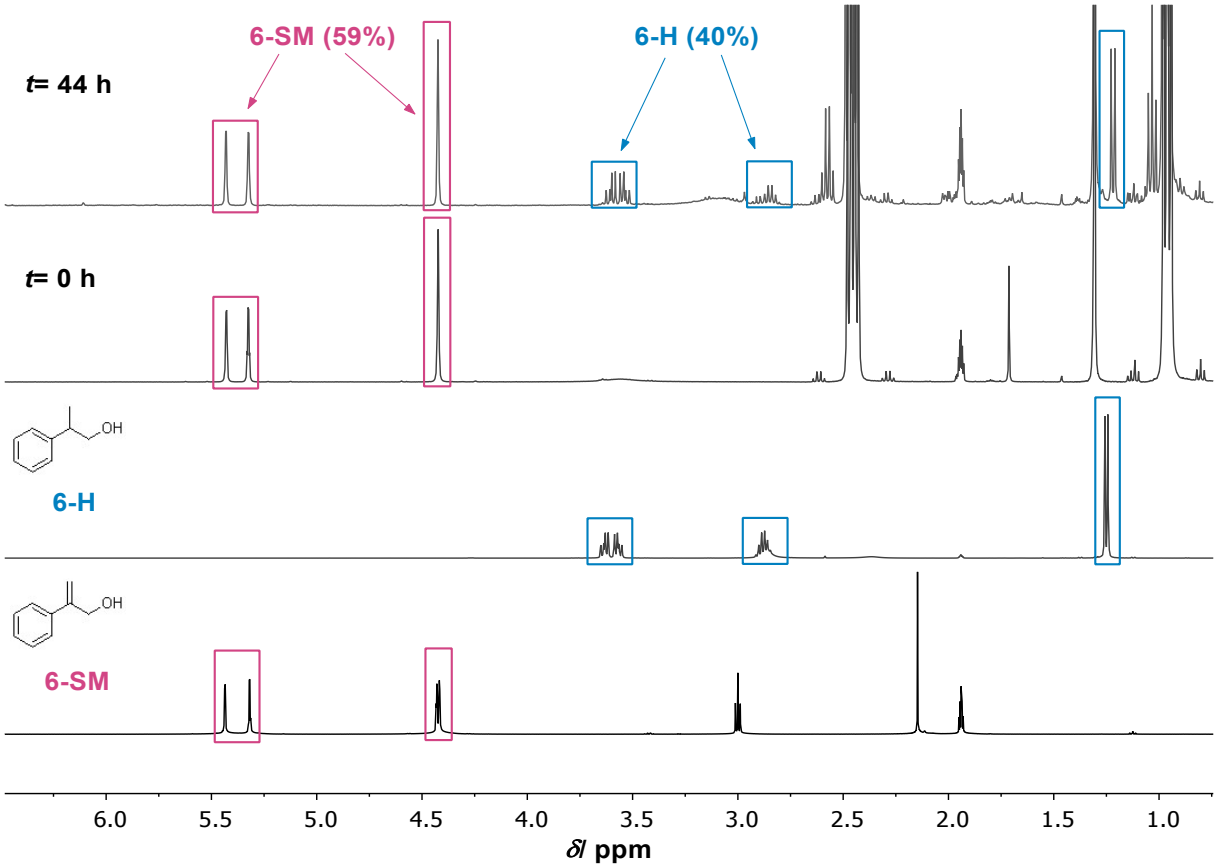

Figure S18. ^{1}H-NMR spectra of the light-driven hydrogenation of 2-phenylprop-2-en-1-ol (**6-SM**) in CD_3CN: The ^{1}H-NMR spectra of the reaction mixture before (t = 0 h) and after (t = 44 h) irradiation are shown in comparison to the ^{1}H-NMR spectra of neat 2-phenylprop-2-en-1-ol (**6-SM**) and 2-phenylpropan-1-ol (**6-H**). The triplet at 1.02 ppm and the quartet at 2.56 ppm in the top spectrum are due to diethylamine resulting from TEA oxidation.

3.2.7 *Light-driven hydrogenation of 2-(3-(benzyloxy)prop-1-en-2-yl)-1,3,5-trimethylbenzene (7-SM)*

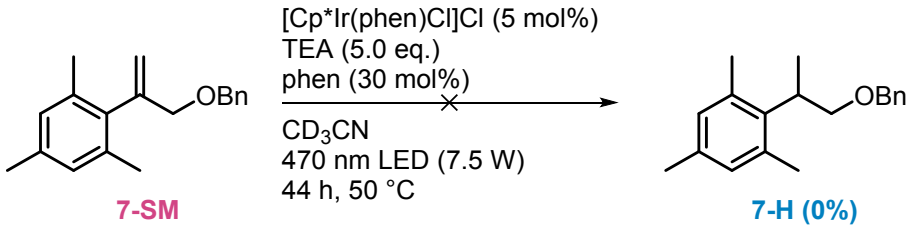

Hydrogenation of 2-(3-(benzyloxy)prop-1-en-2-yl)-1,3,5-trimethylbenzene (**7-SM**) to 2-(1-(benzyloxy)propan-2-yl)-1,3,5-trimethylbenzene (**7-H**) was attempted following general procedure C. However, after irradiating the reaction mixture for 44 h, no conversion of the substrate was observed.

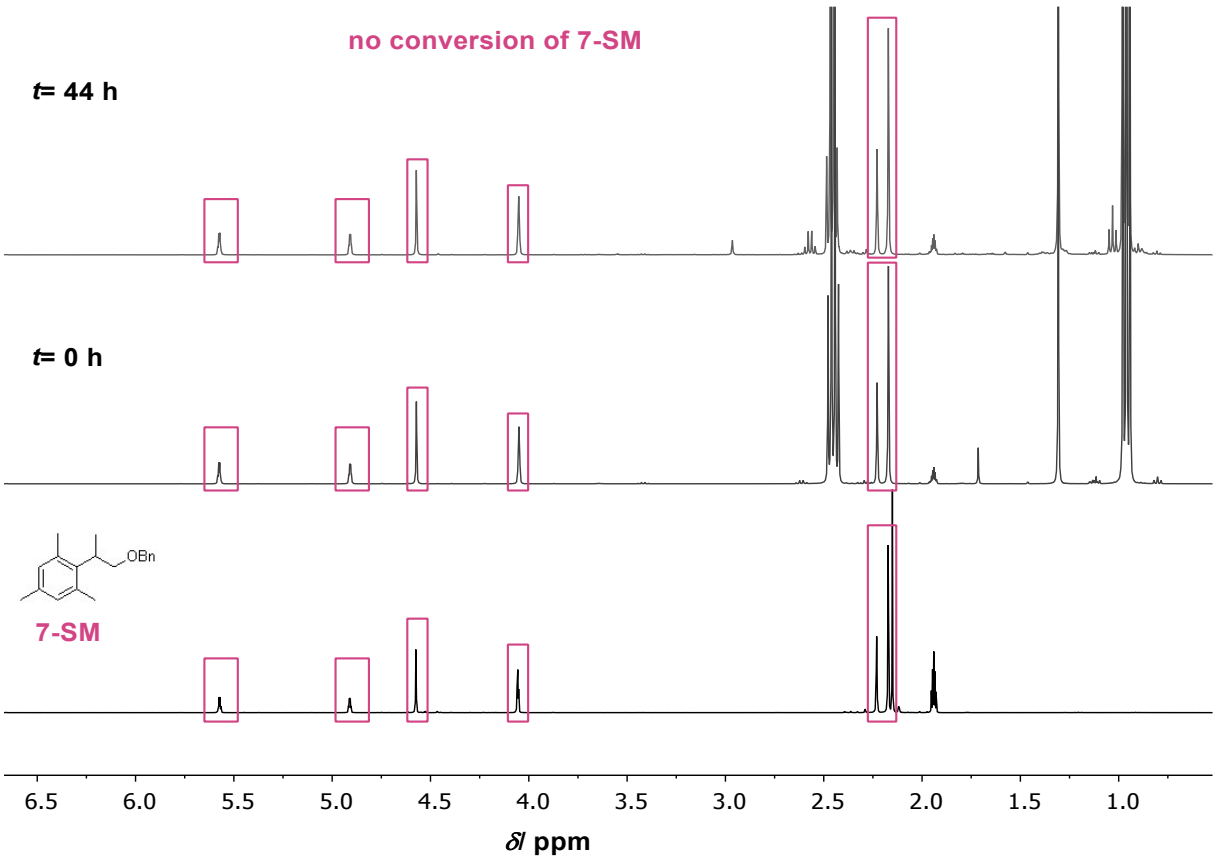

Figure S19. ^{1}H-NMR spectra of the attempted light-driven hydrogenation of 2-(3-(benzyloxy)prop-1-en-2-yl)-1,3,5-trimethylbenzene (**7-SM**) in CD_3CN: The ^{1}H-NMR spectra of the reaction mixture before (t = 0 h) and after (t = 44 h) irradiation are shown in comparison to the ^{1}H-NMR spectrum of neat 2-(3-(benzyloxy)prop-1-en-2-yl)-1,3,5-trimethylbenzene (**7-SM**). The triplet at 1.02 ppm and the quartet at 2.56 ppm in the top spectrum are due to diethylamine resulting from TEA oxidation.

3.2.8 Light-driven hydrogenation of trans-1-phenyl-1-propene (8-SM)

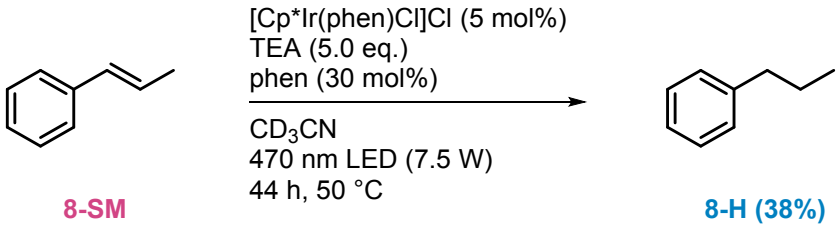

trans-1-Phenyl-1-propene (**8-SM**) was reduced to propylbenzene (**8-H**) according to general procedure C. Based on ^{1}H-NMR spectroscopy, the conversion of **8-SM** was 54%, giving **8-H** in 38% yield. Significant isomerization to *cis*-1-phenyl-1-propene (**8-R**, 16%) was observed. The formation of propylbenzene (**8-H**) was confirmed by GC-MS spectrometry (37% formation of hydrogenation product **8-H** with respect to *tert*-butylbenzene as an internal standard).

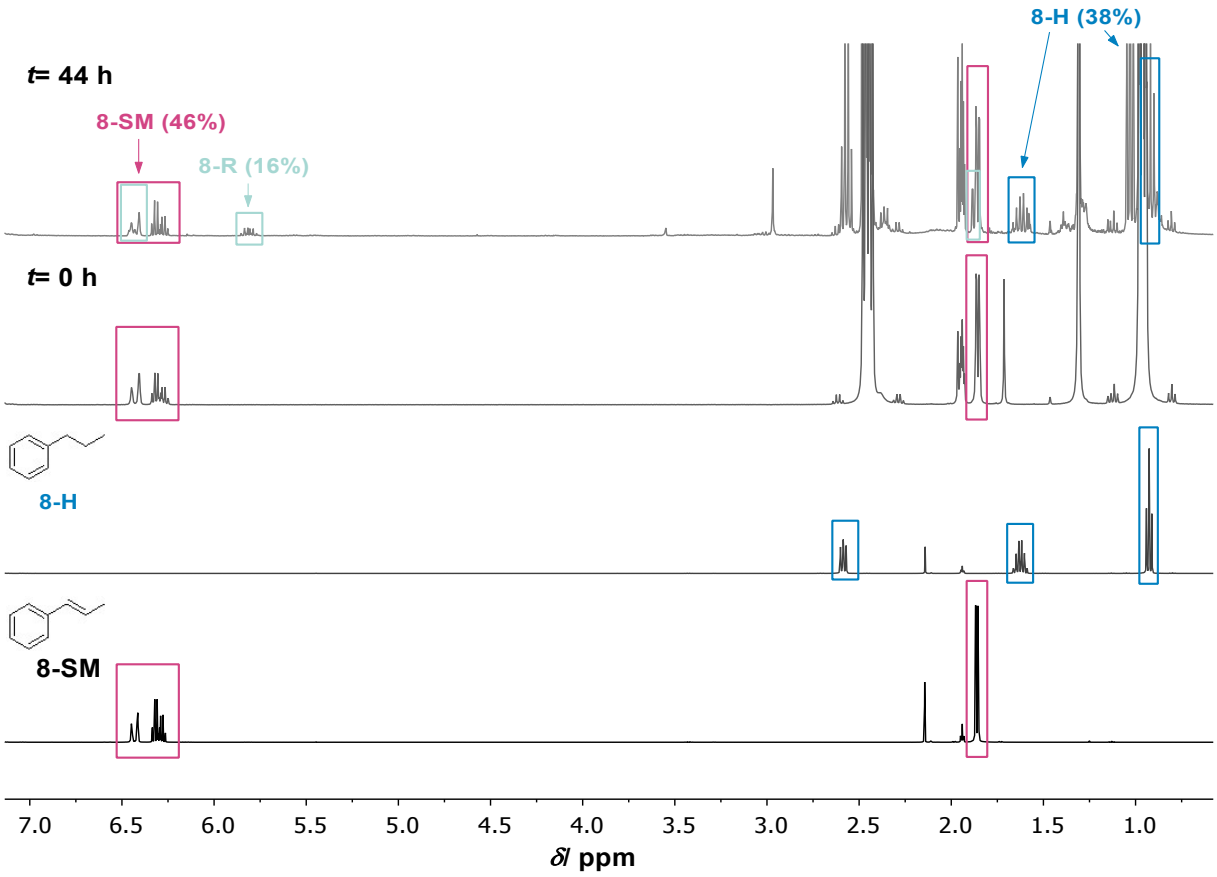

Figure S20. ^{1}H-NMR spectra of the light-driven hydrogenation of *trans*-1-phenyl-1-propene (**8-SM**) in CD_3CN: The ^{1}H-NMR spectra of the reaction mixture before (t = 0 h) and after (t = 44 h) irradiation are shown in comparison to the ^{1}H-NMR spectra of neat *trans*-1-phenyl-1-propene (**8-SM**) and propylbenzene (**8-H**). The triplet at 1.02 ppm and the quartet at 2.56 ppm in the top spectrum are due to diethylamine resulting from TEA oxidation.

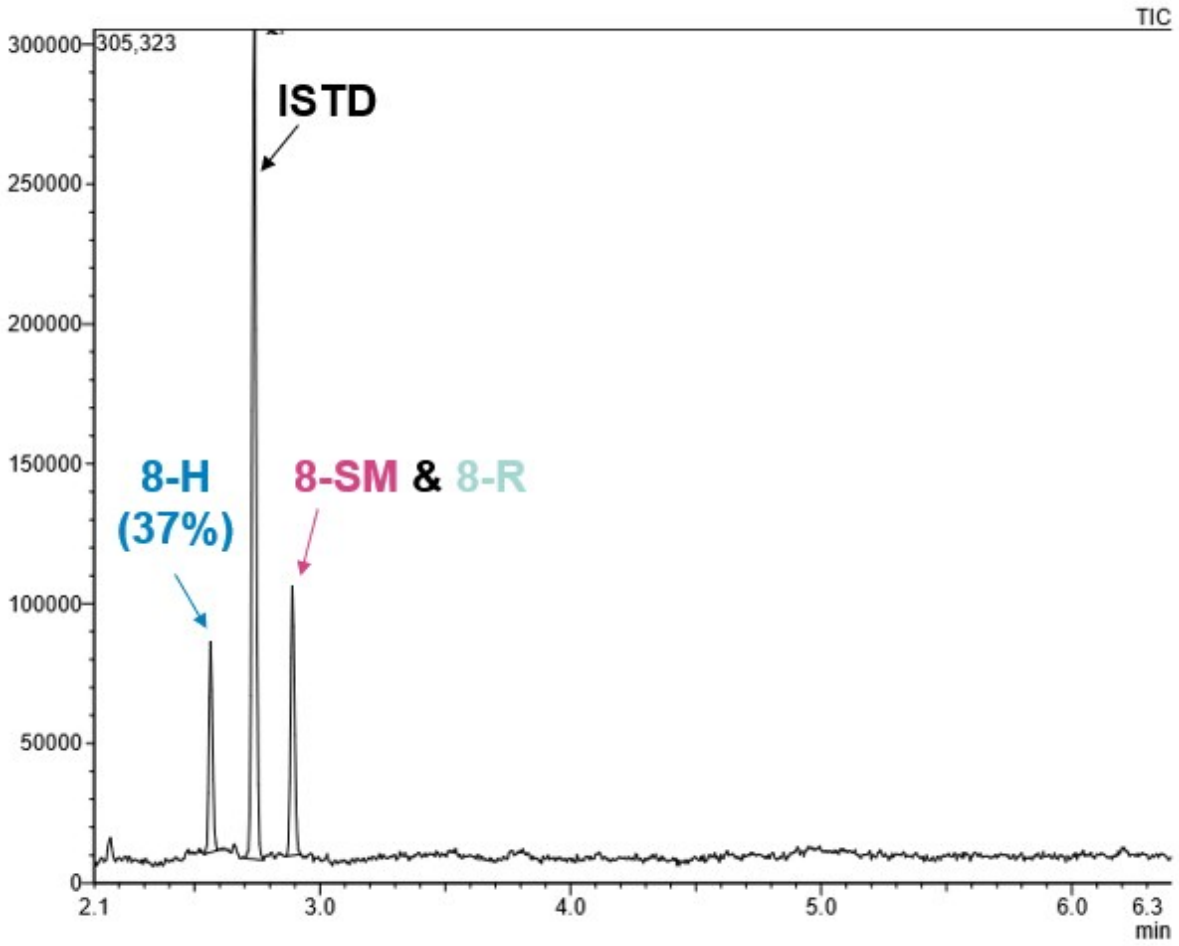

Figure S21. GC-MS trace of the light-induced hydrogenation of *trans*-1-phenyl-1-propene (**8-SM**) to afford propylbenzene (**8-H**) and *cis*-1-phenyl-1-propene (**8-R**). The different analytes were separated using GC method A (see section S1 for details).

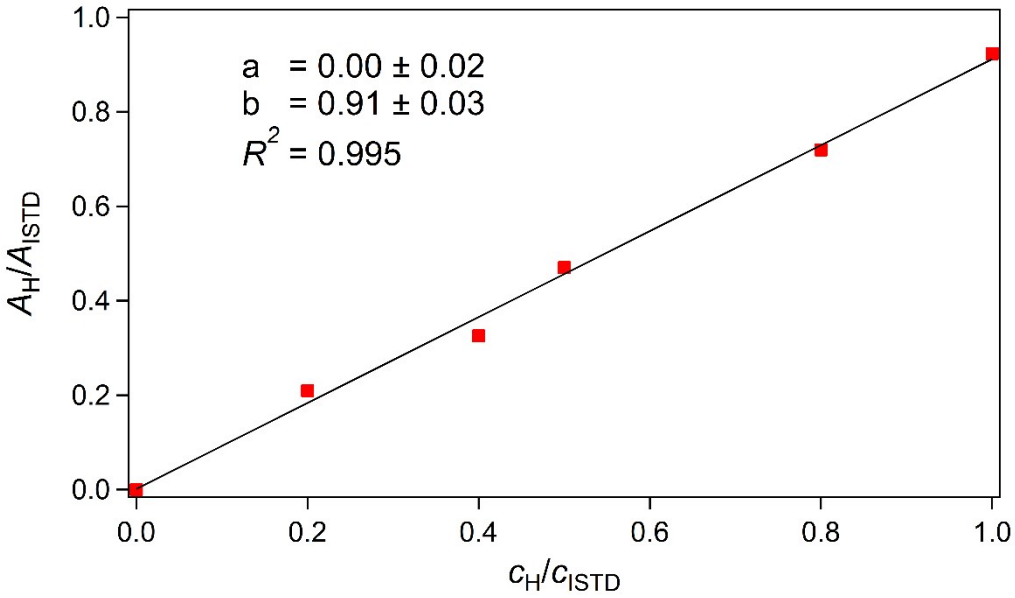

Figure S22. GC-MS calibration curve of propylbenzene (**8-H**) with respect to *tert*-butylbenzene (**ISTD**, 5 mM).

3.2.9 Light-driven hydrogenation of methyl 2-((benzyloxy)methyl)acrylate (9-SM)

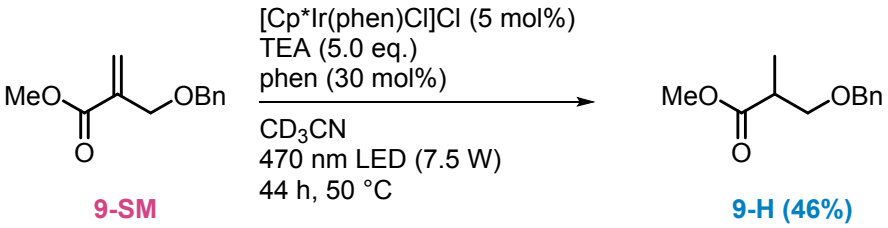

Methyl 2-((benzyloxy)methyl)acrylate (**9-SM**) was reduced to methyl 3-(benzyloxy)-2-methyl-propanoate (**9-H**) according to general procedure C. Based on ^{1}H-NMR spectroscopy, the conversion of the **9-SM** was 71%, affording **9-H** in 46% yield. Significant isomerization to methyl 3-(benzyloxy)-2-methylacrylate (**9-R**, 22%) was detected. In minor amounts, deprotection of the benzylic group (3%) was observed. The formation of methyl 3-(benzyloxy)-2-methyl-propanoate (**9-H**) was further confirmed by GC-MS spectrometry (48% formation of hydrogenation product **9-H** with respect to *tert*-butylbenzene as an internal standard).

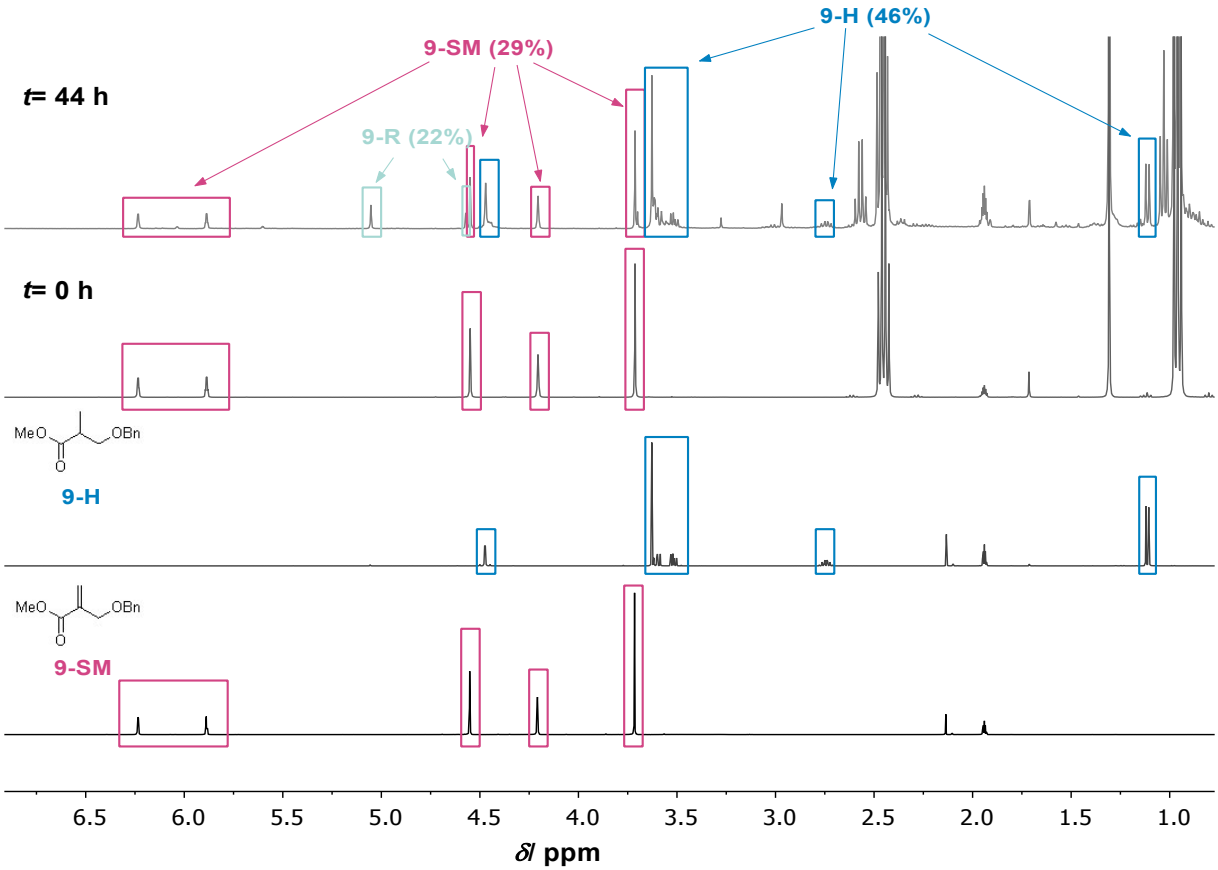

Figure S23. ^{1}H-NMR spectra of the light-driven hydrogenation of methyl 2-((benzyloxy)methyl)acrylate (**9-SM**) in CD_3CN: The ^{1}H-NMR spectra of the reaction mixture before (t = 0 h) and after (t = 44 h) irradiation are shown in comparison to the ^{1}H-NMR spectra of neat methyl 2-((benzyloxy)methyl)acrylate (**9-SM**) and methyl 3-(benzyloxy)-2-methyl-propanoate (**9-H**). The triplet at 1.02 ppm and the quartet at 2.56 ppm in the top spectrum are due to diethylamine resulting from TEA oxidation.

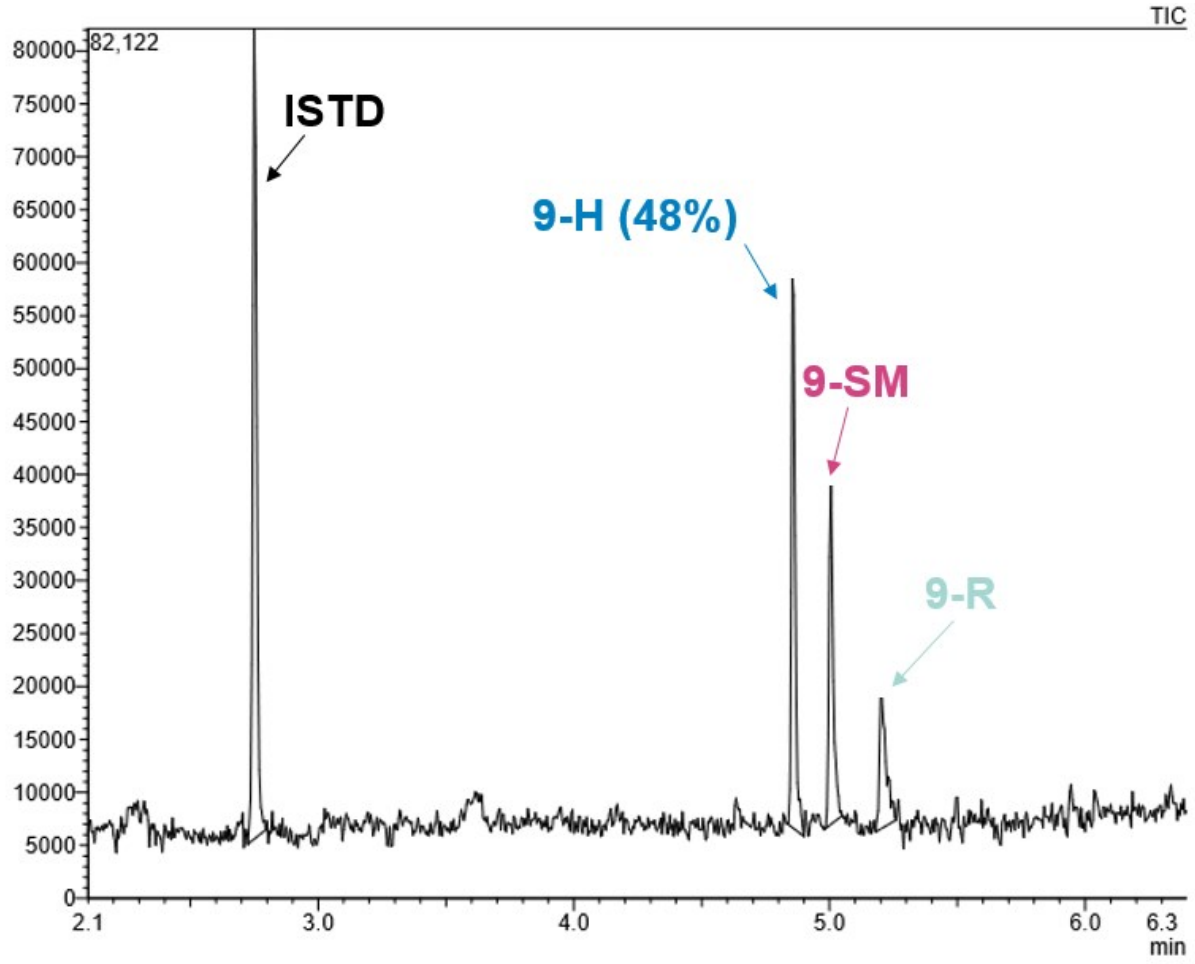

Figure S24. GC-MS trace of the light-induced hydrogenation of methyl 2-((benzyloxy)methyl)acrylate (**9-SM**) to afford methyl 3-(benzyloxy)-2-methyl-propanoate (**9-H**) and methyl 3-(benzyloxy)-2-methylacrylate (**9-R**). The different analytes were separated using GC method A (see section S1 for details).

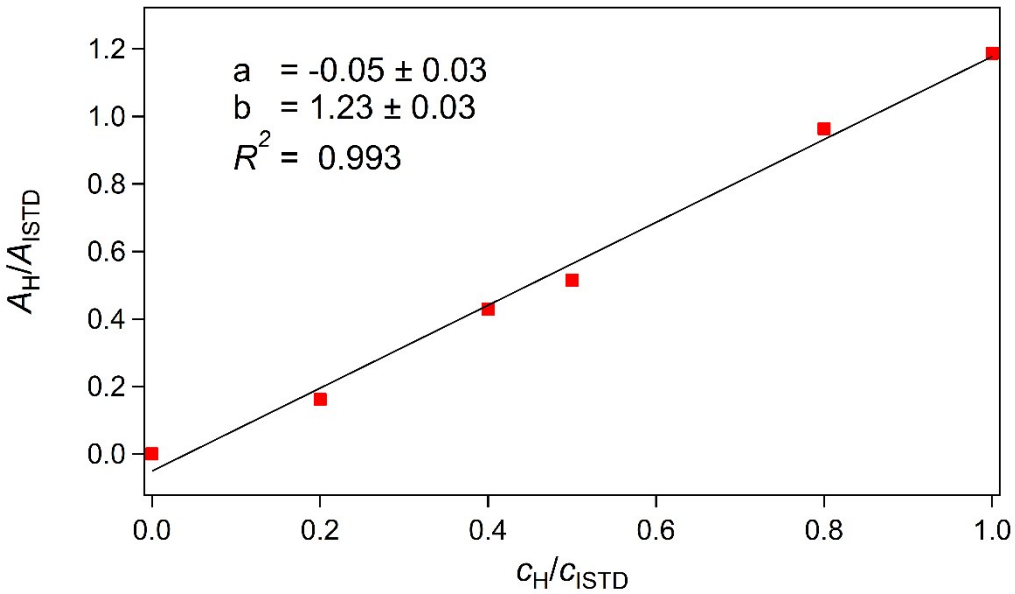

Figure S25. GC-MS calibration curve of methyl 3-(benzyloxy)-2-methyl-propanoate (**9-H**) with respect to *tert*-butylbenzene (**ISTD**, 5 mM).

3.2.10 Light-driven hydrogenation of (((2-cyclohexylallyl)oxy)methyl)benzene (10-SM)

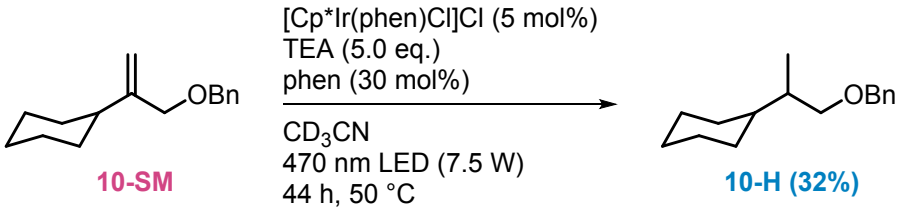

(((2-Cyclohexylallyl)oxy)methyl)benzene (**10-SM**) was reduced to ((2-cyclohexylpropoxy)methyl)-benzene (**10-H**) according to general procedure C. Based on ^{1}H-NMR spectroscopy, the conversion of **10-SM** was 40%, affording **10-H** in 32% yield. Significant isomerization to (((2-cyclohexylprop-1-en-1-yl)oxy)methyl)benzene (**10-R**) was observed (8%).

10-SM and **10-H** could not be separated by GC-MS spectrometry because the retention times of substrate **10-SM** and hydrogenation product **10-H** are too similar. Thus, the conversions were determined by ^{1}H-NMR spectroscopy exclusively.

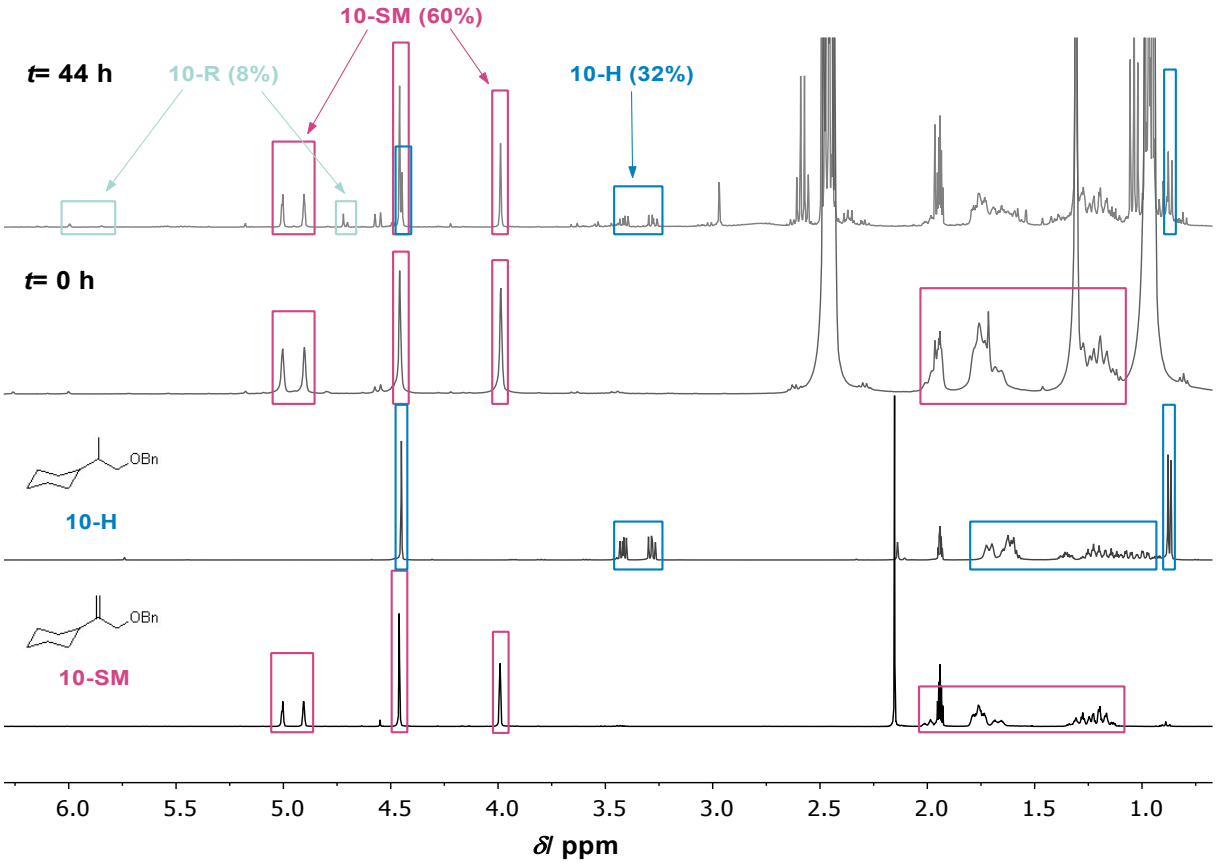

Figure S26. ^{1}H-NMR spectra of the light-driven hydrogenation of (((2-cyclohexylallyl)oxy)methyl)benzene (**10-SM**) in CD_3CN: The ^{1}H-NMR spectra of the reaction mixture before (t = 0 h) and after (t = 44 h) irradiation are shown in comparison to the ^{1}H-NMR spectra of neat (((2-cyclohexylallyl)oxy)methyl)benzene (**10-SM**) and ((2-cyclohexylpropoxy)methyl)-benzene (**10-H**). The triplet at 1.02 ppm and the quartet at 2.56 ppm in the top spectrum are due to diethylamine resulting from TEA oxidation.

3.2.11 Light-driven hydrogenation of ((2-methylallyloxy)methyl)benzene (11-SM)

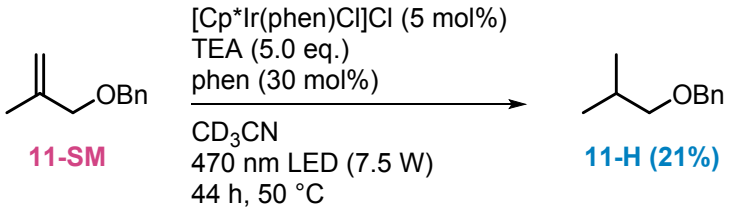

((2-Methylallyloxy)methyl)benzene (**11-SM**) was reduced to benzyl *iso*-butyl ether (**11-H**) according to general procedure C. Based on ^{1}H-NMR spectroscopy, the conversion of **11-SM** was 49%, affording **11-H** in 21% yield. Isomerization to (((2-methylprop-1-en-1-yl)oxy)methyl)benzene (**11-R**, 28%) was found to be the major reaction pathway. The formation of benzyl *iso*-butyl ether (**11-H**) was further confirmed by GC-MS spectrometry (26% formation of hydrogenation product **11-H** with respect to *tert*-butylbenzene as an internal standard).

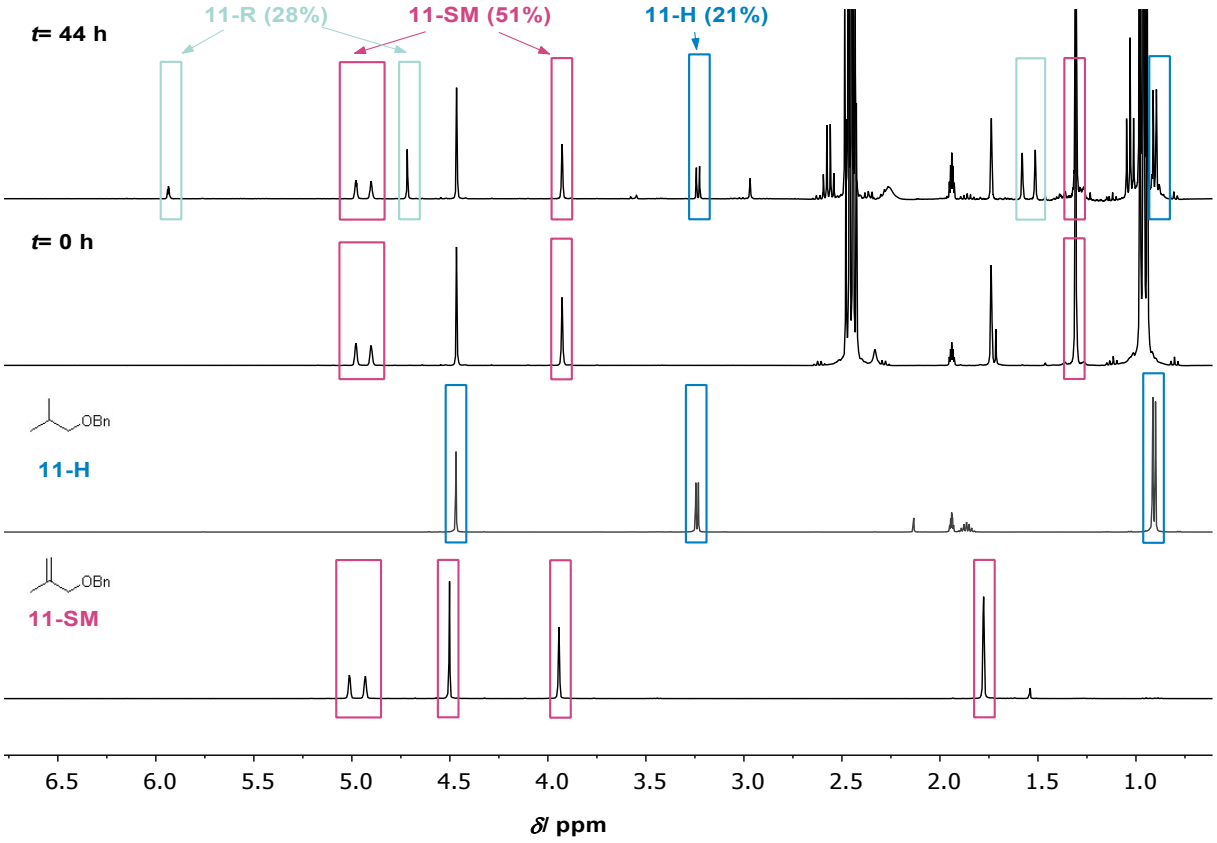

Figure S27. ^{1}H-NMR spectra of the light-driven hydrogenation of ((2-methylallyloxy)methyl)benzene (**11-SM**) in CD_3CN: The ^{1}H-NMR spectra of the reaction mixture before (*t* = 0 h) and after (*t* = 44 h) irradiation are shown in comparison to the ^{1}H-NMR spectra of neat ((2-methylallyloxy)methyl)benzene (**11-SM**) and benzyl *iso*-butyl ether (**11-H**). The triplet at 1.02 ppm and the quartet at 2.56 ppm in the top spectrum are due to diethylamine resulting from TEA oxidation.

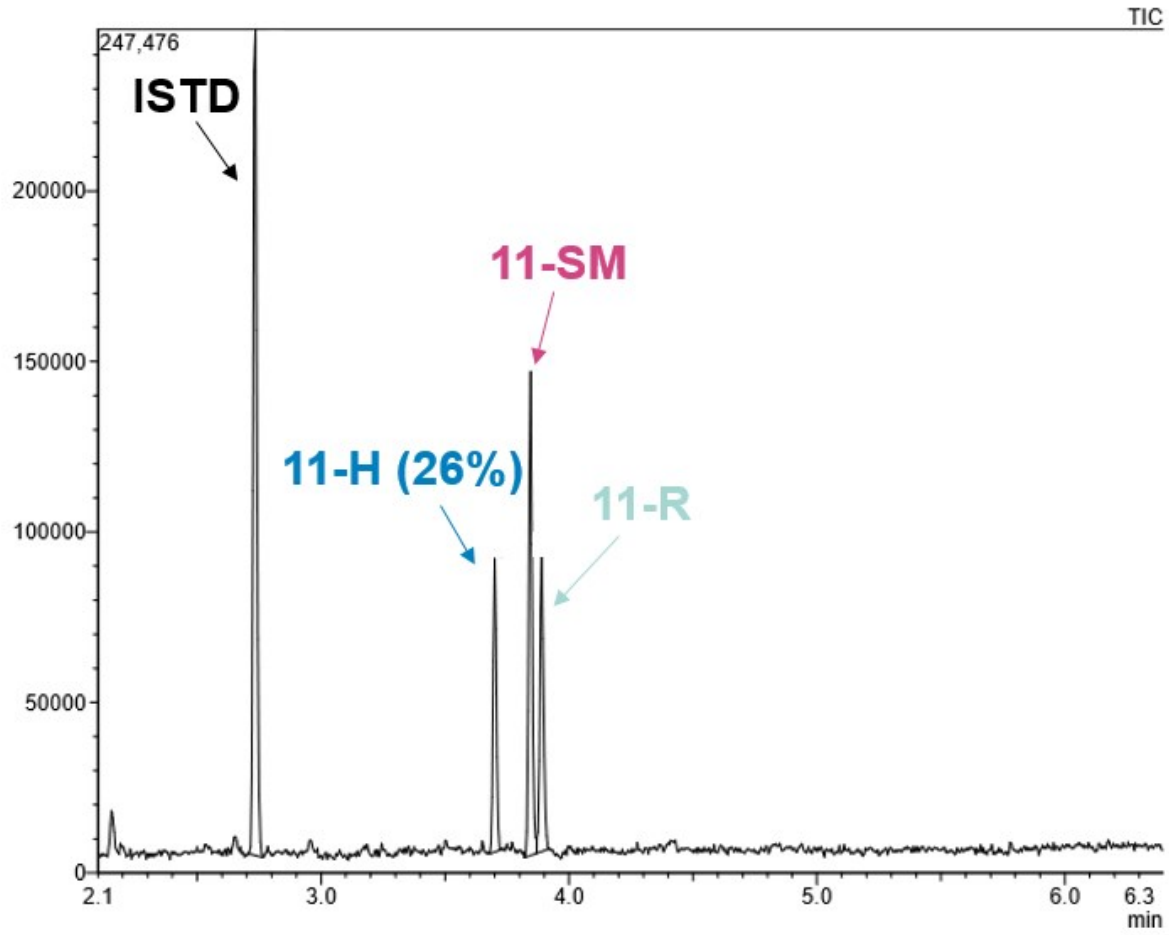

Figure S28. GC-MS trace of the light-induced hydrogenation of ((2-methylallyloxy)methyl)benzene (**11-SM**) to afford benzyl *iso*-butyl ether (**11-H**) and (((2-methylprop-1-en-1-yl)oxy)methyl)benzene (**11-R**). The different analytes were separated using GC method A (see section S1 for details).

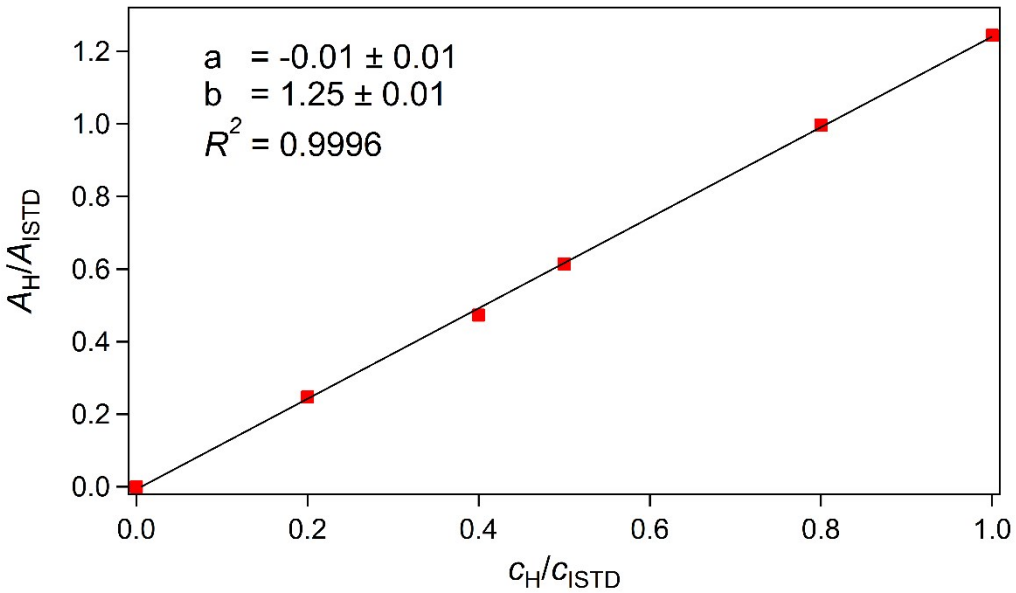

Figure S29. GC-MS calibration curve of benzyl *iso*-butyl ether (**11-H**) with respect to *tert*-butylbenzene (**ISTD**, 5 mM).

3.2.12 Light-driven hydrogenation of ((allyloxy)methyl)benzene (12-SM)

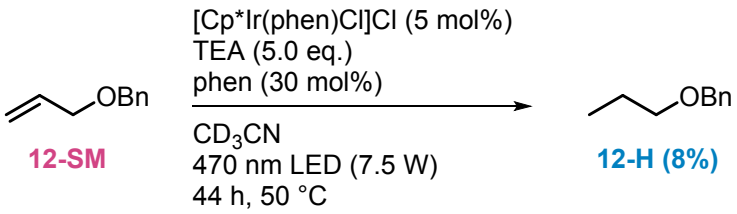

((Allyloxy)methyl)benzene (**12-SM**) was reduced to benzyl propyl ether (**12-H**) according to general procedure C. Based on ^{1}H-NMR spectroscopy, the conversion of **12-SM** was 35%, affording **12-H** in 8% yield. Isomerization to (*E*)-((prop-1-en-1-yloxy)methyl)benzene (**(*E*)-12-R**, 19%) and (*Z*)-((prop-1-en-1-yloxy)methyl)benzene (**(*Z*)-12-R**, 8%) was found to be the major reaction pathway.

12-SM and **12-H** could not be separated by GC-MS spectrometry because the retention times of substrate **12-SM** and hydrogenation product **12-H** are too similar. Thus, the conversions were determined by ^{1}H-NMR spectroscopy exclusively.

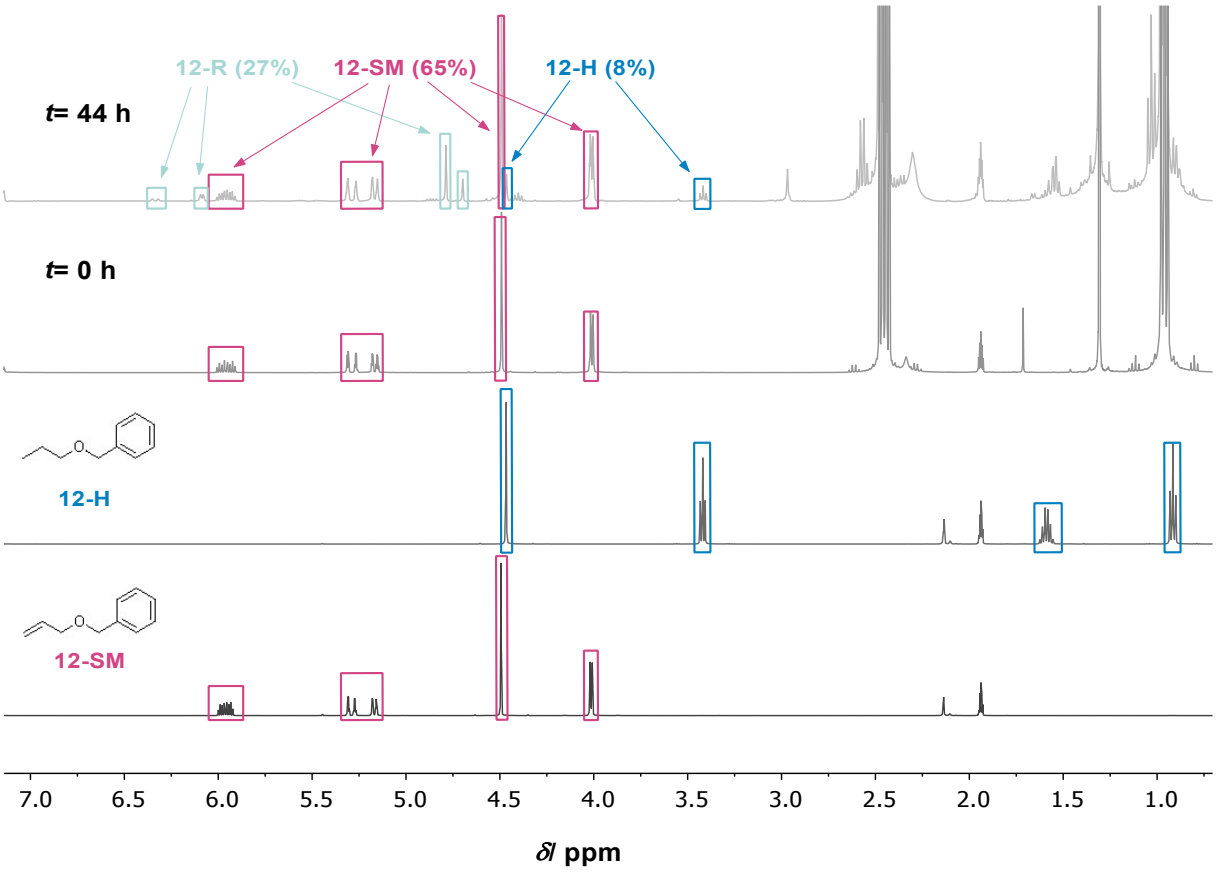

Figure S30. ^{1}H-NMR spectra of the light-driven hydrogenation of ((allyloxy)methyl)benzene (**12-SM**) in CD_3CN: The ^{1}H-NMR spectra of the reaction mixture before (t = 0 h) and after (t = 44 h) irradiation are shown in comparison to the ^{1}H-NMR spectra of neat ((allyloxy)methyl)benzene (**12-SM**) and benzyl propyl ether (**12-H**). The triplet at 1.02 ppm and the quartet at 2.56 ppm in the top spectrum are due to diethylamine resulting from TEA oxidation.

4 Mechanistic studies

4.1 Thermochemistry of the photoinduced HAT

The Ir^{III}-H BDFE of $[Cp^*Ir(phen)(H)]^+$ is not known, but for the $[Cp^*Ir(PMe_3)(H)_2]$ complex the Ir^{III}-H BDFE is ca. 69 kcal · mol^{-1}. (This BDFE value was estimated based on the published BDE value of the Ir^{III}-H bond for $[Cp^*Ir(PMe_3)(H)_2]$ (74 kcal mol^{-1})[30] taking into account an entropic effect of the solvent (MeCN) of 4.8 kcal · mol^{-1}).[31] By contrast, the Ir^{II}-H BDFE of the $[Cp^*Ir(bpy)(H)]^0$ complex is only 43.9 kcal · mol^{-1}.[5] The only difference of that complex to ours is the presence of a phen instead of a bpy ligand, and it seems plausible that this does not much affect the Ir^{II}-H BDFE. Thus, we assume that our catalytically active $[Cp^*Ir(phen)(H)]^0$ complex has an Ir^{II}-H BDFE of 44±2 kcal · mol^{-1}. On the other hand, the BDFE of the newly formed C-H bond radical intermediates **RI•** bearing an aromatic substituent is on the order of 41±2 kcal · mol^{-1}. That proxy value corresponds to the BDE of the C-H bond formed after H-atom transfer to α-methyl styrene (45.6 kcal mol^{-1}[32]) and takes into account an entropic effect of the solvent (MeCN) of 4.8 kcal · mol^{-1}.[31] The initial photo-HAT from the $[Cp^*Ir(phen)(H)]^0$ complex to our aromatic substrates consequently has $\Delta G_{HAT} \approx 0$ kcal · mol^{-1}, see Fig. S31. Thus, in principle reactants and products of the initial HAT step are in equilibrium, similar to what was found previously for thermal (light-independent) metal-catalyzed HAT reactions.[33] Secondary HAT (with oxidation products of TEA acting as H-atom donors, see main paper) is rapid and drives the overall reaction towards the product side. For aliphatic substrates, the BDFE of C-H bond formed after an initial HAT is around 32±2 kcal · mol^{-1} (corresponding to a C-H BDE of the *tert*-butyl radical of 36.6 kcal · mol^{-1}[34]). For these substrates, initial HAT to the olefin is therefore energetically uphill ($\Delta G_{HAT} \approx +10$ kcal · mol^{-1}) and H-abstraction from the radial intermediate **RI•** gets more favored, leading to a greater proportion of rearranged products in comparison to hydrogenated products.

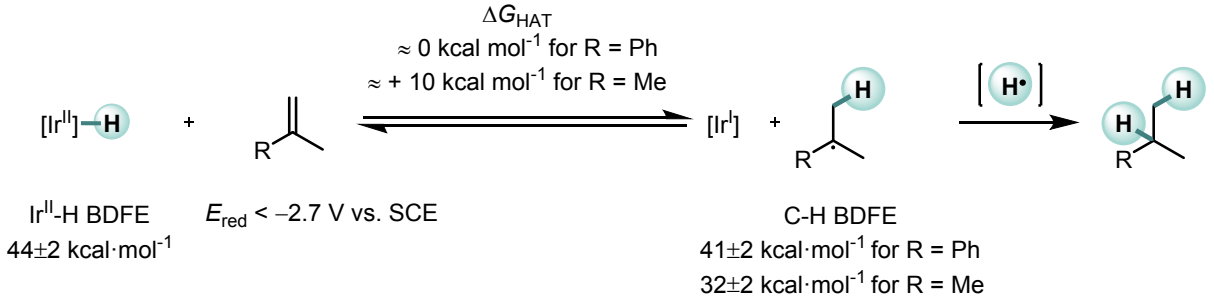

Figure S31. Thermochemistry of the investigated photoinduced HAT.

Aromatic disubstituted germinal olefins have very negative reduction potentials, as illustrated by the reduction potential of α-methyl styrene, which is more negative than −2.7 V vs. SCE (Fig. S31).[35] Thus, electron transfer from $[Cp^*Ir(phen)(H)]^0$ ($E^{0\prime}$(III/II) ≈ −1.4 V vs. SCE[5]) or from ^{3}MLCT-excited $[Cp^*Ir(phen)(H)]^+$ ($E^{0\prime}$(IV/III*) ≈ −1.3 V vs. SCE[5], see Fig. S32) to the investigated olefins is endergonic

by at least 1.3 eV. The reduction potentials included in Fig. S32 were reported for $[Cp^*Ir(bpy)(H)]^+$, but we assume that the reduction potentials of the investigated $[Cp^*Ir(phen)(H)]^+$ complex are similar.

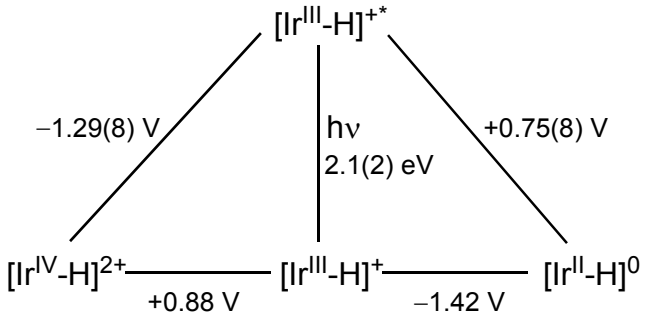

Figure S32. Latimer diagram of $[Cp^*Ir(bpy)(H)]^+$ adapted from Miller and coworkers.[5] All potentials are given in V vs. SCE.

4.2 Role of iridium hydride

Conversion of $[Cp^*Ir(phen)Cl]^+$ (yellow trace, Figure S33) to $[Cp^*Ir(phen)(H)]^+$ (green trace, Figure S33) was monitored by UV-Vis spectroscopy. The increase in absorption at 430 nm and the decrease in absorption at 350 nm as well as the isosbestic point at 375 nm indicate the conversion of [Cp*Ir(phen)Cl]Cl (yellow trace) to $[Cp^*Ir(phen)(H)](PF_6)$ (green trace).

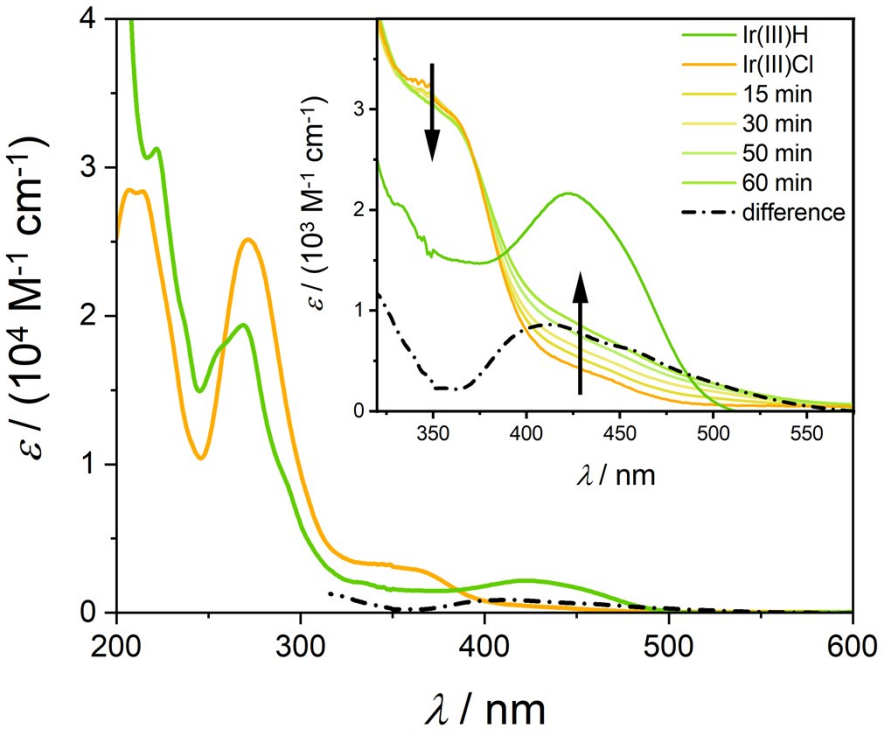

Figure S33. Main plot**:** Absorption spectra of [Cp*Ir(phen)Cl]Cl (yellow trace) and $[Cp^*Ir(phen)(H)](PF_6)$ (green trace) in CH_3CN at room temperature. Inset: Continuous irradiation of a solution containing [Cp*Ir(phen)Cl]Cl (80 µM) and TEA (1.0 mM) in CH_3CN at 455 nm.

The evidence for the photo-driven conversion of $[Cp^*Ir(phen)Cl]^+$ to $[Cp^*Ir(phen)(H)]^+$ in the UV-Vis data of Figure S33 is further supported by the ^{1}H-NMR data in Figure S34. Clearly, the formation of the iridium(III) hydride species (marked by green boxes) from the iridium(III) chloride (yellow boxes) is very slow, but easily detectable in absence of substrate (panels A and C). In presence of substrate (panels B and D), its detection is difficult, presumably due to its efficient turnover with the substrate.

The grey boxes in Figure S34 mark resonances caused by free (unbound) phen ligand (either added in excess (panels A and B), or form as a result of photo-driven dissociation from the iridium complex.

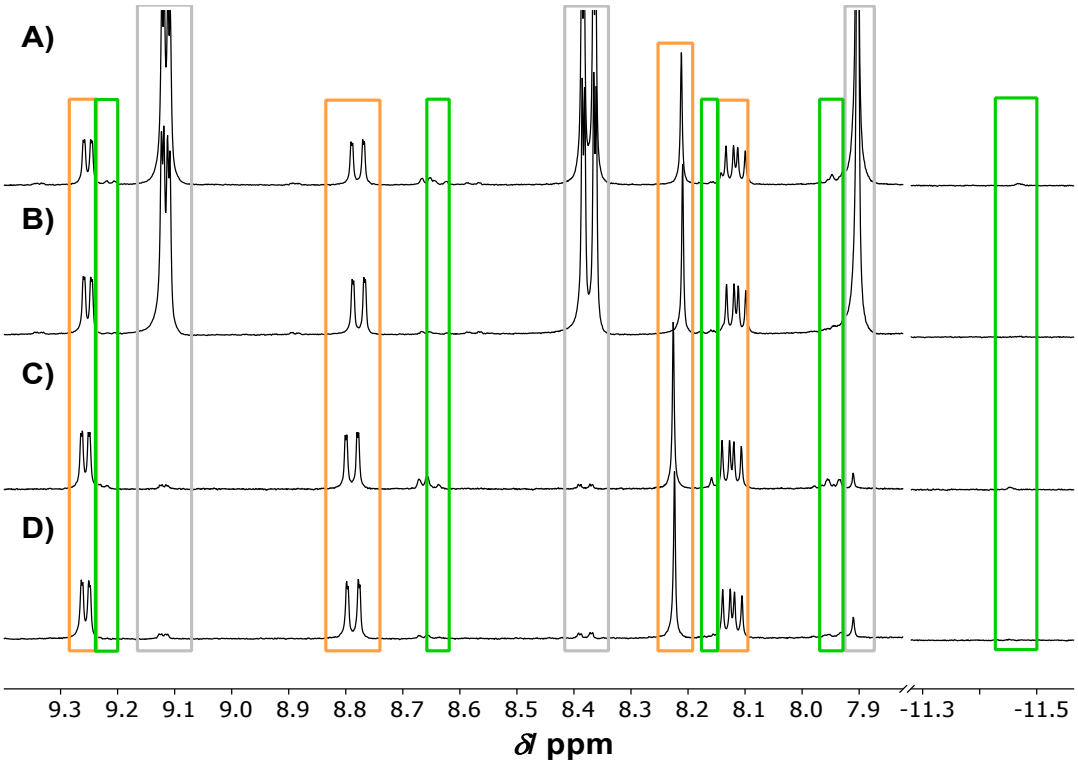

Figure S34: Continuous irradiation of different reaction mixtures containing [Cp*Ir(phen)Cl]Cl] and TEA in deaerated CD_3CN at 470 nm and at 50 °C. A) Reaction mixture containing [Cp*Ir(phen)Cl]Cl] (3.5 mM), phen (21 mM) and TEA (350 mM) in deareated CD_3CN. B) Reaction mixture containing **1-SM** (70 mM), [Cp*Ir(phen)Cl]Cl] (3.5 mM), phen (21 mM) and TEA (350 mM) in deareated CD_3CN. C) Reaction mixture containing [Cp*Ir(phen)Cl]Cl] (3.5 mM) and TEA (350 mM) in deareated CD_3CN. B) Reaction mixture containing **1-SM** (70 mM), [Cp*Ir(phen)Cl]Cl] (3.5 mM) and TEA (350 mM) in deareated CD_3CN.

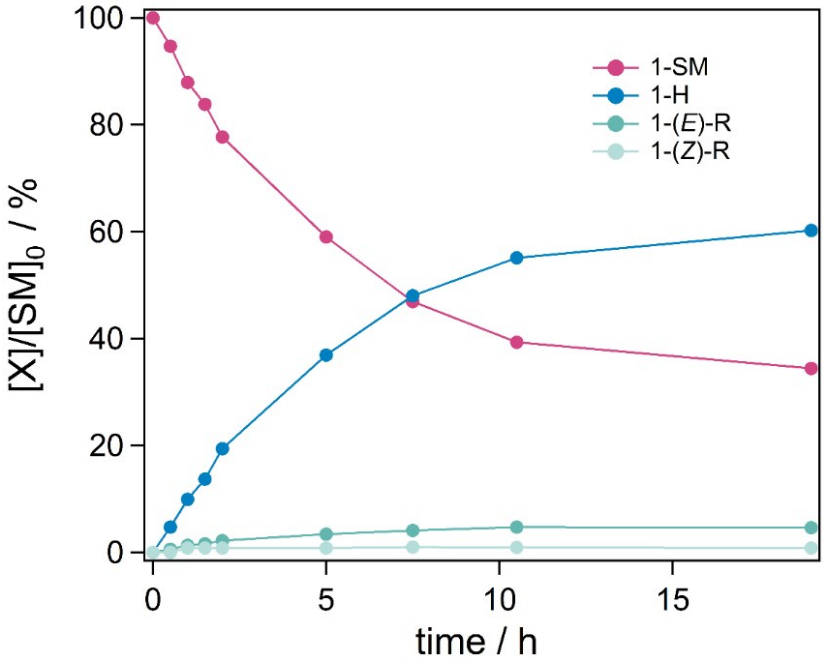

Figure S35. Reaction progress as a function of time when using [Cp*Ir(phen)(H)](PF_6). Conversion of the substrate (**1-SM**, pink trace) and ^{1}H-NMR yields of the different products (**1-H**, blue trace; **1-(*E*)-R** and **1-(*Z*)-R**, turquoise traces) over the reaction course. Monitoring the progress of the reaction mixture containing (3-methoxyprop-1-en-2-yl)benzene (**1-SM**, 50 mM) as a substrate, [Cp*Ir(phen)(H)](PF_6) (2.5 mM), excess 1,10-phenanthroline (15 mM), TEA (250 mM) as sacrificial donor and *tert*-butylbenzene (50 mM) as internal standard while irradiating the reaction mixture at 470 nm (7.5 W). The conversions were determined by ^{1}H-NMR spectroscopy. Acquisition of the NMR spectra occurred in the dark, using 8 aliquots of the same stock solution irradiated in parallel for different amounts of time.

4.3 Excited-state quenching experiments

The MLCT excited-state lifetime τ of $[Cp^*Ir(phen)(H)]^+$ is 148 ns in deaerated CH_3CN containing $[Cp^*Ir(phen)(H)]^+$ (0.2 mM) and NBu_4PF_6 (0.6 mM) at room temperature (Fig. S35), which is in good agreement with the literature,[36] considering that the detected lifetime is concentration dependent.[5] Upon addition of TEA, the emissive MLCT state is quenched with a rate constant of $k_q = 4.5 \cdot 10^8$ M^{-1} s^{-1} based on a Stern-Volmer analysis.

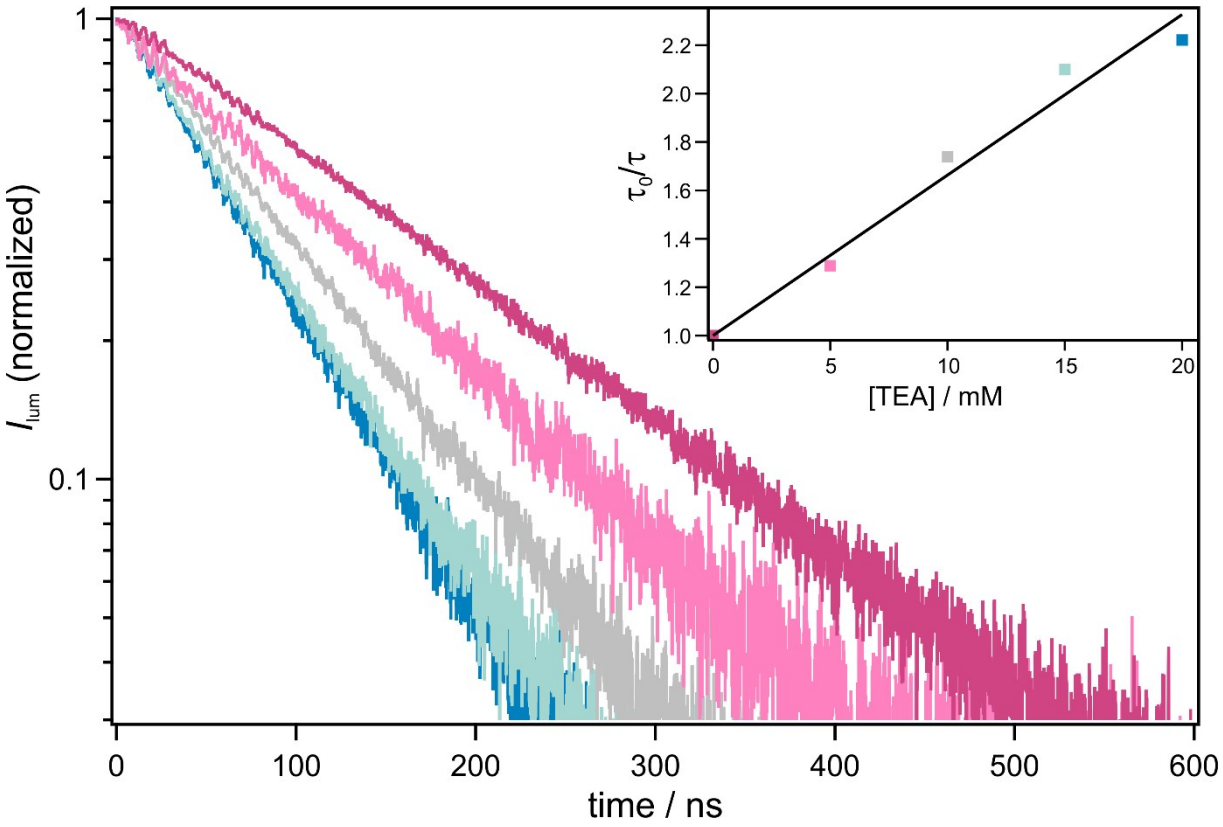

Figure S36. Main plot: Time-resolved luminescence decays of $[Cp^*Ir(phen)(H)](PF_6)$ (0.2 mM) in absence (red trace) and in presence of varying concentrations of TEA. Measurements were performed in deaerated CH_3CN containing NBu_4PF_6 (0.6 mM) at room temperature. Excitation occurred at 455 nm and the luminescence was detected at 700 nm. All decays were normalized to 1.0 at t = 0. Inset: Stern-Volmer plot obtained from the kinetic emission experiments.

Table S5. Lifetime τ at a $[Cp^*Ir(phen)(H)]^+$ concentration of 0.2 mM, Stern-Volmer constant K_{SV} and quenching constant k_q of the reductive quenching of $[Cp^*Ir(phen)(H)](PF_6)$ in presence of TEA in deaerated CH_3CN containing NBu_4PF_6 (0.6 mM) at room temperature.

τ / ns	148
K_{sv} / M^{-1}	66
k_q / M^{-1} s^{-1}	$4.5 \cdot 10^8$

4.4 Mechanistic Overview

The different possible reaction mechanisms of iridium hydrides are summarized in Figure S37. In absence of both the substrate and a sacrificial donor, iridium(III) hydrides undergo efficient bimetallic "self-quenching" ($k_q = 3.8 \cdot 10^9$ M^{-1} s^{-1})[5] and subsequent H_2-evolution upon irradiation with visible light (Figure S37A), as has been previously reported by the group of Miller.[5] In presence of TEA (250 mM) as a sacrificial donor, reductive quenching becomes the major reaction pathway (Figure S37B), as is evidenced by the higher pseudo first-order rate constant ($1.1 \cdot 10^8$ s^{-1} vs. $9.5 \cdot 10^6$ s^{-1} (for TEA and iridium(III) hydride concentrations of 250 mM and 2.5 mM, respectively)). In absence of a substrate, H_2 evolution from the iridium(II) hydride is expected to be the major reaction product, as H_2 formation is exergonic by 16 kcal/mol. $TEA^{\bullet+}$ serves as a proton source for the regeneration of the iridium(III) hydride. When TAA-OMe is used as a sacrificial donor, reductive quenching of the ^{3}MLCT state is again the major reaction pathway, as was evidenced by the formation of the characteristic TAA-$OMe^{\bullet+}$ absorption band in the transient absorption experiment (Figures S37C). When an olefin substrate is added to the reaction mechanism, H_2 evolution from the iridium(II) hydride can be avoided and HAT to the olefin substrate is observed instead (Figure S37D).

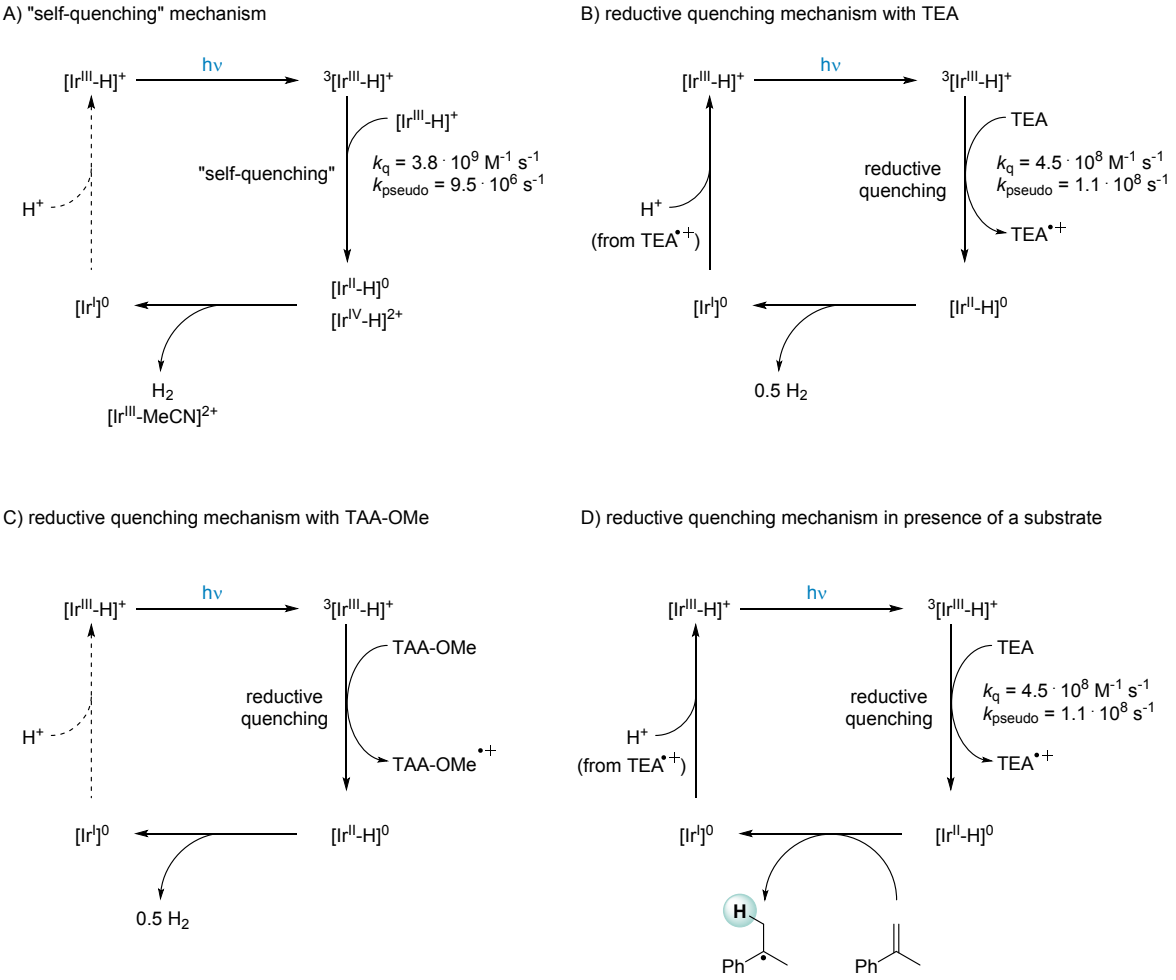

Figure S37. Overview over the different reaction mechanisms of the iridium(III) hydride upon excitation with visible light. A) "Self-quenching" is the dominant reaction pathway in absence of a sacrificial donor.[5] B) and C) Reductive quenching is the major reaction pathway in presence of either B) TEA or C) TAA-OMe as an electron donor. D) In presence of an olefin substrate, HAT to the closed-shell organic substrate takes place.

4.5 Radical clock experiment

Photoinduced H-atom transfer to (1-(2-phenylcyclopropyl)vinyl)benzene (**13-SM**), a radical clock substrate, was investigated to find further evidence for a radical mechanism. The rate constant for the ring opening of this exact substrate is unknown, however, it has been determined for closely related compounds (Table S6). While there is a relatively small difference in the rate constants for the ring opening of secondary and tertiary radicals (compare entry 2 vs. entry 3, Table S6), an additional phenyl substituent on the cyclopropane ring enhances the rate constant k_{RO} (compare entry 2 vs. entry 4, Table S6) by three orders of magnitude. Thus it can be assumed that the rate constant for the ring opening in the structurally related radical intermediate **13-RI1•** (relevant for our studies) occurs with a similar rate constant ($k_{RO} \approx 10^8$ s^{-1}) as in radical intermediate **D** ($3.6 \cdot 10^8$ s^{-1})

Table S6. Rate constants for the ring opening of radical intermediates **A-D** and **13-RI1•**. Whilst the rate constants for radical intermediates **A-D** have been determined previously, the rate constant for the ring opening of radical intermediate **13-RI1•** (relevant for our studies) was estimated by comparison of the different rate constants k_{RO}.

Entry	Radical Intermediate		Rate constant of the ring opening k_{RO} / s^{-1}
1	**A**	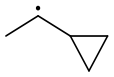	$7 \cdot 10^6$ [37]
2	**B**	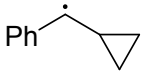	$2.7 \cdot 10^5$ [37]
3	**C**	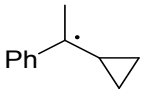	$3.6 \cdot 10^5$ [37]
4	**D**	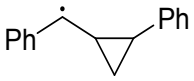	$3.6 \cdot 10^8$ [38]
5	**13-RI1•**	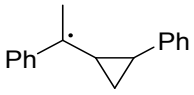	$\approx 10^8$

For the radical clock experiment, degassed stock solutions of (1-(2-phenylcyclopropyl)vinyl)benzene (**13-SM**, 100 µL, 500mM in CD_3CN, 50.0 µmol, 1.0 eq.), [Cp*Ir(phen)Cl]Cl (250 µL, 10 mM in CD_3CN, 2.50 µmol, 5.0 mol%) and *tert*-butylbenzene (100 µL, 500 mM in CD_3CN, 50.0 µmol, 1.0 eq.) as an internal standard were combined and further diluted with degassed CD_3CN (550 µL). TEA (34.7 µL, 250 µmol, 5.0 eq.) was added and 0.5 mL of the reaction mixture were transferred to an NMR-tube. The reaction mixture was then irradiated at 470 nm for 44 h and the conversion was determined both by ^{1}H-NMR spectroscopy and GC-MS spectrometry according to general procedure C.

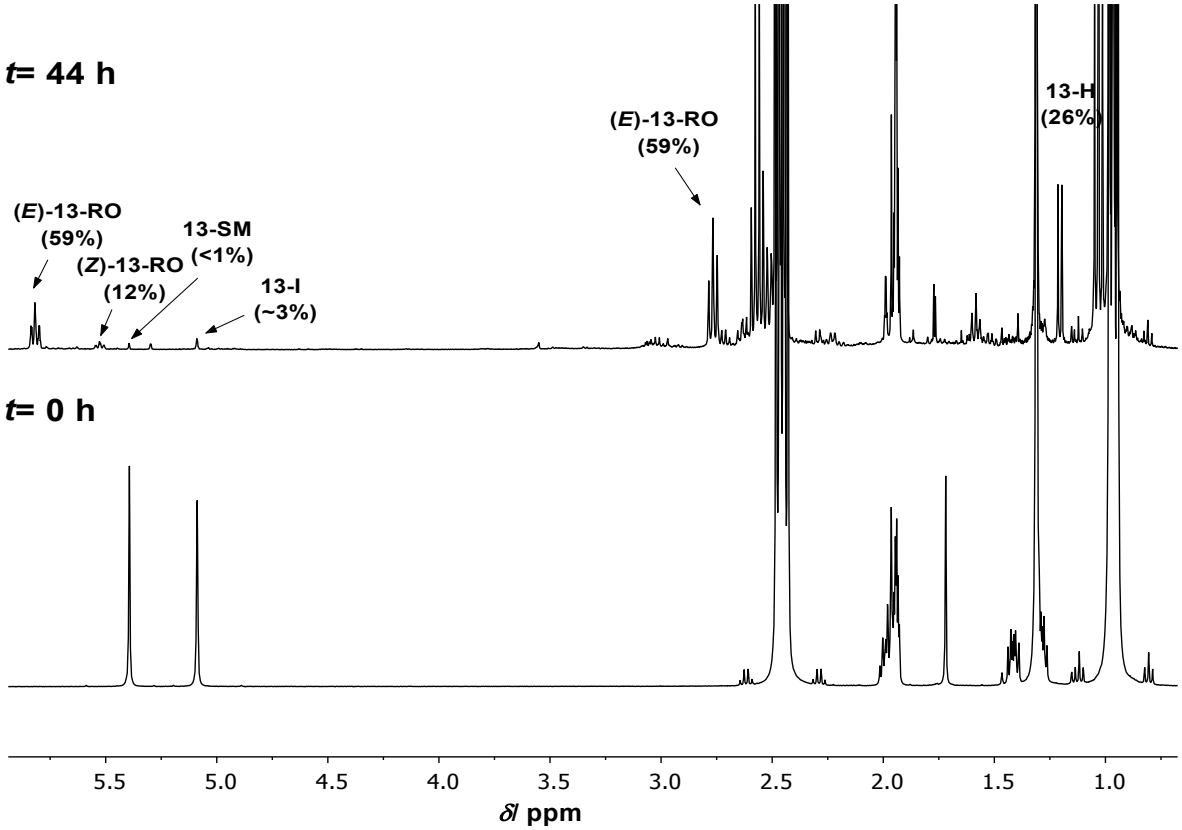

Figure S38. ^{1}H-NMR spectra of the radical clock experiment: The ^{1}H-NMR spectra of the reaction mixture before (*t* = 0 h) and after (*t* = 44 h) irradiation are shown. Visible light-induced hydrogenation of (1-(2-phenylcyclopropyl)-vinyl)benzene (**13-SM**) affords pent-3-ene-1,4-diyldibenzene (**(*E*)-13-RO** and **(*Z*)-13-RO**), pent-4-ene-1,4-diyldibenzene (**13-I**) and pentane-1,4-diyldibenzene (**13-H**).

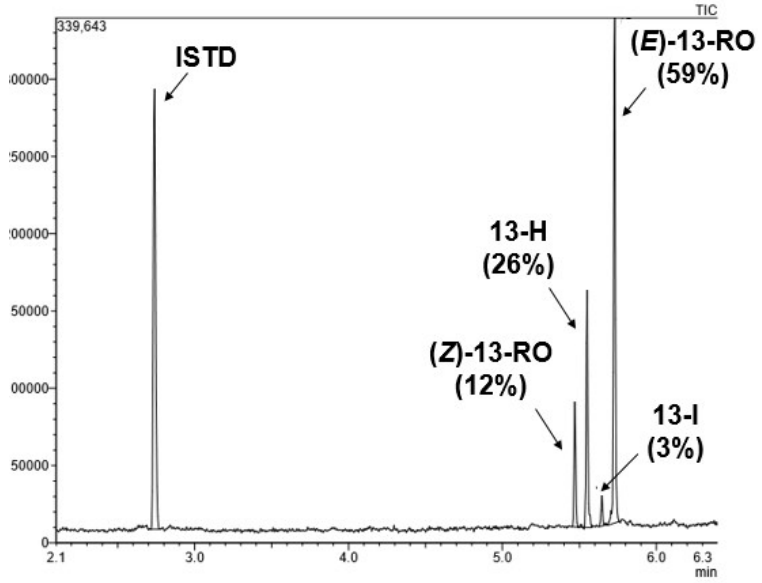

Figure S39. GC-MS trace of the radical clock experiment: Visible light-induced hydrogenation of (1-(2-phenylcyclopropyl)-vinyl)benzene (**13-SM**) affords pent-3-ene-1,4-diyldibenzene (**(*E*)-13-RO** and **(*Z*)-13-RO**), pent-4-ene-1,4-diyldibenzene (**13-I**) and pentane-1,4-diyldibenzene (**13-H**). The different analytes were separated using GC method A (see section S1 for details).

Analysis of the reaction mixture by ^{1}H-NMR spectroscopy and GC-MS spectrometry indicated that no ring-retention product (**13-RR**) is formed (Fig. S38) and that radical intermediate **13-RI1•** undergoes fast ring-opening to give the ring-opened product **13-RO** (71%). Thus, secondary HAT to the radical intermediate is slower than the ring-opening reaction ($k_{RO} \approx 10^8$ s^{-1}). However, **13-RO** is not the only product observed after photoinduced hydrogenation of **13-SM**. Since **13-RO** is a suitable substrate for photoinduced H-atom transfer as well, it can further react under the applied conditions, as confirmed by the formation of both the hydrogenation (**13-H**, 26%) and the isomerization (**13-I**, 3%) products (Fig. S38).

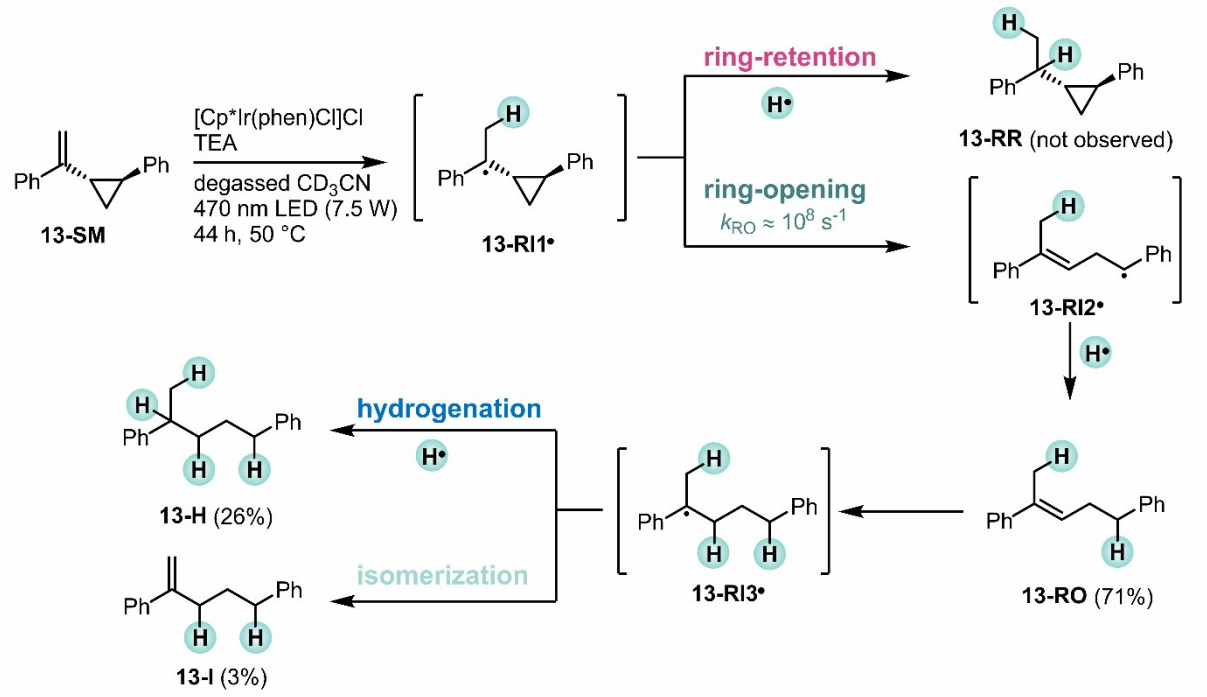

Figure S40. Radical clock experiment with cyclopropane substrate **13-SM** confirms that the reaction proceeds via a radical mechanism. The formed ring-opened product (**13-RO**) can engage in a secondary photoinduced onward reaction to give the hydrogenation (**13-H**) and isomerization (**13-I**) products. For simplicity, only the (*E*)-isomer of the ring-opened product **13-RO** is shown.

4.6 Experiment with a deuterated substrate

To explore the reversibility of the initial photoinduced HAT step, a deuterated substrate ((3-methoxyprop-1-en-2-yl-*1,1,3,3-d*$_4$)benzene, **1-SM-*d*$_4$**) was synthesized and subjected to the reaction conditions. In contrast to traditional studies, where usually a metal-deuteride is used to test the reversibility of hydrogen atoms transfers,[39] we decided to use a deuterated substrate and a non-deuterated hydrogen atom source (TEA). Thus, our method is based on a non-deuterated metal hydride (formed on the basis of the non-deuterated TEA) and a deuterated substrate.

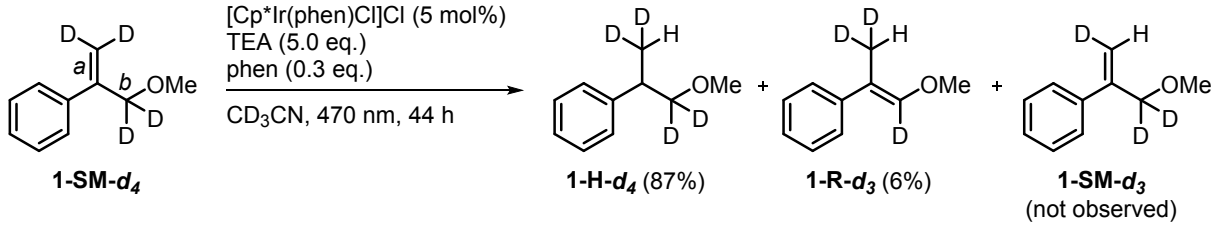

Scheme S7. Experiment with a deuterated substrate **1-SM-*d*$_4$** probing the reversibility of the initial HAT.

(3-Methoxyprop-1-en-2-yl-*1,1,3,3-d*$_4$)benzene (**1-SM-*d*$_4$**) was reduced to (1-methoxypropan-2-yl-1,1,3,3-*d*$_4$)benzene (**1-H-*d*$_4$**) according to general procedure C. The photochemical reaction was followed by integration of the characteristic singlets of the methoxy-groups in the ^{1}H-NMR spectra of the reaction mixtures. To do so, the chemical shifts of the observable methoxy signals were compared to the corresponding resonance of the non-deuterated substrate **1-SM** (Fig. S39). Based on this, the conversion of **1-SM-*d*$_4$** was determined to be 93%, resulting in 87% of the hydrogenation product **1-H-*d*$_4$**. Throughout the experiment, no proton-incorporation into the initial terminal double bond (bond labeled with "*a*" in Scheme S7) to afford **1-SM-*d*$_3$** was observed, indicating that reverse HAT from radical intermediate **1- RI$^{\bullet}$-*d*$_4$** (k_{-HAT1} in Fig. 9 in main paper) is kinetically not competitive with onward reaction to **1-H-*d*$_4$** or **1-R-*d*$_3$**. Since the formed rearranged products **1-R-*d*$_3$** can be further hydrogenated to the corresponding hydrogenation product **1-H-*d*$_4$** (k_{-R}, Fig. 9 in main paper), proton incorporation at the CD_2 group (position labeled with "*b*" in Scheme S7) is possible. However, the exact amount of proton incorporation at this position could not be determined with the applied analytical methods. Also, further identification of the different formed products by mass spectrometry is not possible due to the identical masses of the different isotopomers. Thus, proton incorporation at the CD_2-position (labeled with "*b*" in Scheme S7) is neglected in the schemes for clarity.

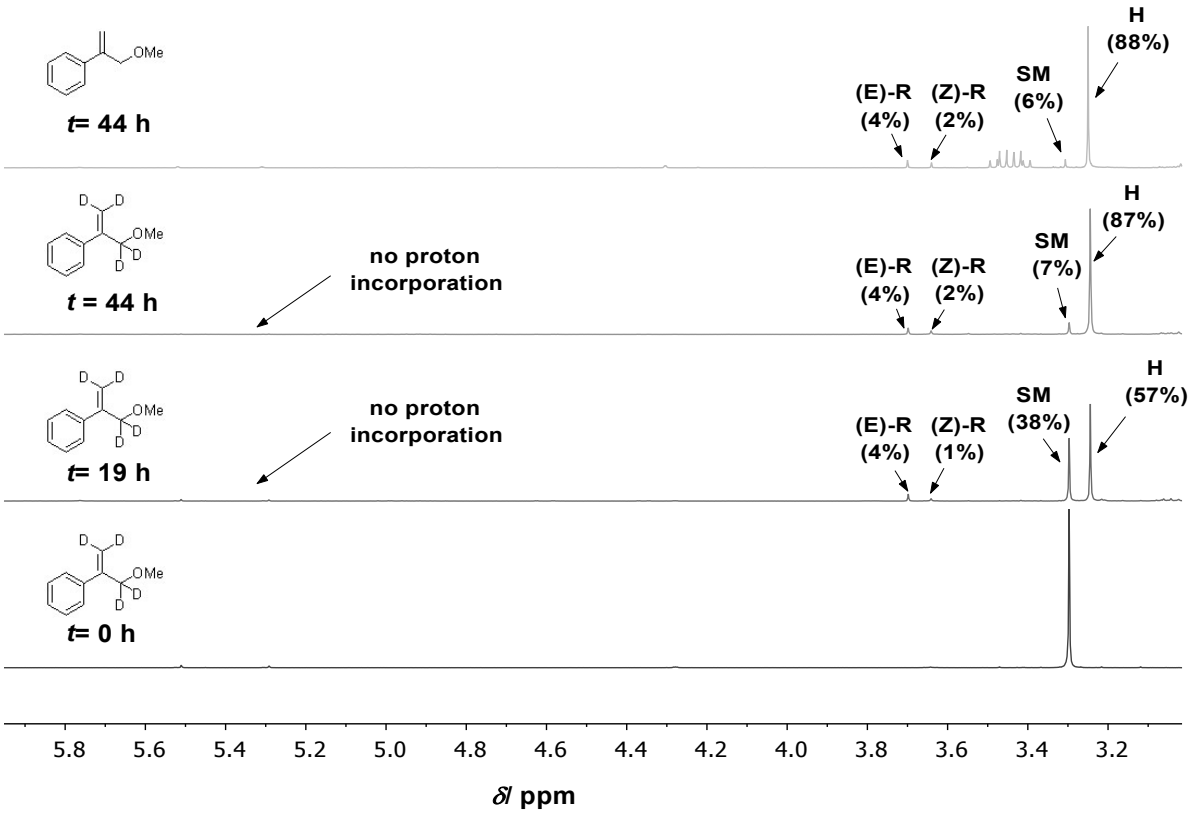

Figure S41. Photochemical experiment with a deuterated substrate: Visible-light driven hydrogenation of (3-methoxyprop-1-en-2-yl-*1,1,3,3-d*$_4$)benzene (**1-SM-*d*$_4$**) at different irradiation times in comparison to the visible-light driven hydrogenation of the non-deuterated substrate **1-SM**.

5 Spectra of new compounds

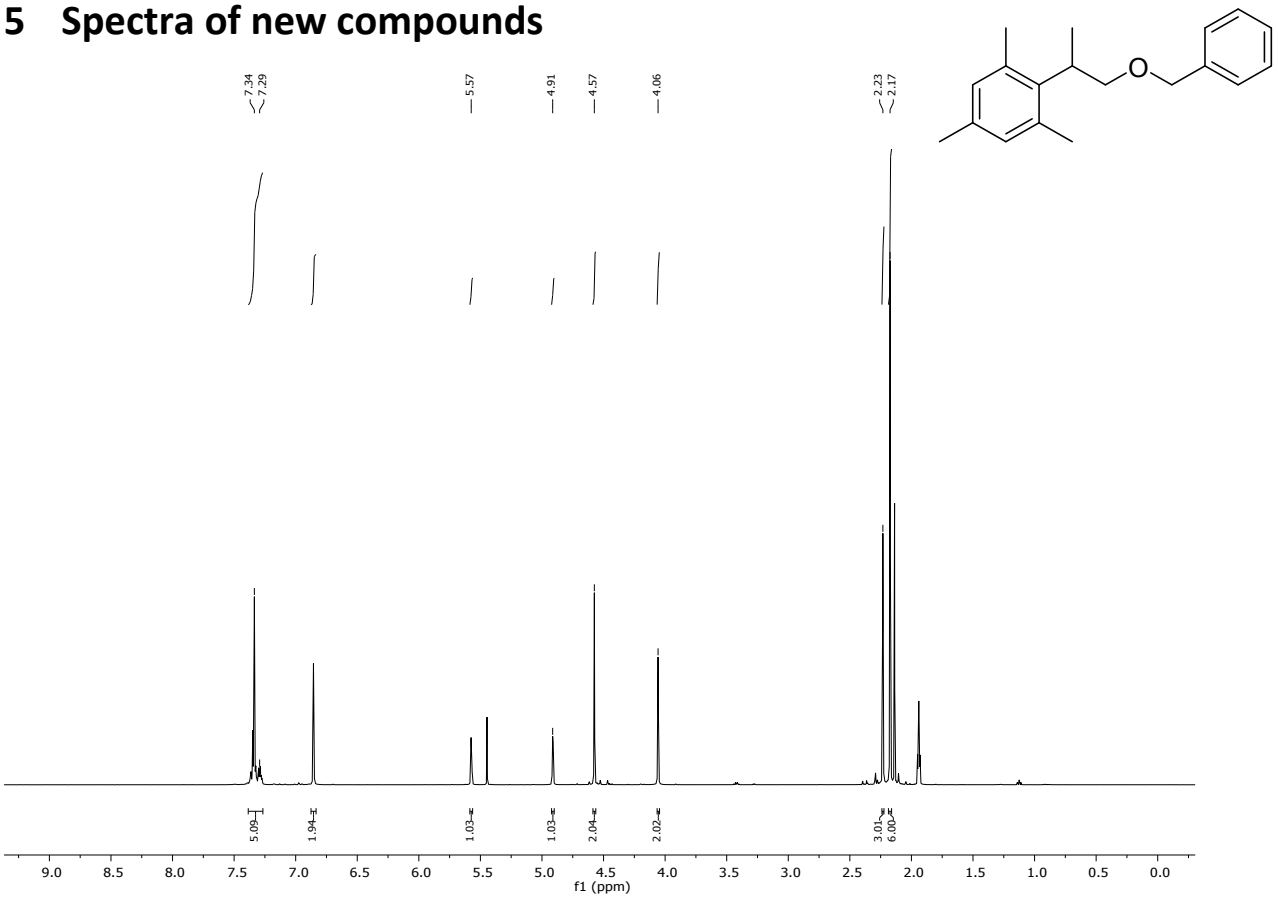

Figure S42. ^{1}H-NMR spectrum of 2-(3-(benzyloxy)prop-1-en-2-yl)-1,3,5-trimethylbenzene (**7-SM**) in CD_3CN.

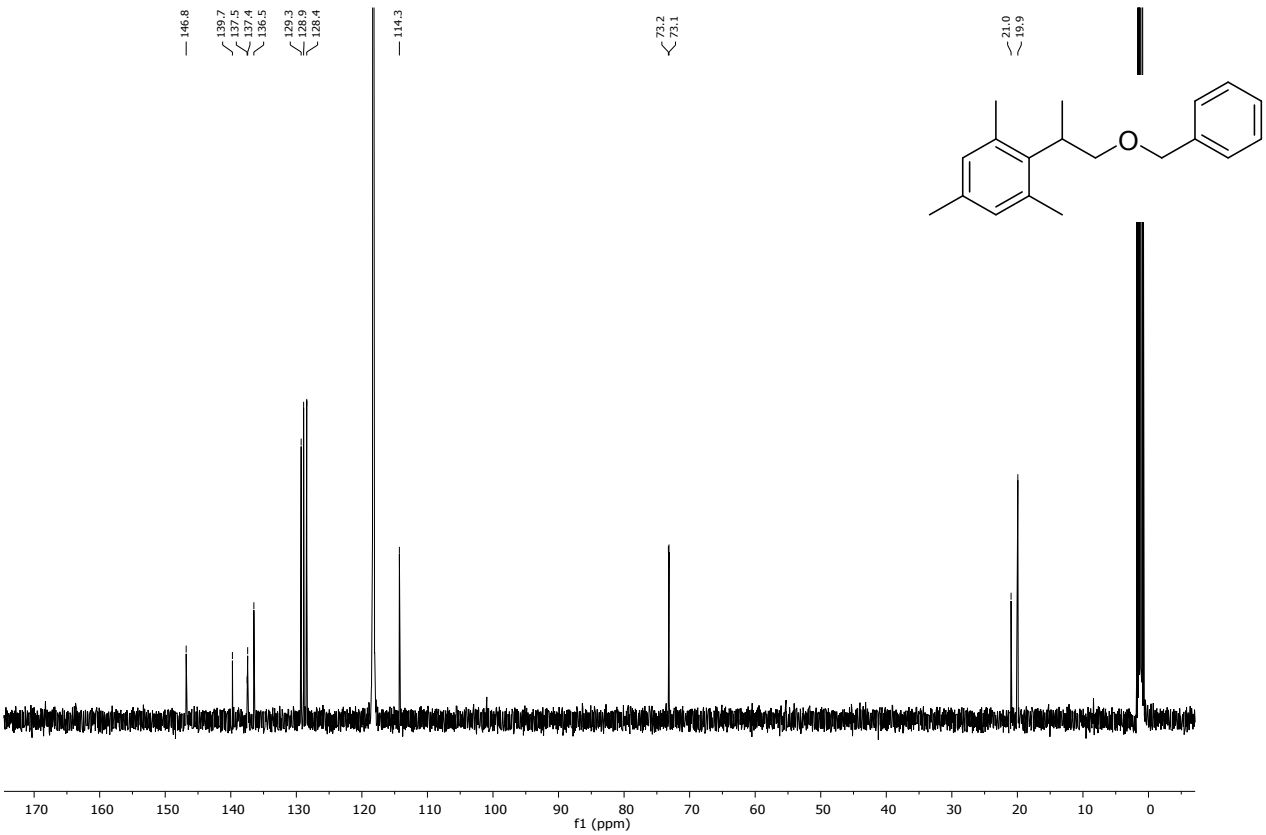

Figure S43. ^{13}C-{^{1}H}-NMR spectrum of 2-(3-(benzyloxy)prop-1-en-2-yl)-1,3,5-trimethylbenzene (**7-SM**) in CD_3CN.

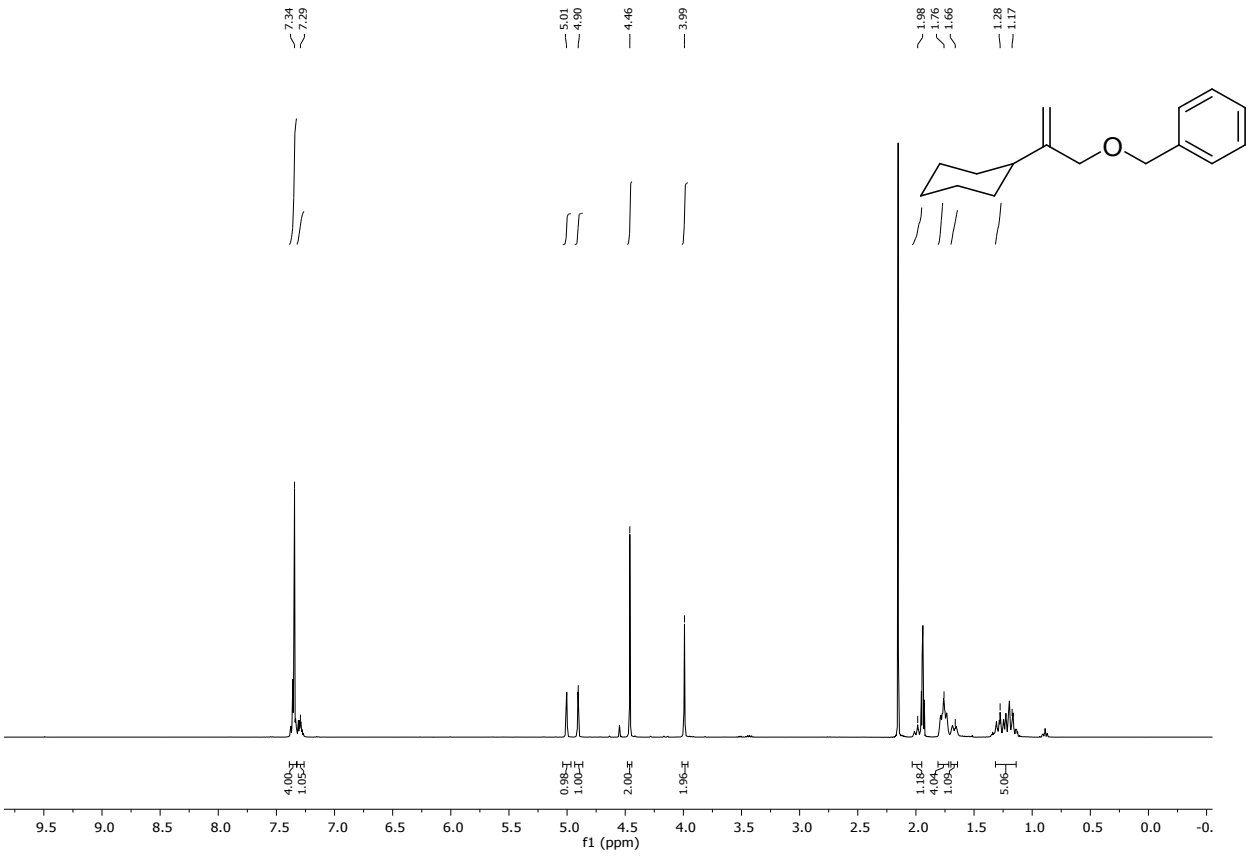

Figure S44. ^{1}H-NMR spectrum of (((2-cyclohexylallyl)oxy)methyl)benzene (**10-SM**) in CD_3CN.

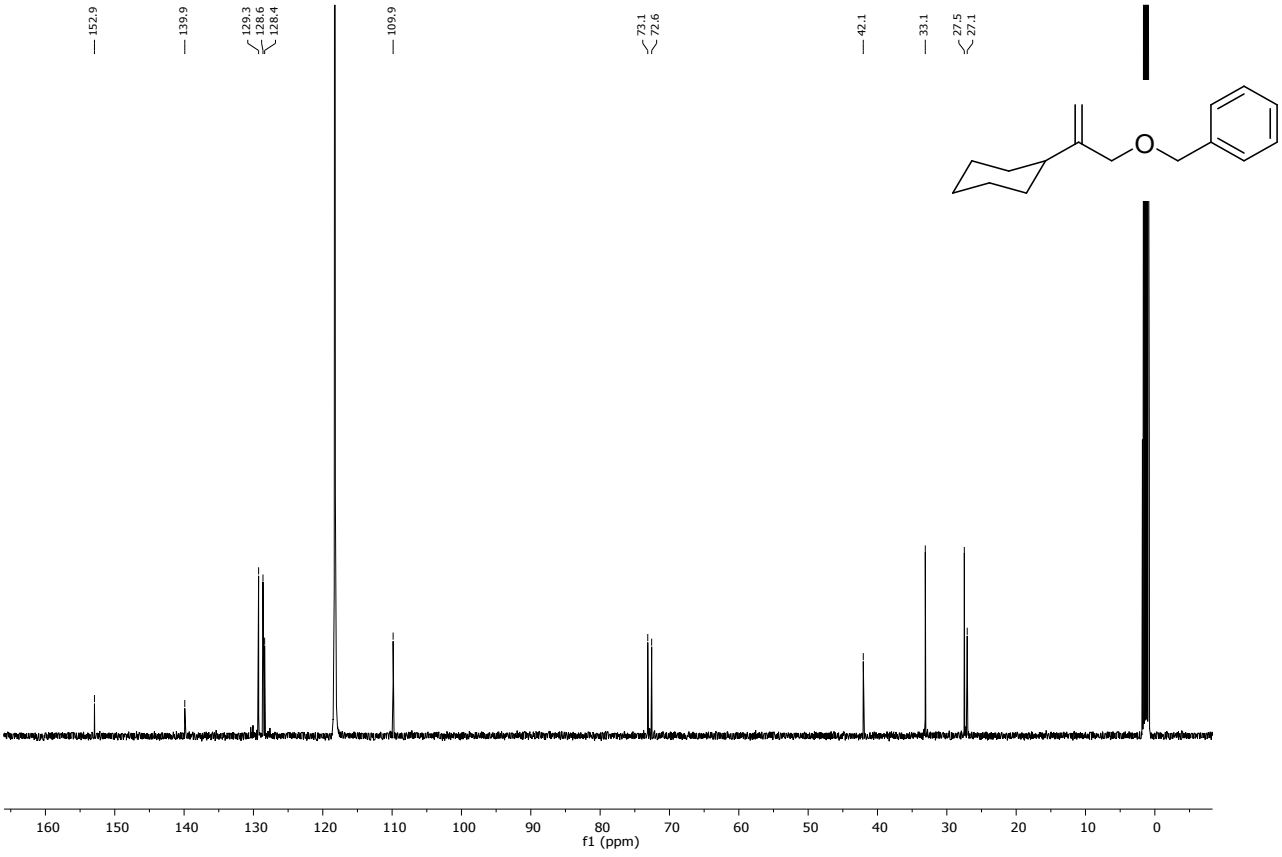

Figure S45. ^{13}C-{^{1}H}-NMR spectrum of (((2-cyclohexylallyl)oxy)methyl)benzene (**10-SM**) in CD_3CN.

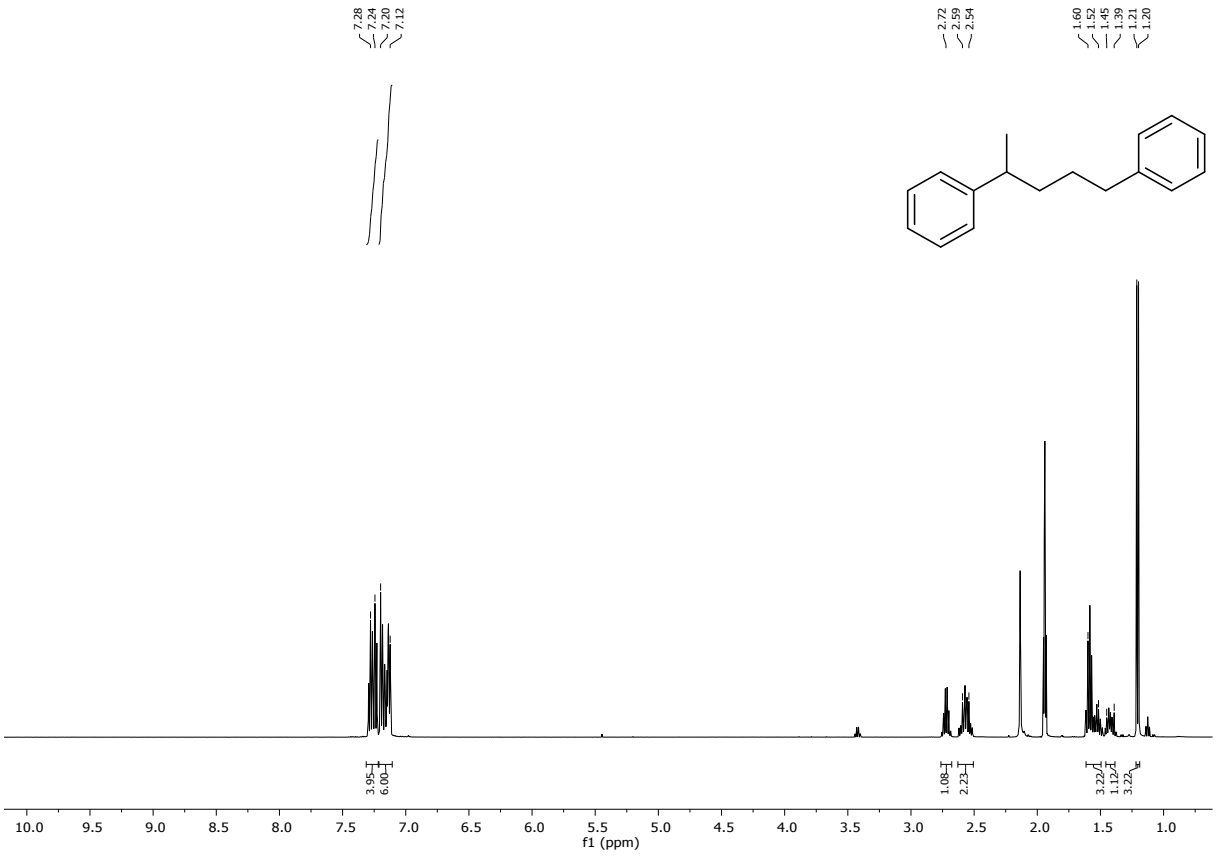

Figure S46. ^{1}H-NMR spectrum of pentane-1,4-diyldibenzene (**13-H**) in CD_3CN.

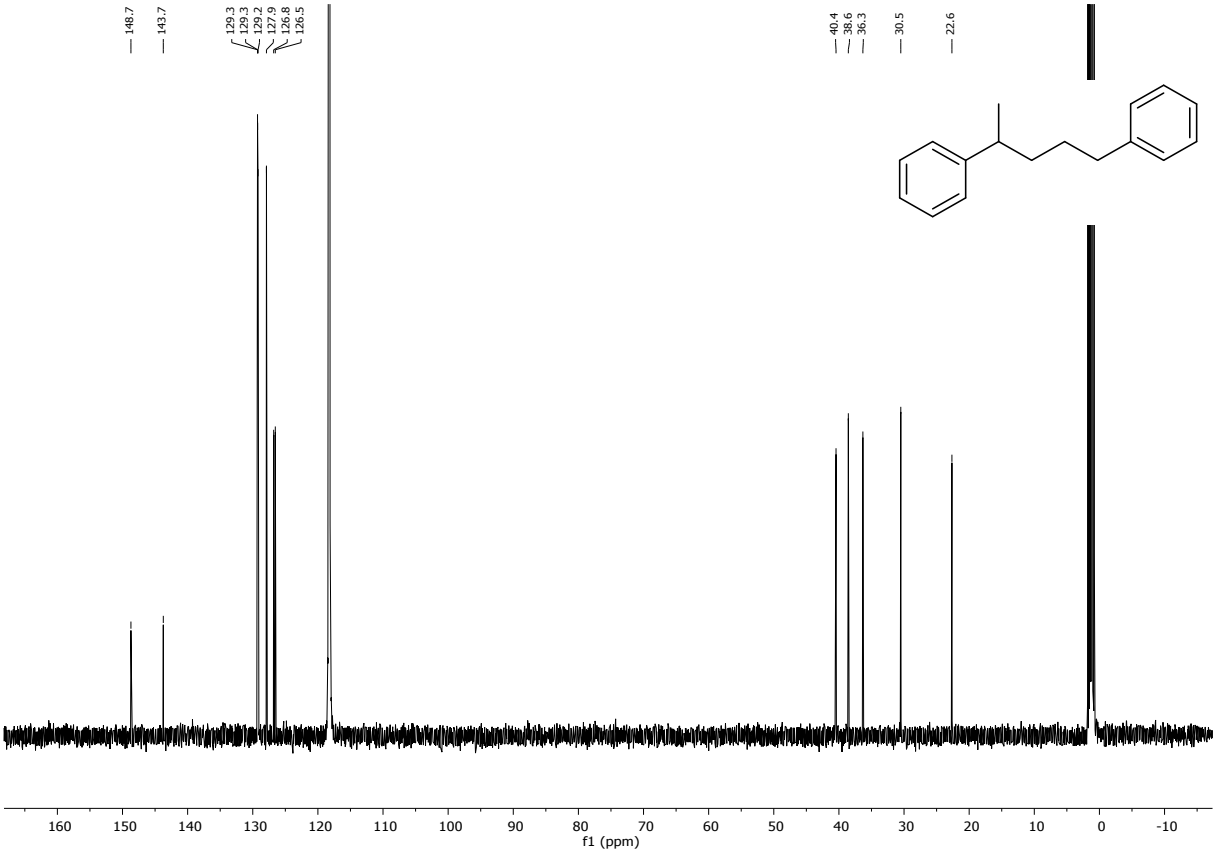

Figure S47. ^{13}C-{^{1}H}-NMR spectrum of pentane-1,4-diyldibenzene (**13-H**) in CD_3CN.

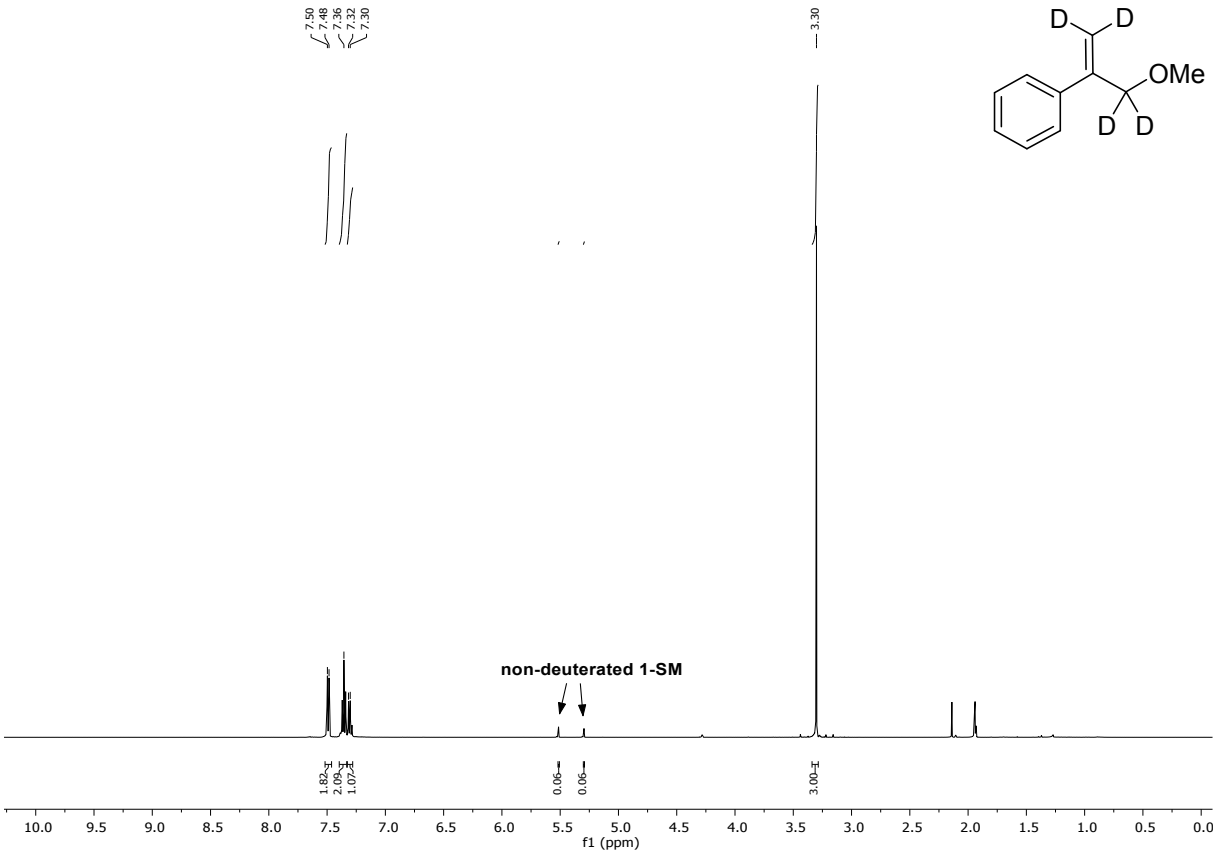

Figure S48. ^{1}H-NMR spectrum of (3-methoxyprop-1-en-2-yl-1,1,3,3-d_4)benzene (**1-SM-*d*$_4$**) in CD_3CN.

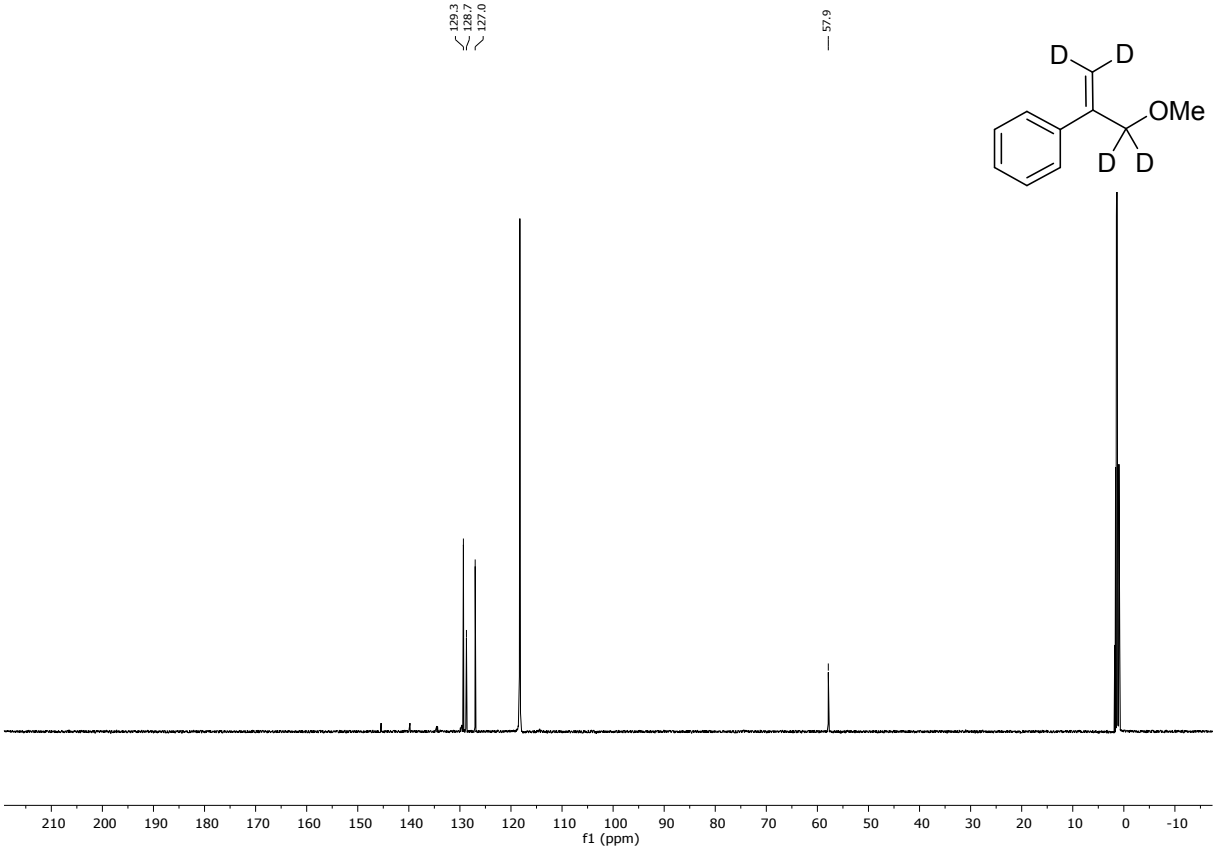

Figure S49. ^{13}C-{^{1}H}-NMR spectrum of (3-methoxyprop-1-en-2-yl-1,1,3,3-d_4)benzene (**1-SM-*d*$_4$**) in CD_3CN.

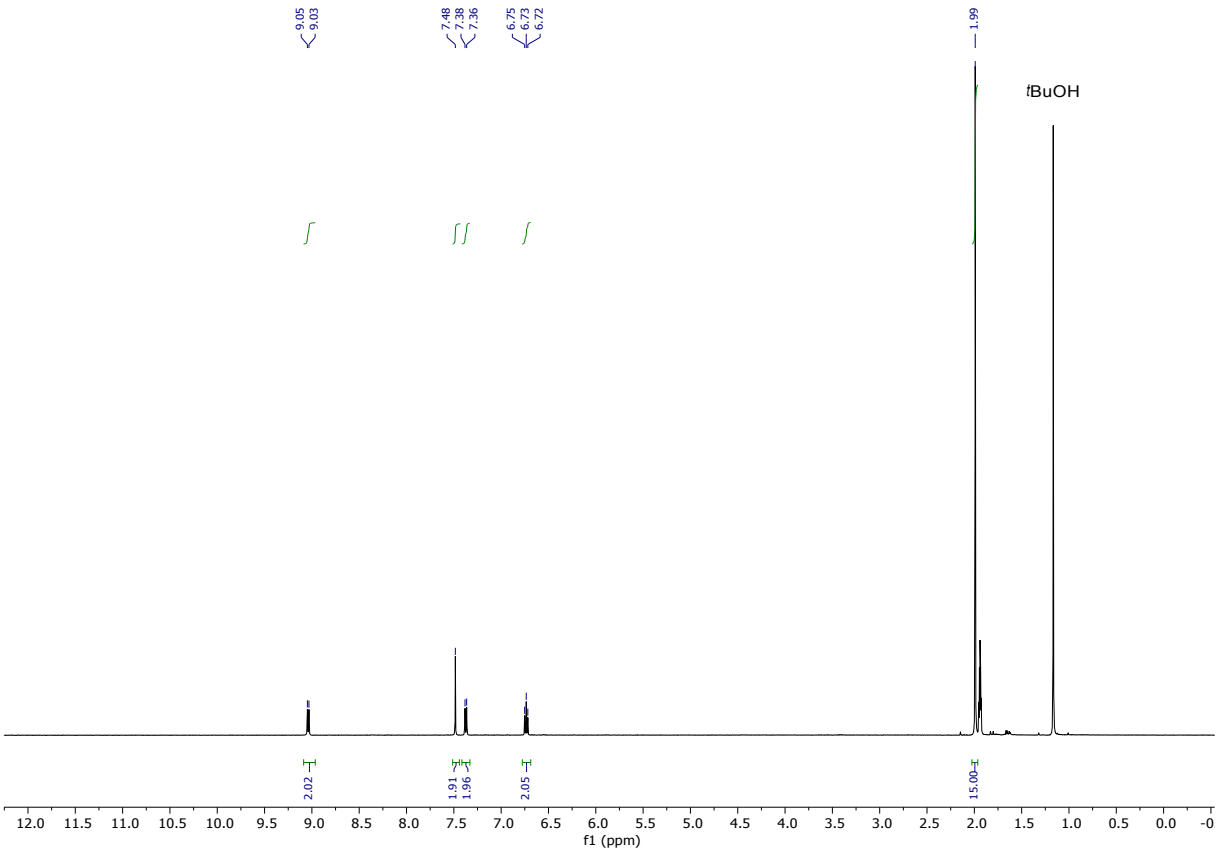

Figure S50. ^{1}H-NMR reference spectrum of $[Cp^*Ir(phen)]^0$ obtained after deprotonation of $[Cp^*Ir(phen)(H)]^+$ in CD_3CN with KO^{t}Bu (1.3 eq.).

6 References

[1] G. R. Fulmer, A. J. M. Miller, N. H. Sherden, H. E. Gottlieb, A. Nudelman, B. M. Stoltz, J. E. Bercaw, K. I. Goldberg, *Organometallics* **2010**, *29*, 2176–2179.

[2] F. Li, C. Sun, N. Wang, *J. Org. Chem.* **2014**, *79*, 8031–8039.

[3] T. P. Brewster, A. J. M. Miller, D. M. Heinekey, K. I. Goldberg, *J. Am. Chem. Soc.* **2013**, *135*, 16022–16025.

[4] M.-T. Youinou, R. Ziessel, *J. Organomet. Chem.* **1989**, *363*, 197–208.

[5] M. B. Chambers, D. A. Kurtz, C. L. Pitman, M. K. Brennaman, A. J. M. Miller, *J. Am. Chem. Soc.* **2016**, *138*, 13509–13512.

[6] S. M. Smith, G. L. Hoang, R. Pal, M. O. B. Khaled, L. S. W. Pelter, X. C. Zeng, J. M. Takacs, *Chem. Commun.* **2012**, *48*, 12180–12182.

[7] A. Garzan, A. Jaganathan, N. Salehi Marzijarani, R. Yousefi, D. C. Whitehead, J. E. Jackson, B. Borhan, *Chem. Eur. J.* **2013**, *19*, 9015–9021.

[8] F. Giacomina, A. Alexakis, *Eur. J. Org. Chem.* **2013**, 6710–6721.

[9] X. Sun, K. Frimpong, K. L. Tan, *J. Am. Chem. Soc.* **2010**, *132*, 11841–11843.

[10] A. Blanc, F. D. Toste, *Angew. Chem. Int. Ed.* **2006**, *45*, 2096–2099.

[11] J. J. Molloy, J. B. Metternich, C. G. Daniliuc, A. J. B. Watson, R. Gilmour, *Angew. Chem. Int. Ed.* **2018**, *57*, 3168–3172.

[12] S. McIntyre, E. Hörmann, F. Menges, S. P. Smidt, A. Pfaltz, *Adv. Synth. Catal.* **2005**, *347*, 282–288.

[13] T. Kippo, T. Fukuyama, I. Ryu, *Org. Lett.* **2011**, *13*, 3864–3867.

[14] P. V. Ramachandran, D. R. Nicponski, *Chem. Commun.* **2014**, *50*, 15216–15219.

[15] E. Sagot, D. S. Pickering, X. Pu, M. Umberti, T. B. Stensbøl, B. Nielsen, M. Chapelet, J. Bolte, T. Gefflaut, L. Bunch, *J. Med. Chem.* **2008**, *51*, 4093–4103.

[16] G. Li, D. Leow, L. Wan, J. Q. Yu, *Angew. Chem. Int. Ed.* **2013**, *52*, 1245–1247.

[17] C. Tao, L. Sun, B. Wang, Z. Liu, Y. Zhai, X. Zhang, D. Shi, W. Liu, *Tetrahedron Lett.* **2017**, *58*, 305–308.

[18] C. Stueckler, C. K. Winkler, M. Bonnekessel, K. Faber, *Adv. Synth. Catal.* **2010**, *352*, 2663–2666.

[19] C. T. Yang, Z. Q. Zhang, J. Liang, J. H. Liu, X. Y. Lu, H. H. Chen, L. Liu, *J. Am. Chem. Soc.* **2012**, *134*, 11124–11127.

[20] D. F. Taber, C. M. Paquette, P. G. Reddy, *Tetrahedron Lett.* **2009**, *50*, 2462–2463.

[21] M. Ficker, S. W. Svenningsen, T. Larribeau, J. B. Christensen, *Tetrahedron Lett.* **2018**, *59*, 1125–1129.

[22] Y. Arai, R. Tomita, G. Ando, T. Koike, M. Akita, *Chem. Eur. J.* **2016**, *22*, 1262–1265.

[23] W. Hüggenberg, A. Seper, I. M. Oppel, G. Dyker, *Eur. J. Org. Chem.* **2010**, 6786–6797.

[24] R. Bejot, S. Anjaiah, J. R. Falck, C. Mioskowski, *Eur. J. Org. Chem.* **2007**, 101–107.

[25] J. C. Anderson, R. H. Munday, *J. Org. Chem.* **2004**, *69*, 8971–8974.

[26] C. Sabot, K. A. Kumar, C. Antheaume, C. Mioskowski, *J. Org. Chem.* **2007**, *72*, 5001–5004.

[27] G. E. M. Crisenza, N. G. McCreanor, J. F. Bower, *J. Am. Chem. Soc.* **2014**, *136*, 10258–10261.

[28] A. C. Hernandez-Perez, S. K. Collins, *Angew. Chem. Int. Ed.* **2013**, *52*, 12696–12700.

[29] C. Quinton, V. Alain-Rizzo, C. Dumas-Verdes, F. Miomandre, G. Clavier, P. Audebert, *RSC Adv.*

2014, *4*, 34332–34342.

[30] J. A. M. Simões, J. L. Beauchamp, *Chem. Rev.* **1990**, *90*, 629–688.

[31] D. D. M. Wayner, V. D. Parker, *Acc. Chem. Res.* **1993**, *26*, 287–294.

[32] D. J. Goebbert, P. G. Wenthold, *Int. J. Mass Spectrom.* **2006**, *257*, 1–11.

[33] S. A. Green, S. W. M. Crossley, J. L. M. Matos, S. Vásquez-Céspedes, S. L. Shevick, R. A. Shenvi, *Acc. Chem. Res.* **2018**, *51*, 2628–2640.

[34] L. Yu-Ran, *Comprehensive Handbook of Chemical Bond Energies*, Taylor & Francis Group, Boca Raton, **2007**.

[35] H. Senboku, H. Komatsu, Y. Fujimura, M. Tokuda, *Synlett* **2001**, 418–420.

[36] D. Sandrini, M. Maestri, R. Ziessel, *Inorg. Chim. Acta* **1989**, *163*, 177–180.

[37] J. Masnovi, E. G. Samsel, R. M. Bullock, *J. Chem. Soc., Chem. Commun.* **1989**, 1044–1045.

[38] R. Hollis, L. Hughes, V. W. Bowry, K. U. Ingold, *J. Org. Chem.* **1992**, *57*, 4284–4287.

[39] G. Li, J. L. Kuo, A. Han, J. M. Abuyuan, L. C. Young, J. R. Norton, J. H. Palmer, *J. Am. Chem. Soc.* **2016**, *138*, 7698–7704.